



Università degli Studi di Cagliari

DOTTORATO DI RICERCA

in Ingegneria Elettronica e Informatica

Ciclo XXVII

TITOLO TESI

Wearable sensors networks for safety applications in industrial
scenarios

Settore/i scientifico disciplinari di afferenza

ING-INF/03 (Telecomunicazioni)

Presentata da: *Claudia Musu*

Coordinatore Dottorato *Fabio Roli*

Tutor/ Relatore *Daniele Giusto*

Esame finale anno accademico 2013 – 2014



*Ph.D. in Electronic and Computer
Engineering*



Dept. of Electrical and Electronic Engineering

University of Cagliari

Wearable sensors networks for safety applications in industrial
scenarios

Claudia Musu

*Advisor: Prof. Daniele Giusto
Curriculum: ING-INF/03 (Telecomunicazioni)
XXVII Cycle*

March 2015

To Luca and my family

Contents

| | |
|--|----|
| Abstract..... | 11 |
| Introduction..... | 13 |
| Chapter 1..... | 16 |
| Industrial port in Europe | 16 |
| 1.1. Navigation..... | 16 |
| 1.2. The port..... | 18 |
| 1.3. Port service area: the Port of Cagliari | 19 |
| Chapter 2..... | 22 |
| Analysis of the processes | 22 |
| 2.1. Current situation of the port of Cagliari | 22 |
| Chapter 3..... | 26 |
| Re-engineering of the processes | 26 |
| 3.1. Port context: re-engineering..... | 26 |
| 3.1.1. Port areas..... | 28 |
| 3.1.2. Control room..... | 29 |
| 3.2. Pre-application analysis | 31 |
| 3.3. Information exchange | 32 |
| 3.4. WebGIS portal..... | 33 |
| Chapter 4..... | 38 |
| Wireless Sensor Network | 38 |
| 4.1. The Internet of Things | 38 |
| 4.2. Wireless Sensor Networks | 40 |

| | |
|--|-----|
| 4.3. Body Area Network (BAN)..... | 46 |
| Chapter 5..... | 49 |
| Wearable Sensor Network..... | 49 |
| 5.1. RFID | 49 |
| 5.2. Wireless Identification and Sensing Platform (WISP) | 51 |
| 5.3. Wearable sensors network | 53 |
| 5.4. The control system | 57 |
| Chapter 6..... | 63 |
| Antennas Design..... | 63 |
| 6.1. Multi-conductor transmission lines..... | 63 |
| 6.2. Calculation of L and C parameters..... | 66 |
| 6.3. Proposed model | 72 |
| Chapter 7..... | 76 |
| Experimental Results | 76 |
| 7.1. Geometry of antennas under test..... | 76 |
| 7.2. First validation..... | 77 |
| 7.3. Test with different multi-conductor | 82 |
| 7.4. Test with substrate wearable | 84 |
| Chapter 8..... | 86 |
| SAR: Specific Absorption Rate..... | 86 |
| 8.1. SAR for different cases of study | 86 |
| 8.2. Wearable Rectangular Patch Antenna..... | 91 |
| Chapter 9..... | 98 |
| Conclusion and future works..... | 98 |
| Appendix | 101 |

| | |
|---|-----|
| 10.1. Computation of the eigenvectors | 101 |
| 10.2. Bisection method..... | 103 |
| 10.3. Discretization | 103 |
| References | 106 |

List of Figures

| | |
|--|----|
| 1.1 Revision map: Source Port Authority Cagliari..... | 20 |
| 2.1 Current nconfiguration in the Cagliari International Container Terminal..... | 23 |
| 2.2 WiFi coverage in the porto of Cagliari | 22 |
| 3.1 Example of a control room architecture..... | 30 |
| 3.2 Screenshot of the port planimetry | 32 |
| 3.3 WebGIS framework | 33 |
| 3.4 Structure of the user interface..... | 34 |
| 3.5 Home Page..... | 34 |
| 3.6 WebGIS Maps..... | 35 |
| 3.7 Map with Open Street Map | 36 |
| 3.8 Different layer | 36 |
| 3.9 Console Layer | 37 |
| 3.10 Workers Marker | 37 |
| 4.1 WSN example | 41 |
| 4.2 WSN network topologies | 42 |
| 4.3 LR-WPAN classification: coverage area | 44 |
| 4.4 BAN Sensors Network for Workplace Safety Management | 47 |
| 5.1 WISP example..... | 51 |
| 5.2 Wisp circuit..... | 52 |
| 5.3 Wearable sensors network..... | 53 |
| 5.4 System architecture | 54 |
| 5.5 Impinj kit..... | 54 |
| 5.6 Wisp-Moo Datasheet..... | 56 |
| 5.7 Axes and rotation angle of a sensor | 58 |
| 5.8 Left: vertical angle α between the acceleration along the X axe with the total acceleration A_m and the Earth's gravitation A_g . Right: vertical angle β between the | |

| | |
|---|-----|
| acceleration along the Y axe with the total acceleration A_m and the Earth's gravitation A_g | 61 |
| 5.9 Planimetry of the area under surveillance | 62 |
| 5.10 General control room..... | 62 |
| 5.11 Worker screen | 62 |
| 6.1 Multi-conductor patch | 63 |
| 6.2 Microstrip Geometry | 66 |
| 6.3 Regular grid for microstrip | 67 |
| 6.4 Interface sampling | 66 |
| 6.5 Closed patch integral of the surface between the dielectric | 68 |
| 6.6 Equivalent circuit of a 4 parallel conductor system | 70 |
| 6.7 Circuital representation | 71 |
| 6.8 Multi-conductor structure | 72 |
| 7.1 Geometry of n-conductors patch..... | 77 |
| 7.2 20-conductors patch | 78 |
| 7.3 Rirr in function of the length | 79 |
| 7.4 12-conductors patch | 81 |
| 7.5 40-conductors patch | 83 |
| 7.6 80-conductors patch | 83 |
| 8.1 CST Model head | 88 |
| 8.2 SAR(W/kg) vs. distance from the human body for varying reader powers | 90 |
| 8.3 Evaluation of SAR at $f=900\text{MHz}$ changing the position of the sensor between 0 and 10 cm..... | 91 |
| 8.4 Geometry of rectangular patch antenna | 93 |
| 8.5 Field distribution at $900\text{MHz} + B_w$ and a $900\text{MHz} - B_w$ for two different cut at 0° and a 90° | 95 |
| 8.6 FarField for different substrate with and without saline solution | 96 |
| 8.7 SAR for substrate jeans | 96 |
| 8.8 SAR for substrate polyacetal | 97 |
| 10.1 Air capacities..... | 104 |

| | |
|----------------------------------|-----|
| 10.2 Dielectric capacities | 104 |
|----------------------------------|-----|

List of Tables

| | |
|--|----|
| 4.1 Wireless technologies for BAN systems | 48 |
| 5.1 RFID characteristic | 50 |
| 5.2 Helmet positioning | 59 |
| 7.1 Parameters of resonance – first test (n=20 and N=16) | 79 |
| 7.2 Parameters of resonance – second test (n=20 and N=36)..... | 80 |
| 7.3 Parameters of resonance – third test (n=12 and N=16) | 81 |
| 7.4 Parameters of resonance | 84 |
| 7.5 Parameters of resonance | 85 |
| 8.1 Dielectric constant of the used materials in the simulation | 91 |
| 8.2 Dimension and parameters of patch antenna at the frequency of 900 MHz..... | 94 |
| 8.3 Result of simulation for different materials | 94 |

Abstract

Industrial contexts, and in particular the port areas, are very complex systems to be monitored and controlled due to the combined presence of vehicles and people. The port areas are the gateway between navigation and terrestrial transportation and are of great importance in transport logistics. Unfortunately, the management of port areas is quite complex because the safety of the workers must be always assured. Therefore, in such a context, a centralized control system for the monitoring and the prevention of risks is of particular importance. In this thesis, a real-time control system for the monitoring of people and vehicles in industrial areas is proposed. The proposed system is based on the Internet of Things paradigm, i.e. a network of “things” (such as sensors, tag RFID, actuators etc.) which can communicate and interact with each other within a shared IP addressing range, in order to share data and contribute to the management and development of advanced applications. Specifically, the thesis is focused on the design of a wearable sensors network based on RFID technology, and specifically on WISP sensors, for assuring the safety of the workers. In this network, wearable devices that can be inserted directly on the textile have been selected. Differently from conventional sensors, wearable sensors ensure a higher level of comfort, and provide higher electromagnetic performance. Furthermore, textile materials are easily available. Microstrips are good candidates for these applications because they mainly radiate perpendicularly to the planar structure, and their ground plane allows a good shielding on the body tissues. Therefore, I have designed specific antennas for RFID, that unlike the classical microstrip antennas have the radiating surface composed of several "side by side" conductive "threads of textile". Since the microwave model does not allow the design of an antenna with these characteristics with a good approximation, a specific microwave model for coupled lines has been designed. With this model, the specific antenna for RFID has been designed, with Jeans as substrate. The particular antenna's substrate allows direct integration into garments, but since the wearable antennas are placed very close to the human body, biological issues which may arise on the human body from the use of these sensors have been analysed. The Specific Absorption Rate (SAR) has been considered and simulations have been conducted for evaluating the effects on the human body, and especially on the head, when irradiated with the electromagnetic waves generated by the wearable antenna realized with different materials. Dosimetric effects have been evaluated in function of the distance from the body, in order to define a safe distance for placing the antenna on the human body. The SAR has been evaluated also for full patches with different textile substrates, whose surface is larger than that of the proposed model of coupled lines. Therefore, if the SAR values evaluated for

the full patch are satisfying, the SAR values for the model of coupled lines will surely be acceptable.

Introduction

Industrial contexts, and in particular the port areas, are very complex systems to be monitored and controlled due to the combined presence of vehicles and people. The port areas are the gateway between navigation and terrestrial transportation and are of great importance in transport logistics. Unfortunately, the management of port areas is quite complex because the safety of the workers must be always assured. Therefore, in such a context dominated by strict rules concerning the safety of people in industrial areas, a centralized control system for the monitoring and the prevention of risks is of particular importance.

Current studies are mostly focused on the designing of wireless sensor networks in open environment (and sometimes in urban environment), rather than dealing with the characteristics of a port service area (safety, architecture, logistics, interaction among different devices). Furthermore, many important topics concerning port areas are not properly covered, such as the integration with network technologies, the development and integration of sensors and actuators, and the distributed computing of data.

In this thesis, a real-time control system for the monitoring of people and vehicles in industrial areas is proposed. The proposed system is based on the Internet of Things paradigm, i.e. a network of “things” (such as sensors, tag RFID, actuators etc.) which can communicate and interact with each other within a shared IP addressing range, in order to share data and contribute to the management and development of advanced applications. The data collected by the proposed control system is managed in real-time by a web platform, with which it is possible to:

- monitor the position and the state of the workers and the means of transportation;
- verify whether the workers are wearing the mandatory safety clothing;
- avoid dangerous situations for workers;

Specifically, the thesis is focused on the design of a wearable sensors network based on RFID technology, and specifically on WISP sensors, for assuring the safety of the workers. In this network, wearable devices that can be inserted directly on the textile have been selected. Differently from conventional sensors, wearable sensors ensure a higher level of comfort, and provide higher electromagnetic performance. Furthermore, textile materials are easily available.

Microstrips are good candidates for these applications because they mainly radiate perpendicularly to the planar structure, and their ground plane allows a good shielding on the body

tissues. Therefore, I have designed specific antennas for RFID, that unlike the classical microstrip antennas have the radiating surface composed of several "side by side" conductive "threads of textile". Since the microwave model does not allow the design of an antenna with these characteristics with a good approximation, a specific microwave model for coupled lines has been designed. With this model, the specific antenna for RFID has been designed, with Jeans as substrate. The particular antenna's substrate allows direct integration into garments. The antenna is a rectangular patch and has been analysed in function of different sizes and materials; in fact, the size of the antenna varies in function of the material used.

The wearable sensors are placed very close to the human body, and are equipped with an antenna for transmitting wireless the acquired information by irradiating a transmission power. Therefore, in the last part of this thesis the possible biological issues which may arise on the human body from the use of these sensors have been analysed. The Specific Absorption Rate (SAR) has been considered and simulations have been conducted for evaluating the effects on the human body, and especially on the head, when irradiated with the electromagnetic waves generated by the wearable antenna. Dosimetric effects have been evaluated in function of the distance from the body, in order to define a safe distance for placing the antenna on the human body. The SAR has been evaluated also for full patches with different textile substrates, whose surface is larger than that of the model of coupled lines studied in Chapter 6. Therefore, if the SAR values evaluated for the full patch are satisfying, the SAR values for the model of coupled lines will surely be acceptable.

The rest of the thesis is structured as follows.

In Chapter 1, the role of industrial ports is presented. The economic importance of navigation and the main characteristics of port areas are described. Finally, the port service area of Cagliari is presented.

In Chapter 2, current ICT solutions implemented to guarantee the safety and to control the workers within the port area of Cagliari are reviewed and discussed.

In Chapter 3 the re-engineering of the processes is described. In order to improve the organization of the port service area of Cagliari and to provide solutions for its limited safety assurance system, a real-time monitoring system able to guarantee the safety of the workers within the port service area of Cagliari has been designed. Furthermore, the WebGIS portal that manages the data acquired by the system is presented.

In Chapter 4, the Internet Of Things (IoT) and the Wireless Sensor Networks (WSN) paradigms are discussed. Furthermore, the characteristic of Body Area Networks (BAN) are discussed.

In Chapter 5, the proposed wearable sensor network is presented. The main characteristics of the RFID and WISP sensors, which are chosen as nodes of the wearable sensors network, are discussed. Therefore, the proposed wearable sensors network and the control system are presented.

In Chapter 6, the design of specific wearable antennas for RFID is presented. Firstly, the design of a patch antenna composed of several "side by side" conductive "threads of textile" is presented. Then, the capacitance and inductance parameters of the antenna are calculated. Finally, since the microwave model does not allow the design of a wearable antenna with a good approximation, a specific microwave model for coupled lines has been designed.

In Chapter 7, experimental results are presented. Firstly, the geometry of the antenna under test is presented. Then, for validating the circuital model, a generic patch composed of the classic FR4 substrate has been studied. Since the multi-conductors model obtained good results, further tests have been conducted with the aim of verifying that such a model is also adaptable to a generic number of conductors connected in parallel. Once the model was validated, a wearable patch using the jeans as the substrate has been studied.

In Chapter 8, the possible biological issues which may arise on the human body from the use of the wearable sensors have been analysed. The Specific Absorption Rate (SAR) is introduced and simulations have been conducted for evaluating the effects on the human body, and especially on the head, of the wearable antenna realized with different materials.

Finally, in Chapter 9 the conclusions and future works are presented.

Chapter 1

Industrial port in Europe

Port areas are the gateway between navigation and terrestrial transportation. Port areas are of great importance for transportation of people and goods, and their management is quite complex because people's safety must always be assured. This thesis focuses on designing an advanced real-time monitoring system for assuring people's safety in a port service area, and especially in the port of Cagliari.

In this Chapter, the role of industrial ports is presented. In Section 1.1 the economic importance of navigation is described, whereas Section 1.2 presents the main characteristics of port areas. Finally, in Section 1.3 the port service area of Cagliari is presented.

1.1. Navigation

Navigation has always been a crucial factor of economic growth in Europe. Navigation services have given a strong contribution to the economy in Europe and to the European companies, so that they can be competitive worldwide. In fact, navigation, and consequently all the maritime companies related to that, are a big source of wealth and employment all over Europe. The 80% of worldwide trade is conducted by navigation, and in Europe short range navigation concerns the 40% of all goods transportation. In the past few years, the navigation transportation of goods has even increased.

In the EU the coastline is 90000 km long (divided into two oceans and four seas). Each state of the EU is responsible of its own coastline, and they are responsible for monitoring the coastline, assuring the safety in the ports and along the coastline, and protecting the coastal waters, the so called EEZs (Exclusive Economic Zone) and the continental platform, maritime infrastructures and maritime resources. With such a geography, the EU is a leader in navigation, which covers the 90%

of foreign trades and the 40% of the internal trades. Navigation trade has increased in the last 40 years by four times and it will again increase by three times within 2020.

With regard to Italy, the coastline is 8000 km long and this, of course, impacts the national economy. The maritime national cluster contribution to the national GDP (Gross Domestic Product) is about 2.7%, whereas the contribution to the transport field is about 11% and involves the 1% of the Italian employees (about 5000 employees in this field) [1]. The Italian cluster has a good level of cohesiveness and a good capacity to support a network of companies and trades, which are highly flexible.

In 2009 the EU Commission has identified the need of enhancing the maritime sector, by funding research projects in the Information and Communication Technology (ICT) field [2]. In order to guarantee an efficient management and monitoring system, it is necessary to base the projects on the existing regulation concerning the tasks of the Port Authority [3] and the procedures to be carried out in case of emergency.

The maritime safety is a matter of the SOLAS (International Convention for the Safety of Life at Sea [4]), whose amendments are maintained by the IMO (International Maritime Organization) [5]. The IMO deals with navigation safety (terroristic attacks, piracy) by promulgating rules with the aim of improving safety for ships, passengers and goods. Major focus is on preventing accidents during transportation, goods handling, and people's transportation. These principles are acknowledged in Italy too, in fact the Ministry of Transport and Infrastructure, along with several maritime associations, created in 2005 the National Technological Maritime Platform (PNTM) [6]. With regard to safety, the project MIELE (Mediterranean Interoperability E-services for Logistics and Environment sustainability) [7] is very important and it is based on the e-Maritime approach [8]. The PTNM proposed the RITMARE project [9].

Port areas are the gateway between navigation and terrestrial transportation. Port areas are of great importance in transport logistics and their management is quite complex because people's safety must always be assured. International researching projects do not deal with the possible issues concerning the monitoring of movements within the port service area, which would have the aim of improving the workers' safety. Many topics are not properly covered, such as the integration with network technologies, the development and integration of sensors and (semi) automatic actuators and the distributed computing of data, with the aim of enhancing the adaptability and the response of the system to the complex scenarios of the port service area. Considering the typical design and implementation difficulties in ICT infrastructures, normally the studies are focused more on designing wireless sensor and actuators networks in open environment (and sometimes in urban

environment), rather than dealing with the peculiarities of a port service area (safety, architecture, logistics, interaction among different devices).

1.2. The port

The port is a natural or artificial place on a coastline (sea or lake) where ships may take refuge from storms. Thanks to its premises, it allows to easily load and unload goods and to embark and disembark passengers.

There are several different types of ports, such as commercial-industrial ports, marinas, river ports, etc. I mainly focus on the commercial-industrial ports, which are usually equipped with several premises:

- external docks: in order to defend the port from the waves;
- internal docks and quays, whose purpose is to let ships dock and to ease loading and unloading of goods;
- lighthouses to reveal the port's presence;
- means of transportation (for instance cranes) to load goods on the ships or to set the ships down into the water;
- storehouses or service areas to store goods;
- terminals for ferries (where available);
- roads or railway to get to the port.

The ports have definitely complex infrastructures and the activities inside them are very complicated to be monitored because of the simultaneous presence of both people and vehicles which continuously move. There are many safety requirements to be satisfied in a port service area, and there is the need of advanced services and communication media. It is possible to make the port service area more efficient and safer by digitalizing and monitoring the processes and the movements of both people and vehicles. The technological evolution of the maritime cluster is currently considered as very interesting by the EU and its members. In general, the monitoring systems concerning the movements of vehicles and people do not deal with the specific characteristics of a port service area, but are mainly oriented to specific needs and applications, with the result that they seem small technologically advanced “isles”, not suitable to evolution and integration into new uses.

The ports are key nodes of great importance in the organization of transportation. They allow to improve the economy of the city where the port is located and this improvement in economy is linked to the possibility to increase the amount of goods and passengers which can be transported on ships. The increase can only be possible reinforcing the pair “transport-safety” and making a good use of the chances originating by the organizational, regulatory and technological context. At the same time, it is necessary to guarantee the safety of the port workers, who work in a complex and dangerous environment in which many accidents can happen, some of them even mortal. The port service area is on the third place of the most dangerous places to work in Italy, just after buildings and metallurgy. It is then necessary to find the best solutions to solve such issues in order to protect the workers and to guarantee them a decent quality of life.

Ports need to be equipped with the most modern and technological safety features, in compliance with the national and international regulation. Specifically in Sardinia, maritime transport has a primary role in the production system and for the economic development of Italy, thanks to the central position of Sardinia in the Mediterranean Sea.

Generally speaking, each port has its own characteristics, which make it difficult to find a broad common protocol about safety. In each port several subjects are involved with a multitude of different activities to be performed and for each of them (and the people involved) it is necessary to keep safety at all times and by all means. The safety’s project to be designed and implemented must involve the whole port service area and it is necessary to make a detailed analysis of risks. Parameters to check the “measure” of safety must be identified and they need to be used in order to prevent accidents and to define proper safety procedures. The safety policy has to base on these concepts: Planning, Putting in place, Checking and Correcting.

1.3. Port service area: the Port of Cagliari

The port service area in Cagliari is located at the centre of the Mediterranean Sea [10]; its geographic position has been strategic and optimal for trading since 2500 years. It was built by the Phoenicians, enlarged by Carthaginians and then increased by the Romans; it has constantly grown and improved. Nowadays, the Port Authority manages the activities in the Port of Cagliari and promotes the new developments in quality, integration and innovation.

The Port of Cagliari has the following purposes:

- commercial or historical port for conventional goods, liquid bulk cargo and roll-

- o on/roll-off ships;
- o industrial port, thanks to the new canal port, for the goods shipped in containers, to be used for transshipment and roll-on/roll-off;
- o industrial for the liquid bulk cargo, in the area of Assemini and Sarroch (Porto Foxi), where around 26 million tons are moved every year;
- o passengers port, in the historical port of Cagliari in Roma street (Molo Sanità, Calata S. Agostino, Molo Sabaudo, Calata Riva di Ponente);
- o fishing activity in the historical port (Pennello di S. Elmo, Calata Darsena and Calata Azuni);
- o touristic purpose as marina, in the historical port (Banchina Ichnusa, Molo Sabaudo, Calata Fiera and Pennello S. Elmo).

The new canal port makes it possible to efficiently use the large space and to increase the number of activities conducted in the port service area (transhipments, trades, passengers transportation, yachting and cruising).

Fig. 1.1 shows a revision map in which it can be seen that in the port of Cagliari the service area is divided in several sub-areas, and each of them is very specific and different from the others. Each sector (sub-area) needs to be covered by its own appropriate monitoring system with specific sensors, in order to ensure safety for both employees and other people who can be present there.

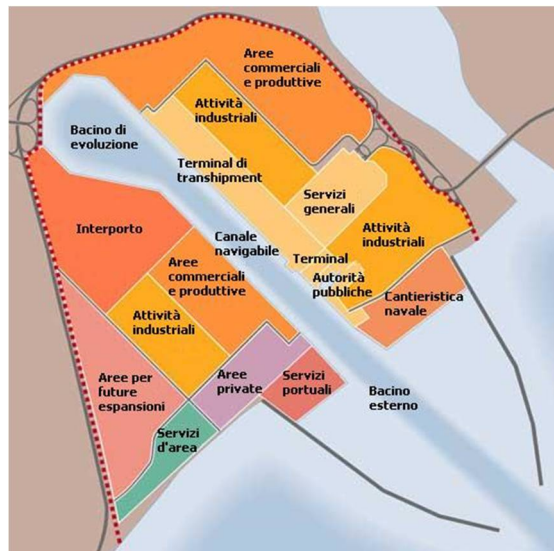


Fig. 1.1: Revision map: Source Port Authority Cagliari.

The problems related to the moving vehicles and people within the port of Cagliari were analysed, in order to design an efficient monitoring system able to provide a high level of safety and

an efficient emergency management protocol within this area. In fact, within the port area there is a huge traffic due to the movements of the workers and of the vehicles for handling goods. There are many different types of machines and vehicles in the port service area, which can be classified according to their use, their traffic flow and the reason why they are moved from one place to another.

Thanks to the Regione Sardegna's funds (tender 15 and 18), I could design an efficient real-time monitoring system able to provide an emergency management protocol which assures the safety in the port service area of Cagliari. A great role is played by the interchange of data among the Port Community, in fact the safety system must be able to provide an easy and automated way to share the data coming from the whole port service area. This becomes possible by using integrated ICT technologies (in compliance with high efficiency and reliability standards), which optimize the logistics inside the port areas both in normal and emergency situations. The system proposed is based on the Internet of Things (IoT) [11-12] paradigm, i.e. a network of "*things*" (such as sensors, tag RFID, actuators etc.) which can communicate and interact with each other within a shared IP addressing range, in order to share data and contribute to the management and development of advanced applications. The implementation of the IoT paradigm allows to increase the opportunities for business and the interoperability between systems, thanks to the innovative way to consider the interaction among people, places and things. The IoT can be used to constantly monitor movements in a port service area and to acquire data from the physical world; the *things* can share these data within their network and manipulate them in order to meet the necessary safety requirements. Monitoring systems, assisted driving, environmental monitoring and augmented maps are the main applications of the IoT in industrial scenarios.

In this thesis, an advanced real-time monitoring system is proposed, which aims at assuring the safety of people in a port service area by using multiple sensors and actuators which are able to communicate with each other. A web platform receives the data acquired in real-time, and it is able to:

- video monitor the port service area: the videos will be sent to a designated control centre;
 - put in place automatic and semi-automatic safety countermeasures, when necessary;
- design systems of augmented reality to display potential dangerous situations.

Chapter 2

Analysis of the processes

In this chapter, the current situation of the port of Cagliari is described. Current ICT solutions implemented to guarantee the safety and to control the workers within the port area are reviewed and discussed.

2.1. Current situation of the port of Cagliari

A port service area is a very complex reality. In order to allow each thing to work properly, everything has to be designed very carefully. Loading and unloading (of ships and containers) must work in a way that they do not cause any risk to the safety of the people nearby [13-15].

The port of Cagliari manages the loading and the unloading of containers with a system named Quay Cranes (QC). The containers are moved on authorized vehicles to a storage place and organized in ordered lines. The vehicles can be of two types: normal cranes or straddle carriers (SCs). Cagliari is the fourth most important commercial port in Italy, and it handles around 708000 TEU (Twenty-foot) containers per year, from more than 900 ships. The terminal is 400 thousand square meters wide, and the quay is 1520 meters long, with 7 gantry cranes and a moving crane; it has a storage capacity of 24000 TEU.

The port of Cagliari has already a communication network, which is managed by the CICT (Cagliari International Container Terminal) [16]. Fig. 2.1 illustrates the current network configuration in the CICT.

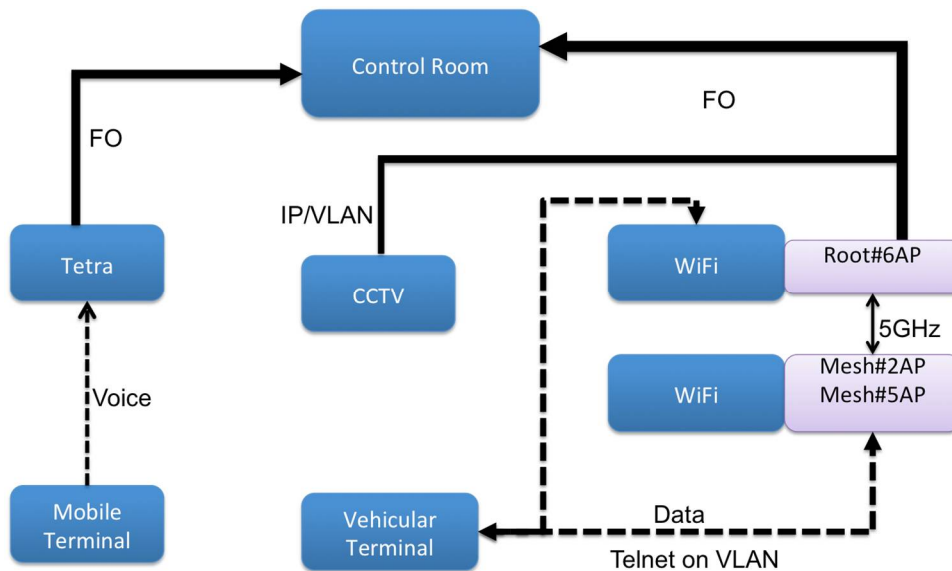


Fig. 2.1: Current network configuration in the Cagliari International Container Terminal

In the past few years the CICT has updated the Wi-Fi infrastructure by implementing a network composed of 13 Access Points (APs) based on the standard IEEE 802.11b/n, in order to cover the quay and the storage area. The APs are placed on different heights and places in the terminal area in order to cover the wide area of 1550x310 square meters:

- 6 APs on the perimeter of the area, 23m height, connected to the control service by Optical Fibre (OF 62.5/125 multimode);
- 2 APs along the quay, 14m height in MESH (5 GHz frequency);
- 5 APs on the quay cranes.

The Wi-Fi coverage is illustrated in Fig. 2.2.

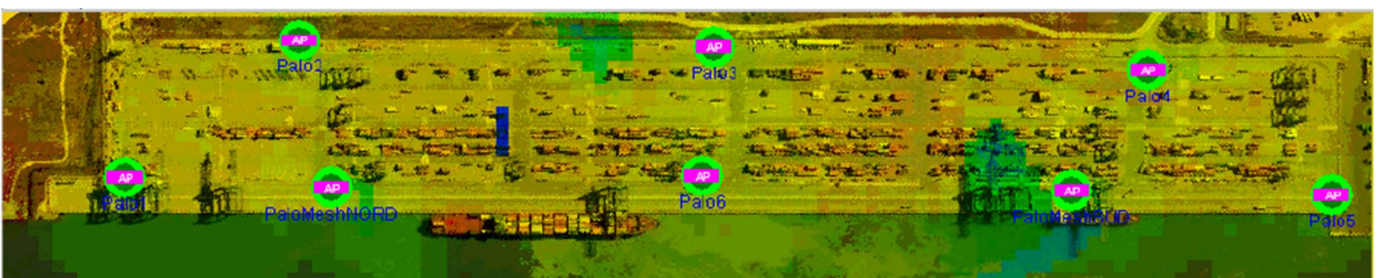


Fig. 2.2: WiFi coverage in the port of Cagliari.

The 23m high APs are in root mode and are cabled to the OF network along the quay and on the side of the internal enclosure. Each AP is linked to the central control point by an industrial switch, which is located in the operational building, by multimode OF 62.5/125. The 14m high APs along the quay have their antennas in Mesh Mode (5 GHz) and communicate with the Root APs in

POE (Power Over Ethernet) mode (standard IEEE 802.3af), which means that the power supply comes from the same RJ45 cable used to transfer data. The choice of having a POE Mesh network was made because this type of network can guarantee a wider coverage and permits to save costs, especially on the quay area, where the majority of activities are performed and major coverage and resilience are needed.

All the devices are RUCKUS, both the APs (Ruckus ZoneFlex 7762 Series) and the Wireless LAN controller (Ruckus ZoneDirector 1100), which manages all the APs. A new controller is going to be purchased for redundancy purposes, as the controller is the key factor in a Mesh network. In fact if the controller stops working, the whole Mesh network would stop working.

Together with the APs there is also a video surveillance system all along the perimeter of the area. The radio waves are sent back and forward through the TERrestrial Trunked RAdio (TETRA), [17-18] and it is possible to know the position of the authorized vehicles thanks to the embedded GPS systems in each vehicle. Each vehicle is equipped with a radio that uses TETRA, but a dedicated system to locate the worker is not available yet, as well as a system that allows to know whether the worker is fine and is using the proper and mandatory safety equipment.

The safety requirements of the whole port service area must be identified, and in particular those of the infrastructures, the loading and unloading processes, the workers and the vehicles. The movements of vehicles must be monitored both in real time and at specified time intervals. The legislation (both national and international) for such activities of monitoring must be considered. The proposed system allows to identify critical situations and anomalies, and for such cases automated or semi-automated procedures solve the issues and avoid risks.

Inside the port service area, many operations are continually performed in order to load and unload containers. Each vehicle has its own sensor network, which is controlled by the electronic control unit. The vehicle will be equipped with more sensors in order to have a unique sensor network which constantly evaluates the working parameters of the vehicle. Both vehicles and workers will be under control by the same control unit and therefore workers' safety will improve.

One or more sensors will be placed on several vehicles and on the worker's body. These sensor will get all the data related to the vehicle or the worker so that all their movements within the port service area can be monitored; the vehicle's maintenance parameters will also be monitored. In case of entrance in a forbidden area, excessing of speed limits, approaching of another vehicle or any other forbidden activity, all proper alarms will be activated. There are ongoing simulations of possible forbidden activities in order to check how the sensor would react to them.

The technical solution which has been chosen is based on a continuous exchange of data and information with the workers and especially with the maintenance area in order to highlight the practical needs and the existing operational protocols. The vehicle is periodically stopped due to mandatory maintenance port checks, in particular it is stopped every 500 hours, 1000 hours and 1500 hours of vehicle's use. The recording of using hours is done through the data sheets which are ad hoc data sheets provided by the workers of the Port Society. The problem is that they are often not up to date and they include errors; moreover, it is still a long and slow procedure to be carried on by hand. Therefore, the monitoring of the vehicles will be done by the GPS. With regard to the workers, once they have entered their working area their position is checked by the perimetral cameras only in the proximity of the loading and unloading areas; on the other hand, their moving from service area to their designated position is not monitored in any way.

In the current system I have noticed that:

- it is not possible to check whether the worker wears or not all the mandatory working clothes by using the available cameras;
- it would not be known, in case of fire or other sudden danger, the current position of all the people within the area;
- every worker can enter every service area, even without having the permission to enter; there are not barriers to prevent unauthorized access to the areas;
- the only available signal warnings (both acoustic and visual) are the ones that are activated when a Quay Crane moves, but there are not warnings when other vehicles start moving or when workers are in an area where vehicles are moving.

Starting from the points listed above, I have decided to make a re-engineering of the processes, in order to improve the organization of the port service area of Cagliari and to provide solutions for the described safety limits. The ICT technologies will help to improve safety in the area and avoid accidents in the port service area.

Chapter 3

Re-engineering of the processes

In this Chapter, the re-engineering of the processes is described. In order to improve the organization of the port service area of Cagliari and to provide solutions for its limited safety assurance system, an effective monitoring system able to guarantee a satisfying level of safety and emergency management has been designed. Section 3.1 describes the re-engineering of the port area whereas in Section 3.2 the pre-application analysis is discussed. Section 3.3 explains how information is exchanged within the network and Section 3.4 presents the WebGIS portal.

3.1. Port context: re-engineering

In the port areas, the management and transmission of the information have a significant role among the various participant of the Port Community. In fact, the safety system has the objective of automatically interchange the information on the basis of the data acquired by the control and monitoring system of the port area. This would be possible by expanding the existing port area technologies with ICT technologies that must have high standard of efficiency and reliability and must be able to optimize the management of logistics by making port procedures faster and cheaper. The proposed system is an integrated control and monitoring system that makes use of procedures aimed at scalability, flexibility, innovation, distributed data monitoring and quality of service. Furthermore, it is focused on interoperability and integration of communication networks (sensors, radio, telematics, etc.). In order to add these characteristics to the system, network infrastructure models (hybrid multihop mobile ad-hoc networks, vehicular networks, wireless sensor networks, etc.) and data processing models have been studied, which must consider transmission, sensing, safety and processing requirements as well as the available infrastructure resources.

The proposed system is focused on the functions of monitoring, preventing accidents and warning, with the aim of guaranteeing people safety through the utilization of sensors, actuators and heterogeneous communication channels able to communicate with each other. The objective is to implement a real-time information platform able to:

-
- monitor the means of transportation;
 - monitor the workers within the port area;
 - verify whether the workers are wearing safety clothing;
 - decide prevention measures and automatic and semi-automatic safety measures.

Movements of goods and people must be monitored in real-time or at constant time intervals, accounting for national and international safety laws and making possible an instant detection of critical and dangerous situations. The constant control allows to reduce the number of accidents because of the preventive alert sent by the system. In fact, the system has the capability to detect critical situations and working anomalies, making the solution instantaneous through automatic and/or semi-automatic procedures with the worker assistance. Current people and vehicular monitoring systems works independently from each other and do not account for port peculiarities but they are aimed at specific needs and applications.

In order to satisfy scalability and integration requirements, Service-Oriented Architecture (SOA) technologies have been considered. This choice is coherent with current management services in new generation networks and allows to implement different types of applications through the utilization of software with specific characteristic oriented at integration and reutilization.

Within the port area, loading and unloading operations are continually executed. The idea which is on the basis of the technology/safety union is to make use of the “objects” (i.e. the sensors) to create a controllable architecture. The research has been focused on people and means of transport to solve the critical points evaluated from the analysis of the current situation.

With regard to people, the research has been focused on the possibility of providing the workers with sensors capable of monitoring the interested area and of guaranteeing the highest safety levels by evaluating whether the worker is working lawfully (control whether he is wearing the mandatory clothes for protecting his safety). Furthermore, by meshing the information concerning the worker and the means of transport acquired by the sensors, the worker could be alerted in case of danger (e.g. whether he is too close to a moving vehicle) or in case of the malfunctioning of a means of transport.

With regard to the means of transport, they are provided with a sensor network controlled by an electronic control unit: the idea is to expand this system with other sensors to create a unique sensor network capable of evaluating the control parameters of the means of transport. For this reason, a dedicated system has been implemented, which automatically computes the hours of utilization of the means of transport, alerts whether the means of transport needs inspection, monitors the vehicles positions in the port area, and controls the parameters of the mains of

transport. This system has been implemented by installing an electronic board within the vehicle dashboard, which is powered through a 5V-1.5A cable at the vehicle ignition. Once powered, the board starts a data communication with the Remote Server. Precisely, the board is provided with a Wi-Fi dongle that sends the data to the Wi-Fi network of the port area. The Remote Server manages the received data through the WebGIS portal that is discussed in Section 3.4.

The proposed board is composed of:

- mother board: *Raspberry pi model B* (<http://www.raspberrypi.org>);
- accelerometer: *Xloborg* (<https://www.piborg.org>);
- GPS receiver: *NaviLock NL-464US* (<http://www.navilock.de>);
- Wi-Fi antenna: *TP-Link TL-WN722N* (<http://www.tp-link.it>);
- power supply: *12V to USB power converter*

The definition of a unique operative centre allows to continually control the workers and the means of transports and, as a consequence, the safety of the workers increases. The current scenario consists of a complex system of workers and means of transport that operate in the same port area. Many danger situations can occur when very heavy means of transport move in the same area where the workers are working.

The objective is to create a sensing network, defined by a distributed architecture, composed of different types of devices such as: electronic, hydraulic, electrical, and electrostatic. These devices must be able to acquire data from the environment, from the means of transport and from each person within the considered area. In order to reach these objectives, the port system has been divided in two subsystems:

- the port areas;
- the control room.

3.1.1. Port areas

The physical architecture of the port is nonlinear and there are some areas where there is not a constant number of people and means of transport. The port has some areas where only the means of transport are allowed to entry. On the other hand, there are some areas where only the workers are allowed to entry. The proposed system must distinguish among the permissions and the prohibitions that the people and the means of transport have to respect in the different areas. Each worker will be provided with specific permissions and sensors on the basis of his area of interest.

Workers movements will be controlled in order to continually know the position of each worker. Furthermore, in order to monitor the areas where the worker is allowed to entry and whether he is operative, each worker should be provided with a badge (with RFID technology) and with a control system which consists of the union of sensors embedded on the clothes with a GPS sensor. In this way, it is possible to better evaluate the current position of the worker and even to know whether the worker is wearing the mandatory safety clothes [19]. In addition, by analysing the data acquired by the wearable sensors, possible worker problems can be monitored; for instance, by equipping the safety helmet with a specific sensor it is possible to verify whether the helmet is on the floor or in the worker's head, and if necessary an alert can be sent to the control centre in order to promptly activate first aid procedures.

This architecture guarantees a safety increase but do not guarantee any prevention system. With regard to the prevention and the guarantee of the port area, each possible risk should be evaluated and a scalable control system able to increase the safety of the workers has to be defined. Because of the sea-land interaction, additional risks have to be considered i.e. those concerning the presence of other workers such as truck drivers, passengers, staff of the port company, staff of the public company with control rules, etc. One critical point is the risk of fall from the height due to the moving of containers in the air, which could fall down.

With regard to dangerous goods, giving correct information to the workers is fundamental. The workers must know the exact nature of the goods in order to use adequate instruments and equipment. Because of the possible set of problems that have to be integrated in the same centralized system for the safety, the adequate sensors and communication system to be used must be accurately evaluated. The specific characteristics of the sensors are presented in the next chapters, in function of the monitored parameters.

3.1.2. Control room

In the control room, the port areas can be displayed and controlled. In Fig. 3.1, an example of a control room architecture is shown. Generally, the control room is equipped with a workspace where a worker can monitor and control the workers and the means of transport in the port area. The worker can make use of video walls, PCs and radio stations. The user interface displays graphically the state of the sensors activated in the port area, as well as videos of the area (currently the port is equipped with video surveillance systems which mainly monitors the quay). The graphical and video services have the task to make the communication between the system and the

worker as intuitive as possible. The background of the graphical presentations is a digital geographic map of the port area of interest, where the workers can be monitored.

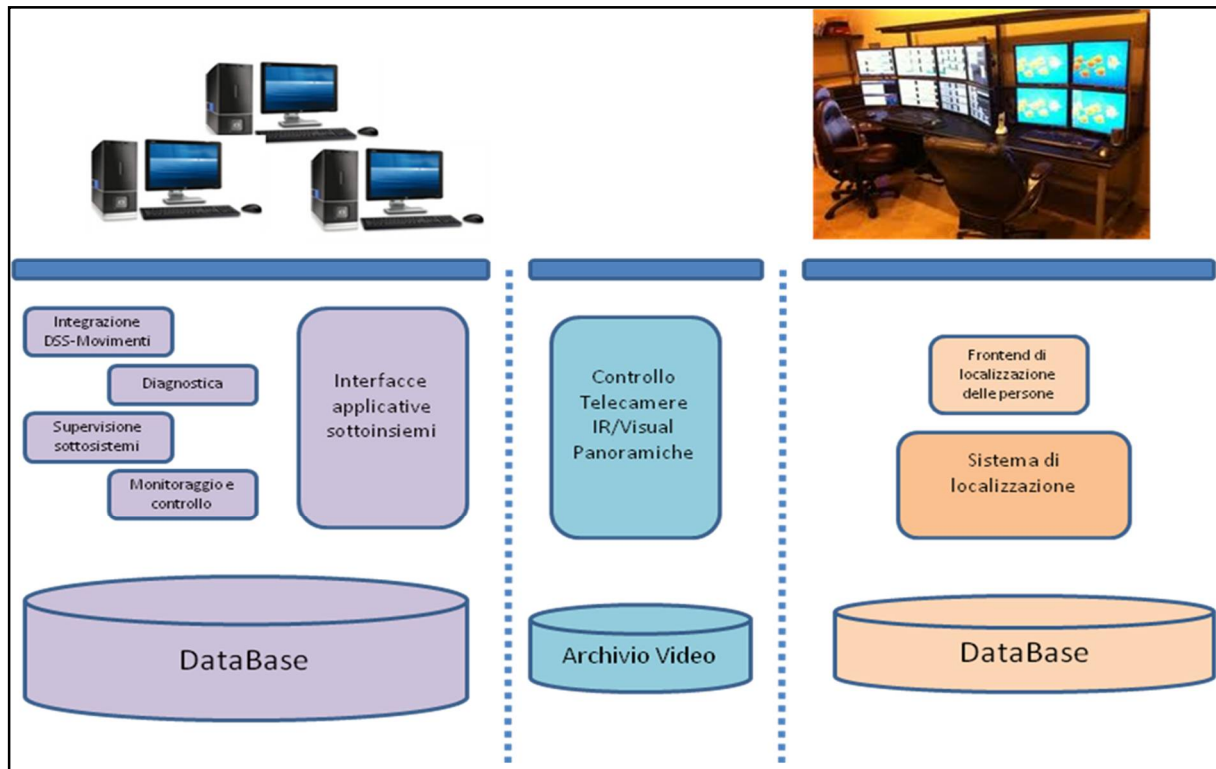


Fig. 3.1: Example of a control room architecture.

Servers, file archives, and network devices must be organized within the control room in order to guarantee the working of the network. Furthermore, statistical data must be collected concerning the controlled parameters and the anomalies, in order to distinguish critical situation from random operational problems. The monitoring and control interfaces places should be remotely reachable (by using Microsoft Remote Desktop software, VNC or similar TCP/IP client-server systems) by administrators and authorized workers. Furthermore, the system should be upgradable at any time to new security levels of the system and new monitoring and control functionalities.

The control room should be provided with a video wall for the displaying of high resolution images. In the video wall it should be possible to:

- display the people and the means of transport currently working within the port area;
- control the parameters of the means of transport in order to promptly react in case of alarms;
- control whether the workers are wearing the mandatory safety clothes.

3.2. Pre-application analysis

The proposed control and monitoring system will be mainly used by people responsible of security and maintenance for the following functions:

- monitoring of workers, equipment and vehicles within the port area;
- detection and warning of possible irregular and dangerous situations.

The information acquired by the system can be constant or real-time. The constant information are as follows:

- port planimetry including mobility indication;
- vital statistics of the workers;
- information about port equipment;
- threshold values for the monitored parameters.

On the other hand, the real-time information are as follows:

- activities conducted by the workers;
- GPS coordinates of equipment and means of transport;
- speed of mobile equipment and vehicles;
- information about the alarms and the equipment parameters monitored.

The application which has been studied for the people responsible of the safety allows to display on the planimetry the following information:

- map;
- list of workers;
- list of the equipment;
- list of external vehicles.

Fig. 3.2 shows a screenshot of the port planimetry displayed by the application.

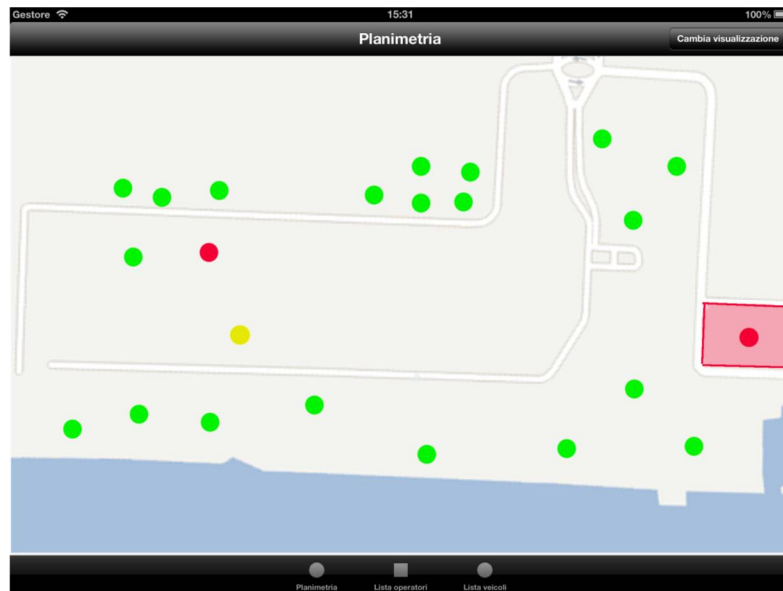


Fig. 3.2: Screenshot of the port planimetry.

In the planimetry it is possible to:

- control whether a worker enters into an area in which is not authorized to enter;
- open a screen with the worker details, the equipment details or the vehicle details.

Different types of port equipment (vehicle or buildings) are classified in different lists. The equipment can be selected from the list or by clicking on an equipment displayed on the map.

3.3. Information exchange

The server is connected with the control and coordination centre and records the information about the workers and the vehicles of the port area. A web service provides the information which must be updated in real time. When the application starts, and at regular time intervals, the web services send updated information about each worker and vehicle. Therefore, the position and the information of the workers and vehicles are updated in the map.

Information flows are exchanged between the server and the devices applications of the means of transport and of the workers. The server compares the recorded values with the threshold values and automatically send push communication to the control room in case of irregular situations. If a worker or a vehicle is in danger, an advise is sent to the video wall of the control room, where the worker or the vehicle of interest can be displayed.

3.4. WebGIS portal

The WebGIS portal [20], is a Geographic Information System (GIS) published on the web especially created for data management and displaying on the port cartography. It consists on cartographic services implemented on a web server that allow to interact with the cartography and its data through the web. The development of a support framework permits to integrate the information of the different systems. The framework is composed of:

- server: it consists of the physical server, the web server, and the database;
 - web server: implemented with Apache (XAMPP) and PHP;
 - database: PostgreSQL 9.1 integrated with PostGIS;
- control workstation: Acer Aspire AX3810 with Microsoft Windows 7.

The general working scheme of the framework is illustrated in Fig. 3.3.

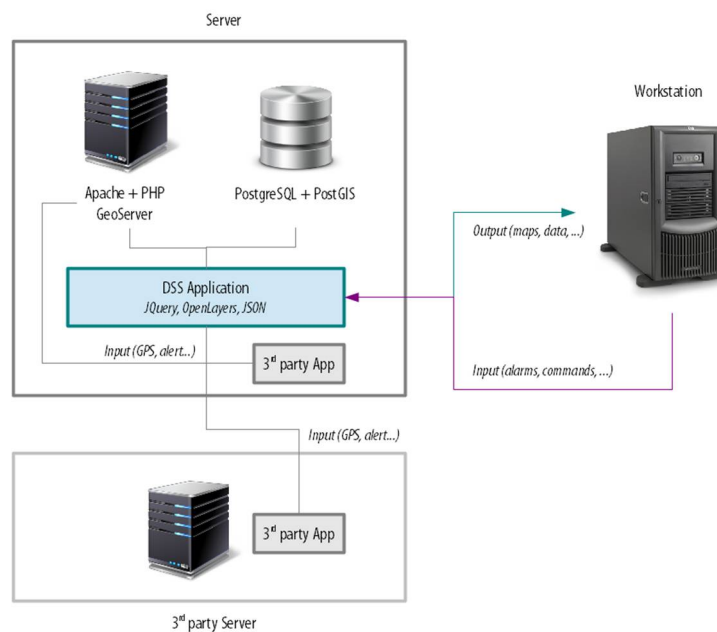


Fig. 3.3: WebGIS framework.

The relational database PostgreSQL has been chosen because it represents the best open source database in terms of reliability, data integrity and accuracy. With regard to the user interaction, the console is the main element on which the user-system interface is based. The console has been developed by using the CakePHP framework, which implements the Model-View-Controller (MVC) architectural pattern. The “page” has the main rule for the displaying of system

data, since it represents the user interface with which the user interacts with WebGIS. The general structure of the page is shown in Fig. 3.4.

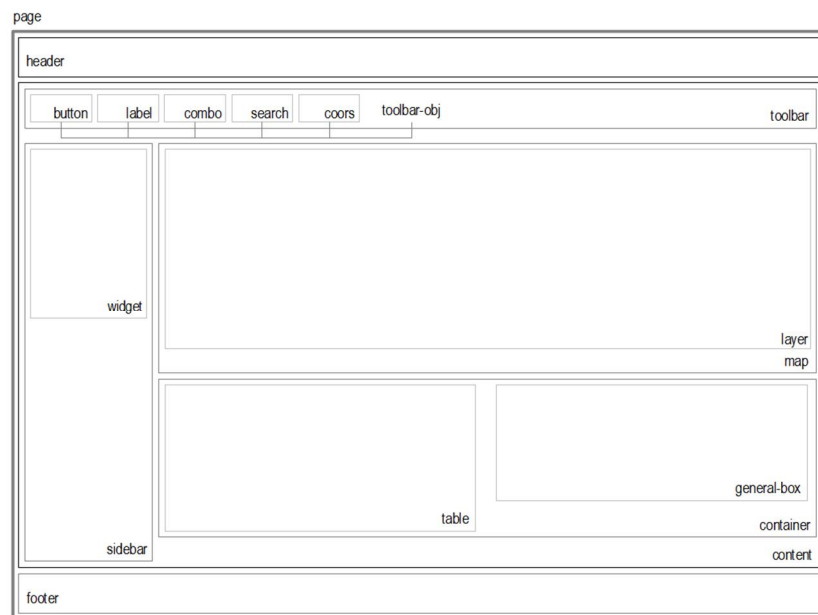


Fig. 3.4: Structure of the user interface for a single page.

The pages included in the system are defined into the view. Then, the pages for data representation are created. In Fig. 3.5 the Home Page is shown.



Fig. 3.5: Home Page.

The main elements of WebGIS are the maps, which are reachable by clicking the “Map” button placed on the home page. The WebGIS map is shown in Fig. 3.6.

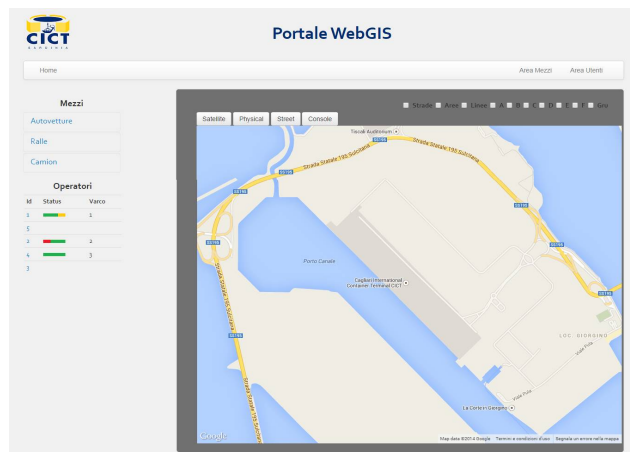


Fig. 3.6: WebGIS Maps.

The Map functions are:

- display the means of transport and their movements on the terminal container;
- display the workers on the terminal container;
- display the areas in which the terminal container can be divided.

The maps have been developed with the OpenLayers framework, which is an open source library completely written in JavaScript that allows to create maps also with different sources. Furthermore, it is displayable in any browser without dependency from the server side since it works on the client side. OpenLayers is not a map server web, but it simply provides the data requested by these, giving them back in form of layers. The layers form the base of the map and can be arbitrarily modified, placed side by side and in a variable number. In the application, the user can select among five layers:

- Google Satellite;
- Google Physical;
- Google Street;
- OpenStreetMap;
- Console Layer.

The first three are Google maps, available on the Google Maps API. OpenStreetMap is a project that makes cartographic data freely available without legal and technical limits. The whole world map is available and downloadable, and it can be also used offline unlike Google maps which are only available online. In Fig. 3.7 a map with OpenStreetMap is shown.

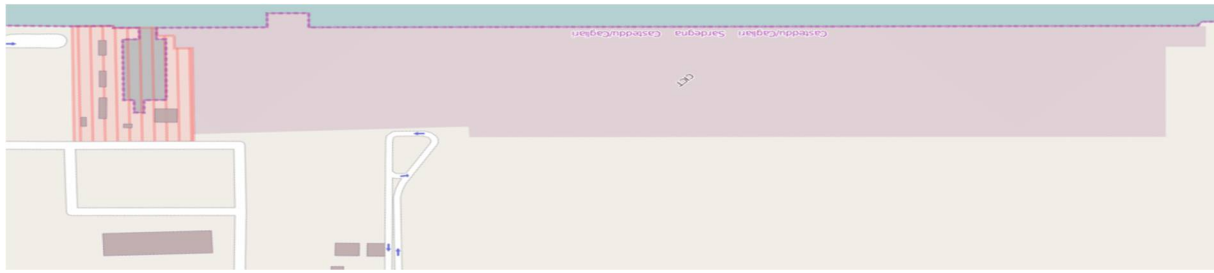


Fig. 3.7: Map with Open Street Map.

It is possible to select among the satellite map, the physical map, and the street map. Furthermore, it is possible to select the map in console mode.

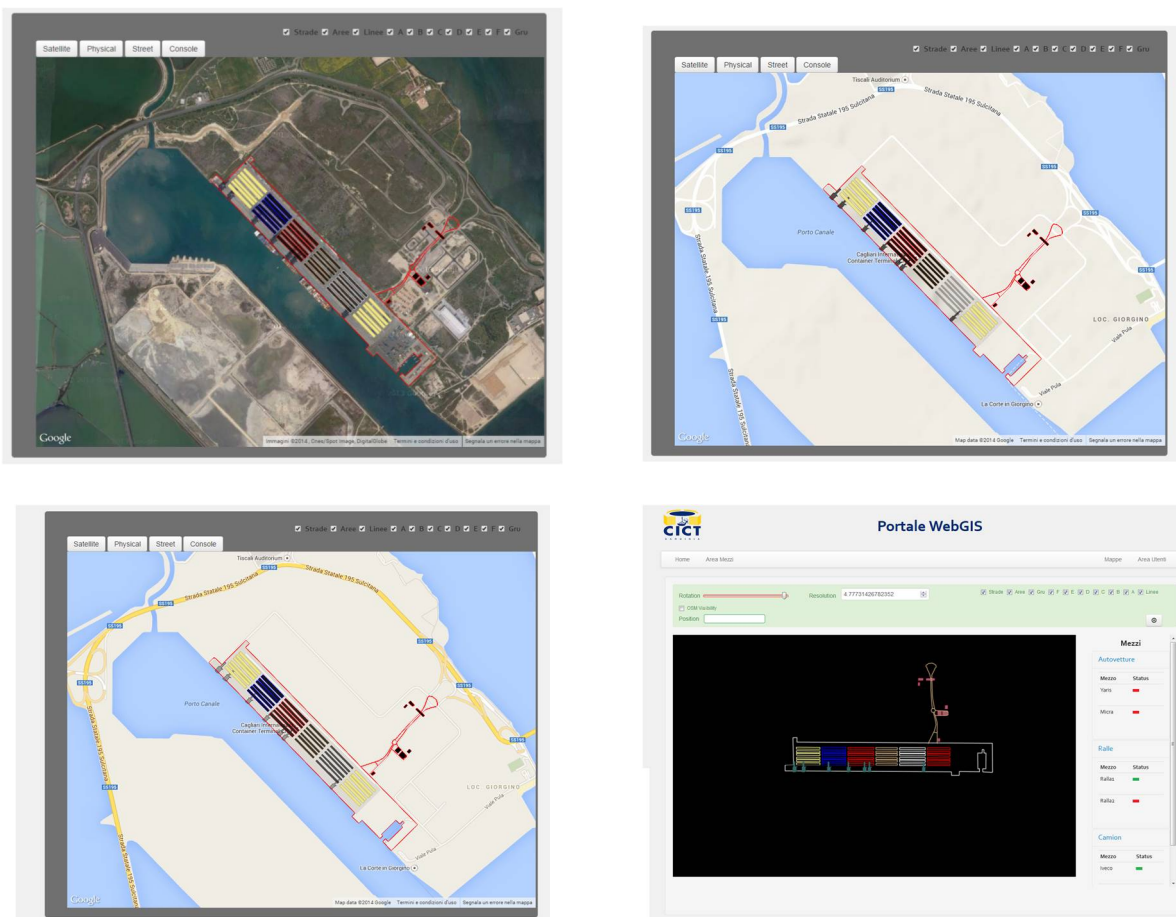


Fig. 3.8: Different layers.

The fourth map shown in Fig. 3.8 is the Console layer: it has a black background in which the shapefile of Porto Canale can be loaded. A zoom of this map is shown in Fig. 3.9

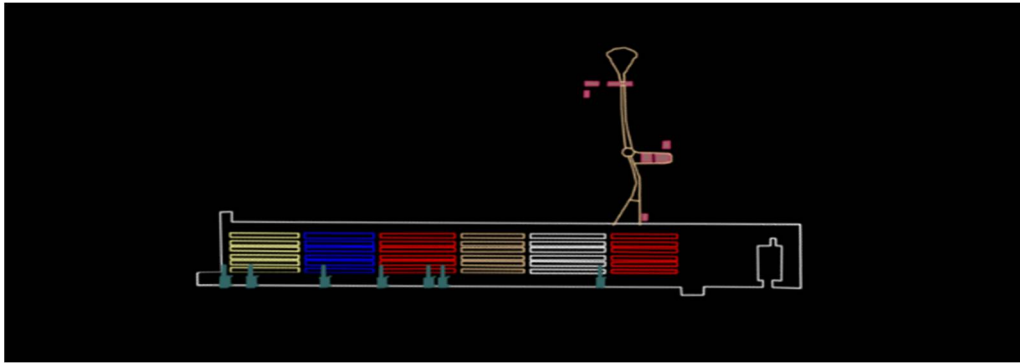


Fig. 3.9: Console Layer.

A very important function of the map is the possibility of inserting the markers. The markers are used to signal a desired position by using an icon. In the proposed system, markers with different type and colours have been used to identify workers and means of transport, in order to instantly identify the type of vehicle and whether they belong to the CICT or they come from the outside. The marker used for the workers is shown in Fig. 3.10.



Fig. 3.10: Workers Marker.

By clicking on the markers it is possible to obtain extra information about the workers and the means of transport.

Chapter 4

Wireless Sensor Network

In this Chapter, the Wireless Sensor Network (WSN) are presented. Section 4.1 introduces the Internet Of Things (IoT) paradigm, whereas in Section 4.2 the main characteristic of Wireless Sensor Networks (WSN) are presented. Finally, Section 4.3 discusses the characteristic of Body Area Networks (BAN), which are a particular type of WSN.

4.1. The Internet of Things

The massive spread of personal computer, cell phones, radio positioning systems and, more in general, all the electronic devices defined as “intelligent systems”, made technology and personal computers part of everyday life. Development was made possible thanks to the lower prices of both materials and components and to the capability and attitude to miniaturize these components. The spread was made possible also by the development of Telecommunications protocols and wireless systems, which permitted to design and realize complex communication architectures that allow to reach places which were not reachable yet, and to unbind the device from the physical location concept, giving the kick start to network mobility. For these reasons, in the past few years a new communication paradigm has emerged, i.e. the Internet of Things (IoT) [11-12]. The meaning of “Internet of Things” has a wide range, as it refers to a worldwide network of interconnected “things”, which communicate with each other using standard protocols and processes [21]. The key concept of the IoT is that *things* such as sensors, tag RFID, actuators, etc. can communicate and interact with each other using a definite IP range in order to share information and to support in the management and development of advanced applications. Implementing IoT allows new business opportunities to be pursued and more efficient operations, thanks to its innovative way to see interconnections among people, places and things.

The aim of the IoT is to build a dynamic scenario that will deeply change the way of interaction between users and things and especially the interaction with the surrounding

environment. The IoT will be the infrastructure by which all the nodes will share data and deliver complex services. The power of this paradigm is the strong impact that communication among “things” will have on people’s everyday life. Some examples are: in healthcare the device would be able to interact with the patient dosing medicines and sending alerts in case of need; in industry and trading processes, the transport of goods would improve and become more efficient, etc.

The National Intelligence Council [22] forecasts that “by 2025 Internet nodes may reside in everyday things – food packages, furniture, paper documents, and more”. The future of “things” will certainly be linked to the development of IoT technologies, and thanks to them there will be an improvement in life conditions and in the overall economic progress. There are still some open topics about the IoT, related to social and technological aspects, to be cleared before this paradigm can be fully accepted worldwide. Studies are currently focused on the possible connections among the devices, giving them higher computing capabilities in order to be able to automatically adapt to the surrounding environment with tight constraints on safety and privacy matters.

There are two main technological components of IoT applications:

- Identification and communication technologies:
 - Radio-Frequency Identification tags: a RFID is basically a microchip equipped with an antenna which has a unique identifier associated to a “thing”. RFIDs are a major component in implementing communication among “things”; they have one or more tag readers and can read one or more tags; it is possible to receive and send data about the “thing” using the tag readers on the RFID. RFIDs are not the only ones used in the IoT, but there are also the Near Field Communication (NFC), the WISP (Wireless Identification Sensing Platform [23]), and many others;
- Wireless Sensor Networks: a WSN is a network composed of a cluster of nodes which communicate with each other using wireless technology and multi-hop mode. RFID systems can be integrated into WSNs in order to check the status of the “things”, their position, their temperature, etc., and in order to transmit data concerning the “things”. RFID technology is surely the most appropriate technology for this purpose, thanks especially to its low cost.
- Middleware: it is the software layer between the communication layer and the application layer. This layer is very important in the IoT, because it allows to simplify the implementation of new services and to integrate different technologies at the network layer and the application layer. The architecture is SOA (Service

Oriented Architecture) [24-25], which allows to decompose complex systems into smaller and well defined subcomponents.

The integration of the IoT with RFID tags allows to monitor in real time every single “thing”, animal or person which is equipped with a tag, even when they are not in view. A network can be developed in order to reach the tag wherever it is located and at every time, thanks to the sensors and to their capability to communicate with each other in multi-hop mode. So far, RFIDs have been mainly used for the monitoring of goods or to verify the presence or the absence of people in a specific place (for instance, a worker would use his badge equipped with RFID to announce his presence at work). The idea has then been extended to the safety of workers who work in industrial environment, in which monitoring is rather complex. RFID tags are very simple to implement and cheap. Many different tags (with different size and for different purposes) are already and easily available. The most common are, for example, workers’ badges, adhesive tags on goods or label tags used usually for animals. Safety in work environment is surely a very important matter, and monitoring in industrial environment can be very complicated because of the high costs and because of the complexity of the different environments. Therefore, the utilization of RFID tags in these scenarios can help ensuring the safety of the workers. RFID are further discussed in Chapter 5.

4.2. Wireless Sensor Networks

Wireless Sensor Networks are networks composed of several autonomous electronic devices capable to achieve data from the surrounding environment and to communicate and exchange these data with each other. The network can be depicted as a cluster of interconnected nodes that send the acquired data to a centralized data collector centre named gateway; the gateway is the point of conjunction between the network and the data elaboration centre. In Fig. 4.1 is shown an example of a WSN.

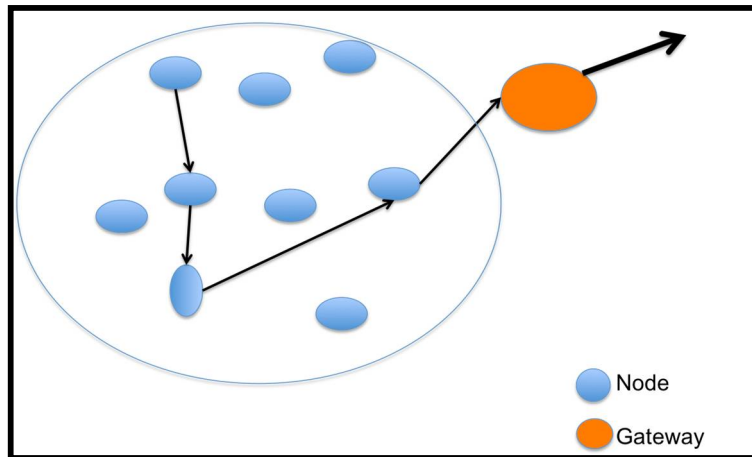


Fig.4.1: WSN example.

Each wireless sensor is equipped with a microcontroller that has little computational capabilities, a radio chip for communicating with other nodes, a power supply unit and one or more sensor for acquiring environmental data. Basically, each sensor is composed of one or more transducers, which are connected to blocks of A/D converters: analogical signals coming from the transducer are digitalized and sent as input to the microcontroller. The microcontroller allows the nodes to communicate with each other and provides the nodes with computing capabilities. The power unit must be composed of power scavenging modules, for instance solar cells and/or batteries, as the sensor nodes are often located in impervious areas, and the operations of each node depend on the power supply.

WSNs are very little invasive, thanks to the dimensions of the nodes and to the fact that not cabling is needed, so their installation is very easy, especially in those cases when installing complex networks is not possible. The sensor nodes are essentially static devices, which means that they are not moved or relocated. Nevertheless, WSNs are not immune to the problem of defining optimal topology and defining routing protocols which could guarantee reliability even in case of changes on the topology.

WSNs are dependent on energy (they could turn off if their battery is low) and are highly scalable [26], and ready for new nodes insertion, which leads to a consequent change in topology. They can be programmed in order to be able to self-redesign themselves in different network topologies as follows:

- Star topology: there is a central node (star centre) which has control and coordination functionalities over the whole network and among network's nodes. This is the easiest topology, it makes it possible to use simple routing protocols; it is useful in case of a network with a central node, which requires high power supply, and several

secondary nodes with little power supply needs. Usually, the star centre can also work as bridge towards other connection systems;

- Mesh or peer-to-peer network: there is not a central control-function element, but all the nodes are identical and have the same functions; they can interconnect to each other. This topology is more efficient and reliable than the previous one, as it allows redundancy to be implemented, but it also needs more complex routing algorithms;
- Tree topology: it is composed of clusters of nodes and each cluster has a central node with controlling functions. The advantage of this topology is that the number of possible paths to reach each node is reduced to the minimum, leading to less complex managing systems.

Network topologies are illustrated in Fig. 4.2.

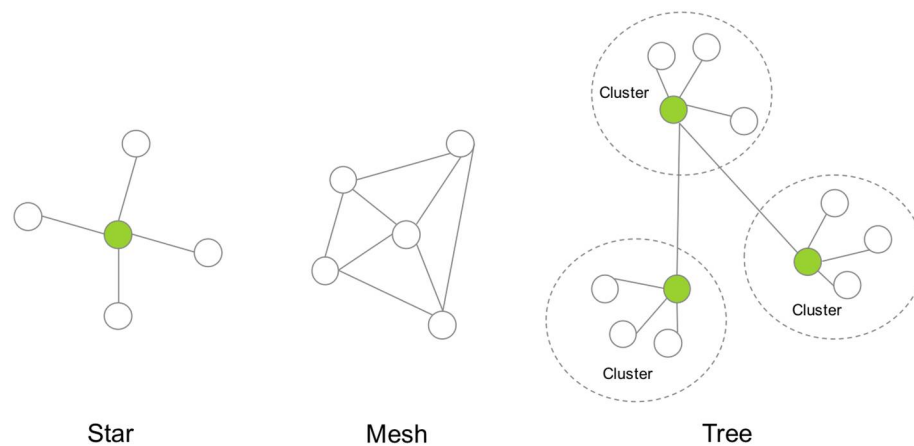


Fig.4.2: WSN network topologies.

The design of a WSN needs the evaluation of several different technological features which can lead the designer towards a choice among all the available technologies. Here are some examples:

- Fault tolerance: the network must be able to go on working although one or more nodes stop working. The sensor nodes can stop working, for instance, because of a lack in power supply, but it is mandatory that the no-working elements do not affect the functioning of the entire network. When designing a WSN it is necessary to implement the desired tolerance with the right algorithms. These algorithms need to be reliable in the specific context of application of the network;
- Scalability: the number of sensor nodes in the area covered by the network is highly variable and it depends on the specific application the network is intended to. It is quite normal to have an average of 20 devices in 1 m². Such a quite high density is to

be taken into account while designing the network, in order to guarantee its correct functioning and avoid interference among the sensors. Moreover, the position and the function of the nodes can change in time;

- Production costs: the cost of each device must be low. In fact, if the cost of the nodes was more than the cost of a normal cabled network, there would be no advantage in implementing a WSN;
- Operational environments: the network sensors can be used in highly inhospitable environments, such as battlefields, or in places with too high temperature or pressure. This is why the design and the choice of the sensors is tightly bound to the places where they are to be used. It is very important to choose the right package for the sensors, in order to protect them from severe high temperatures or pressure or vibrations and so on, depending on where they are to be used, with obvious fulfilment of the requirements described above.

A WSN can be used for several different purposes, for instance: data collecting, monitoring and more, in a range of different uses:

- Environmental use: in order to survey for wild fires and to test air in proximity of industrial plants;
- Home Automation (Domotic) use: in order to make a connection between the environment and humans and to adapt the environment to humans' needs automatically;
- Medical use: in order to monitor constantly patients' vital signs and to automatically dose medicines.

Sensor networks can be implemented with different types of sensors, with the aim to monitor several environmental features: temperature, moisture, movements, lighting conditions, pressure, noise, presence or absence of specific objects, mechanical stress, speed, direction and size of objects. The major goal of a sensor network is to spread the data collected by each node. A sensor could be used in different ways: it is possible to periodically interrogate the sensor in order to have a continuous flow of information, or to use it only when a defined condition happens, or even to have a mix of these two, i.e. periodically checking a specific variable, so that if a threshold is exceeded, the sensor would send a warning message to the controller.

WSNs belong to the Low Rate Wireless Personal Area Networks (LR-WPAN), which are small networks which transmit at low transfer rates. In WSNs, many application fields require low kbps transfer, therefore the primary goals when designing them are cost saving and power consumption. In Fig.4.3, LR-WPANs are classified on the basis of the network coverage area: WAN (Wide Area Network), MAN (Metropolitan Area Network), LAN (Local Area Network),

PAN (Personal Area Network), and BAN (Body Area Network). This type of classification is normally used for cabled networks, but it can also be extended to include different types of wireless networks, with small error induced by the fast and continuous growth and progress of wireless technology.

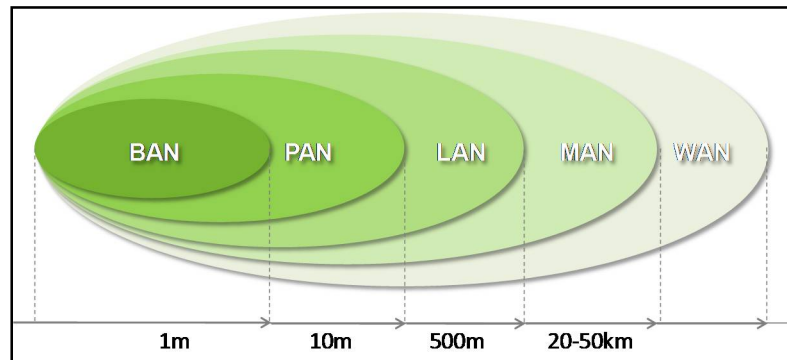


Fig.4.3: LR-WPAN classification: coverage area.

The great part of current available sensors are based on IEEE 802.15.4 [27]. This standard defines the physical layer and MAC address for low power and low bit-rate wireless applications on WPAN [28]. In order to extend the coverage on a larger area (metropolitan services with middle-to-long range networks), the WSNs are integrated with radio/wireless transport infrastructures, which are complementary to the 802.15.4 standard, such as 802.11 [29], 802.16 [30], UMTS [31] and satellite networks. A new committee (IEEE 802.15) is born specifically for PANs, which cover distances up to 10m; the committee has defined three different types of WPAN, depending on their data rate, power consumption and QoS:

- High data rate WPANs: they are described in IEEE 802.15.3 standard and include technologies developed for multimedia application which need high QoS (WiMedia and Bluetooth2);
- Medium data rate WPANs: they are described in IEEE 801.15.1 (Bluetooth) standard and are designed for electronic devices, such as mobile/smartphone technology and Personal Digital Assistant (PDA);
- Low data rate WPANs: they are the LR-WPAN, described in IEEE 802.15.4 standard and ZigBee; these are intended for low power consumption networks and low cost networks since they cannot be implemented with other WPAN technology; sensor networks belong to this group. IEEE 802.15.4 does not compete with already existing wireless technologies, but its aim is to integrate the available low rate wireless application range.

When designing a WSN it is necessary to take into account the same functional requirements as for every kind of network, i.e. for instance cover range, security, power consumption, and other which are to be customized for the specific network, i.e. for instance network size, transmission speed. To get a good design of the network, it is necessary to analyse the differences between WSNs and traditional networks, such as:

- it is necessary to provide an auto configuration mode, as per the IEEE 1451 standard [32];
- the user should be able to enter each device in order to check the construction settings in detail and should also be able to change the settings in order to calibrate them adequately to the purpose for which the device is to be used;
- each node must be identifiable in the network;
- the information acquired from the sensors must be collected in a synchronous way; it is necessary to have a time stamp saying when a datum was collected; in a sensor network a strong mechanism of synchronization is mandatory and it has to be more timely deterministic than a classic computer network.

These are all reasons why, to design a WSN, specific network designing tools and procedures are needed. There are many examples of protocols and algorithms to be used in order to design and implement ad hoc wireless networks (i.e. networks where a central coordinator is not needed and where each node works both as a node and as a router), but none of these protocol is perfectly suitable for WSNs, because of the specific features of this kind of networks.

In order to better show these features, here is a list of the most tight requirements of a WSN:

- the number of sensor nodes can be higher (some orders of magnitude) than an ad hoc network;
- the sensors are positioned very closed to each other (high spatial density, i.e. dozens or hundreds of sensors in few meters);
- some nodes could stop working or could not work properly, but they must not influence the behaviour of the entire network;
- the topology of the network can change quite frequently;
- the sensors normally send data in broadcast;
- the sensors have tight power constraint, as the power supply (batteries) cannot be frequently replaced.

The list above shows that, to adequately design a WSN, it is necessary to find the best compromise between performance and duration of the batteries. Multi hop strategies can be the optimal way to achieve high efficiency in routing and low transmission power, and they could avoid

the problems which might arise from the high spatial density of the sensors. Furthermore, multi hop strategies can help to mitigate the problem of power requirement, which is one of the most tight requirements in designing such networks.

4.3. Body Area Network (BAN)

In order to define a real-time control system able to constantly monitor the safety conditions of the workers by using wearable sensors, I focused on the study of Body Area Networks (BAN) [33-35]. The BAN is defined by the IEEE 802.15 as a "*communication standard optimized for low power devices and operation on, in or around the human body to serve a variety of applications including medical, consumer electronics/personal entertainment and others*" [28].

Some common use cases for BAN are: Body Sensor Networks (BSN), Monitoring, Mobile Device Integration, Personal Video Devices. Sensors and actuators are the key components of BANs used for calculating and for data transfer to a central unit via wireless links. The BSNs are composed of little devices placed on the human body that can provide information about people health state, and the way people move and interact with the environment. Such devices are generally composed of a radio interface for data wireless communication and a little microprocessor capable of implementing the communication protocol and of calculating part of data.

It is possible to basically distinguish among three devices:

- sensor node: device that collects and calculates the needed information and, if necessary, sends this information via wireless;
- actuator node: device that operates accordingly with the data received from the sensors or because of the user interaction;
- Personal Device (PD): device that collects data from the network sensor and transmits to an analysis engine or a data visualisation system. The components are the battery, a processor more powerful than that of sensors and actuators, the memory and the transmitter receiver. This device is also known as Body Control Unit (BCU). Frequently, the BCU is a smartphone, a PDA or a local PC.

In order to decide the best strategy to define an architecture able to guarantee the maximum safety for the workers, the equipment for personal safety of the workers in industrial environment have been studied. Precisely, the workers have to wear clothes in compliance with safety rules. Such clothes have been designed to protect the worker body from a possible accident, and must be appropriately worn, respecting strict rules.

In the port area of Cagliari, the workers have to wear:

-
- safety helmet (there are two different types of safety helmet to be worn, which depends on the area where the worker works);
 - safety jacket;
 - safety shoes.

The BAN Sensors Network for Workplace Safety Management is shown in Fig. 4.4.

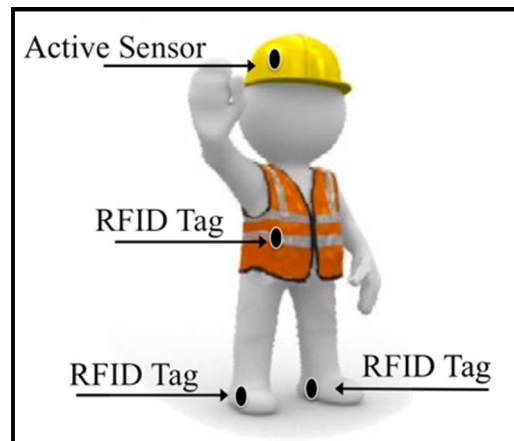


Fig. 4.4: BAN Sensors Network for Workplace Safety Management.

The safety helmet is provided with an active sensor, while the safety jacket and the safety shoes are provided with RFID tags. Technical specifications of these devices will be discussed in Chapter 5.

The real time monitoring of these safety devices requires the utilization of advanced sensor systems and communication techniques. The sensors must be able to signal, in addition to the PD presence, also useful data for the safety such as temperature and sensor orientation, in order to verify its correct working.

The main requirements of the monitoring through the PD are the wearability of the sensors connected to the safety device, the sensors size, and the battery duration. During the study, different wireless standards have been evaluated, as: Bluetooth Low energy (BLE), ZigBee, ANT, NFC and RFID [36-39].

Table 4.1 compares these wireless technologies for BANs.

TABLE 4.1 Wireless technologies for BAN systems

| Wireless technology | Bluetooth low energy | ZigBee | ANT | NFC | RFID (passive) |
|------------------------------------|----------------------|------------|---------------|---------------|----------------|
| Power supply duration | Some years | Some years | Some months | Some months | Unlimited |
| Max number of connection nodes | Not available | 64000 | Unlimited | Not available | Unlimited |
| Max Operative distance (m) | 50 | 70/100 | 7/30 | 0.2 | 4/10 |
| Max Data communication rate (Mbps) | 1 | 0.25 | 1 | 0.424 | 0.1/1 |
| Transmission current (mA) | < 15 | 35 | Not available | < 15 (reader) | > 20 (reader) |
| Battery | Yes | Yes | Yes | Not always | No |

Based on the comparison in Table 4.1, I considered NFC technologies and RFID with passive sensor tags as the most viable alternatives, due to the fact that they do not require a power source for the sensors but only for the central unit. The final choice to use RFID over NFC was motivated by the reduced range of the latter technology, unsuitable for an industrial environment. Although ZigBee and Bluetooth-LE are both low-cost and low-power technologies, flexible and small enough to meet the needed constraints, they were discarded for the necessity of having a power source.

Chapter 5

Wearable Sensor Network

In this Chapter the proposed wearable sensor network is presented. Section 5.1 discusses the main characteristics of the sensors chosen for the network, the RFID. Section 5.2 presents a particular class of RFID that makes use of the passive tag capabilities combined with computation capabilities: the Wireless Identification and Sensing Platform (WISP). In Section 5.3 the proposed wearable sensor network is presented, whereas Section 5.4 discusses the control system.

5.1. RFID

RFID (Radio Frequency IDentification) is a wireless technology used for data reception and remote data storage. It is mainly composed of three elements:

- the tag or transponder that, placed on the object to identify, is the real data support on the system and it is composed of a microchip for data storage and an antenna;
- the reader that, communicating with the tag, reads or writes the data into the memory, and is composed of a radiofrequency module (TX and RX), a control unit and antennas for the transponder;
- data processing system (for example, a PC).

RFID systems can be classified on the basis of:

- working frequency;
- working range (max applicability distance);
- type of physical coupling.

RFID technology works in different frequency bands, as shown in Table 5.1:

TABLE 5.1 RFID characteristic

| <i>Frequenza</i> | <i>Working field</i> | <i>Type of Tag</i> | <i>Max working distance in open space (m)</i> |
|------------------|----------------------|--------------------|---|
| LF 135 kHz | Near field | Passive-Inductive | 0.5 |
| HF 13.56 MHz | Near field | Passive-Inductive | 3 |
| UHF 869 MHz | Near and far field | Passive or active | 9 |
| MW 2.4 GHz | Far field | Passive or active | 15 |
| MW 5.8 GHz | Far field | Passive or active | 20 |

The wavelengths in the microwave (MW) range are largely absorbed by the human body, causing severe limitations in BAN scenarios. This made us take into consideration only the lower frequencies for the purpose of the present research activities. Among these frequencies, I opted for the UHF systems [40-42], taking into consideration the low data rate provided by the LF systems and the limited range of both LF and HF systems and the fact that the system will be operated mainly outdoors.

There are mainly three type of RFID tags: passive, semi-passive, and active.

- **Passive:** the radiofrequency wave generated from the reader is used as energy source for powering the circuit and for data transmission. The maximum working distance is 4-5 meters, due to the fast power attenuation and to the not very high power transmission that can be used. In fact, current regulations prohibit to produce high power electromagnetic fields in the UHF range;
- **Semi-Passive:** have built-in battery then do not need energy derived from the reader to power the integrated circuit. For this reason, the working distance is longer (up to 15 meters) although lower power levels are used. The working distance in this case is limited due to the integrated transmitter that does not make use of the reader field for data transmission;
- **Active:** are self-powered by a battery and are provided with an active transmitter. They transmit autonomously the information then can cover higher working distance.

Although the active and semi-passive tags can cover high working distances, they have more disadvantages in terms of higher costs, reliability and environmental impact. Then, in the RFID systems the passive tags are the most used.

5.2. Wireless Identification and Sensing Platform (WISP)

Among the various RFID systems in commerce, a very interesting alternative for the developing of the project are the WISP. The WISP [43-44] are passive sensors (battery-free) equipped with a microprocessor that provides detection and computation features to the tag. Being a passive tag, it is powered and read by a RFID reader (which can be static or mobile) from which it absorbs the needed power for communicating with the reader. It works at the UHF American standard (915 MHz). In Fig. 5.1 a WISP sensor is shown.

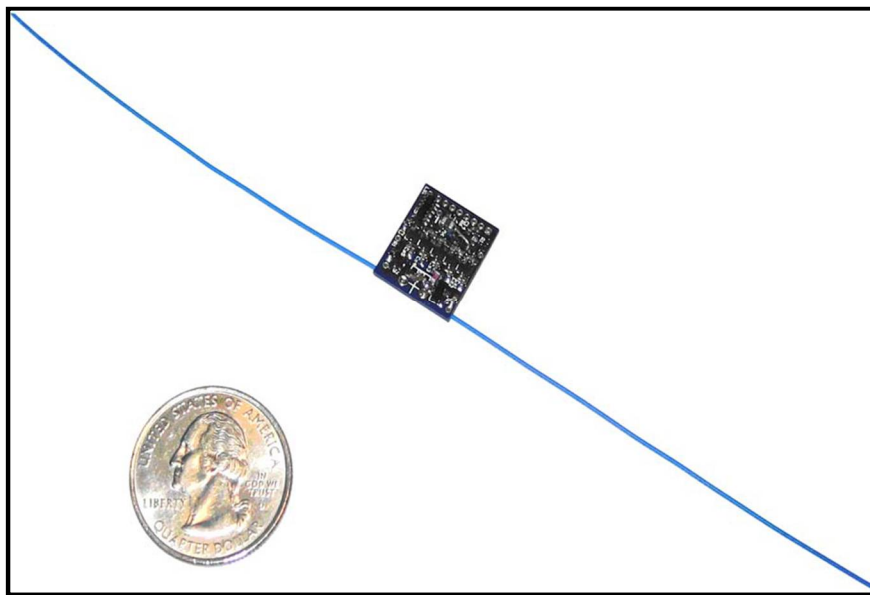


Fig. 5.1: WISP example.

The idea on the basis of the WISP is the development of a device equipped with sensors that, when asked by a reader, instantaneously measures physical quantities through the sensors and returns these measures and the identification. The WISP is not equipped with a battery but it is powered by the energy coming from the reader through the back-scattering phenomenon. Precisely, the WISP is a 16-bit-general-purpose microcontroller developed by Intel and the Washington University. Similarly to the RFID, the WISP is a passive sensor, but, in addition, it supports also sensorial and computing functions since it is equipped with a microprocessor. The device can be read and powered by the radio signal of a common UHF RFID. Commonly, it is used in conjunction with sensors of light, temperature, acceleration, and voltage. Furthermore, it is frequently used to develop embedded safety applications.

The WISP is readable through EPC (Electronic Product Code) protocols, managed by EPCGlobal, but rather than transmit only a static identification, it is able to:

- analyse sensors and return their values;
- write on flash memories;
- compute cryptographic calculations.

The energy received by the passive tag is collected and used to power the 16-bit microcontroller. The EPC Class 1 Generation1 and Class 1 Generation2 are two standard highly accepted for this technology, and work at frequencies considered in our project, i.e. UHF.

The WISP is an electronic card composed of:

- modulator;
- demodulator;
- microcontrollers;
- external sensors;
- other components such as EEPROM and LED.

Such sensor has been tested in industrial environment and resulted in compliance with the project. Fig. 5.2 shows the WISP circuit.

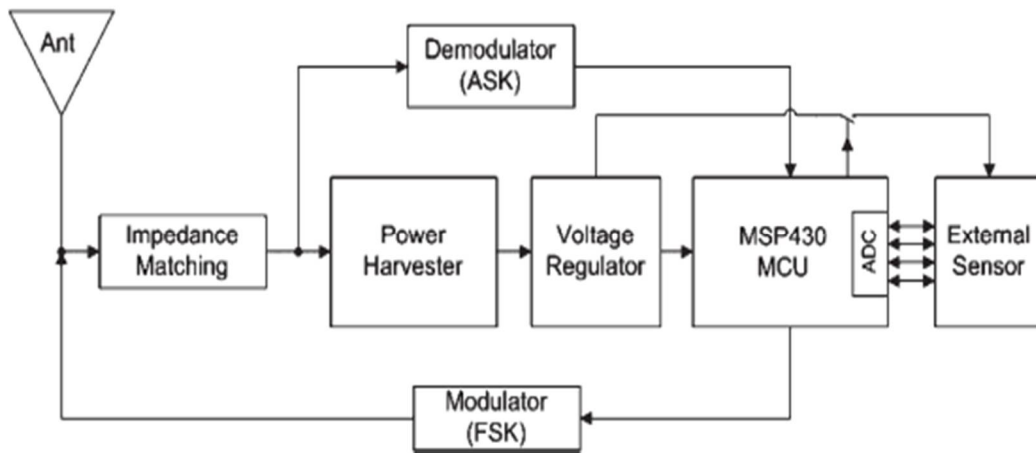


Fig. 5.2: Wisp circuit.

5.3. Wearable sensors network

The proposed wearable sensors network is a network of wearable sensors appropriately placed in the worker's clothes [45]. The sensors, as previously said, are passive sensors that receive the needed energy for working by their reader.

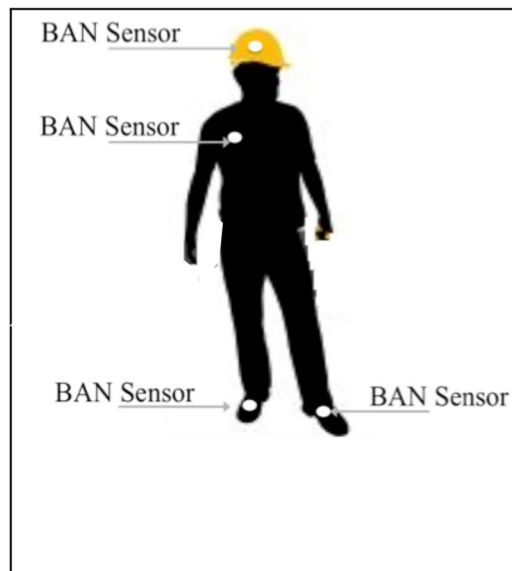


Fig. 5.3: Wearable sensors network.

The proposed wearable sensors network, shown in Fig. 5.3, is composed of the following nodes: a sensor in the helmet, one in the jacket and two in the shoes. These sensors communicate wireless with an access point that sends the information to the working central that verifies and re-elaborates the received data.

Within the industrial area the workers must wear the proper safety equipment: helmet, jacket and shoes. Each sensor is characterized by an integrate RFID tag with an unique identification code. Some tags are passive whereas others have computational abilities. I choose to place passive RFID tags into the shoes and the jacket, whereas in the helmet has been placed a WISP equipped with an accelerometer, in order to detect the presence of the worker and the correct use of the helmet.

The Body Control Unit (BCU), which is responsible of collecting data from the wearable sensor network, is composed of RFID readers placed in strategic control points of the industrial scenario. For instance, they can be placed in the bus that transports the workers in specific working areas, in the crane access points, in the areas in which heavy means of transport pass, etc. The

system is composed of RFID gates placed in strategic points of the industrial environment. All readers are connected through an Ethernet port to the local LAN through which the status of the tags and the information returned by the sensors can be read and stored in the database. A schematic diagram of this architecture is presented in Fig. 5.4. By constantly monitoring the checkpoints and the data written in the database, a human operator or a software can notice missing safety equipment and/or out-of-range output values of the sensors denoting wrong position of the helmet.

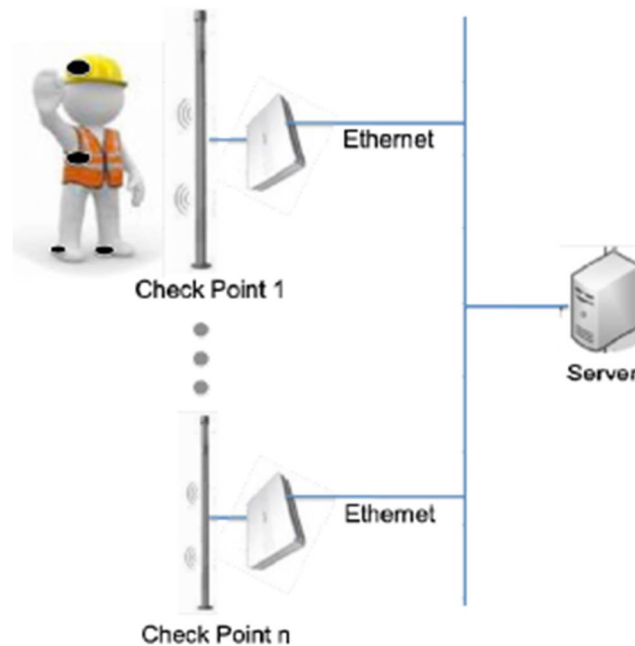


Fig. 5.4: System architecture.

The instruments bought for the test are:

- 1 reader Speedway Revolution R420;
- 1 power supply;
- 2 far field antennas;
- 1 antenna very short-range Mini Guardrail;
- console cable;
- 1 cable AMA/R-TNC 2m;
- tag sample pack;
- 2 WISP-Moo [46-47].

RFID technologies have been evaluated and the Speedway Revolution reader [48] has been chosen since it represents a reliable and flexible solution for these type of systems. This reader has the Autopilot function, through which it is able to do a self-configuration reducing interferences and

consumptions and increasing the performance. The dynamic antennas management allows to focus for a longer time the working range on the system areas in which the greatest number of tags are detected. Such systems belongs to the UHF Gen2 category, and are ideal for the identification and authentication of goods and people, for access control and for each action which needs the moving of multiple tags.



Fig. 5.5: Impinj kit.

The sensors bought were Moo sensors, which work at 915 MHz within the range of UHF American standard (from 902 MHz to 928 MHz). Since in Europe the range of UHF is from 865 MHz to 870 MHz, the internal clock signal of the Moo sensors has been modified in order to adapt its working frequency to European standards. Therefore, some internal registries of the sensor have been modified to change its working frequency from 2.7 MHz (ideal value in America) to about 3.8 MHz (value consistent with European standards).

The technical characteristics of the reader adapted to European standards are:

- modulation: PR-ASK (Phase Reversal-Amplitude Shift Keying);
- TARI (Type a Reference Interval): 20 μ s;
- DR (Divide Ratio): 64/3;
- backscatter link frequency: 320 kHz.

The Wisp-Moo is a sensor produced in America and has been set to a Backscatter link frequency of 256 kHz and a TARI oscillating in the range 16-20 μ s. In order to adapt the system, the values of the registries BSCLT1 and DCOCTL have been measured with the oscilloscope in the pin P5.5 (pin 49) to obtain 3.84 MHz, a value consistent with the ETSI standard.

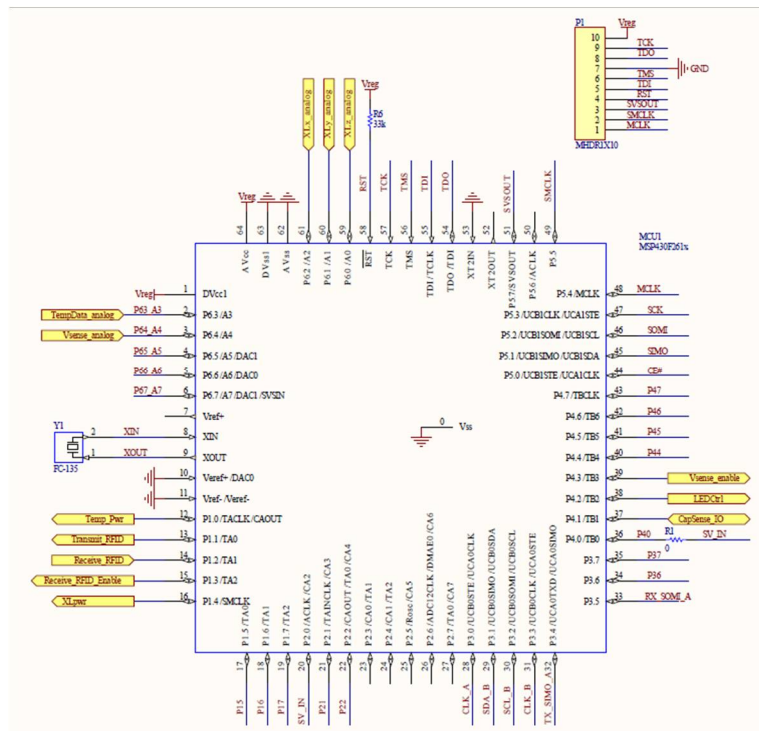


Fig. 5.6: Wisp-Moo Datasheet.

Such values have been added into the MACRO SEND_CLOCK in the board.h file, because it has been noticed that the frequency change occurred into the sendtoreader routine written in assembler. From the results obtained with the oscilloscope, the following changes have been done:

```
// SEND_CLOCK □ MOV.B #0x8b, &0x57 □ MOV.B #0x60, &0x56
```

Generally, for such systems the encoding techniques have different characteristics on the basis of:

- the difficulty to rebuild the reception timing;
- the spectrum occupancy in the base band;
- the decoding complexity;
- noise sensibility;
- the transferred energy.

Typically, the encoding between the reader and the tag is chosen to maximize the energy delivered in reception, whereas the encoding between the tag and the reader is chosen to minimize the energy. It can be distinguished between the encoding based on the pulse duration (PIE, Pulse Interval Encoding) and the encoding based on the transitions (Manchester, Miller, FM0). Manchester and PIE are preferred in reader-tag communications whereas Miller and FM0 are preferred in tag-reader communications.

The encoding used for the WISP is:

- Reader-Wisp encoding: PIE;
- Wisp-Reader encoding: MILLER 4.

Once the encoding was chosen, the modulation was evaluated. For communications between reader and tag and vice versa, traditional techniques with low circuital complexity are used. The most used modulations are the Amplitude Shift Keying (ASK), the Phase Reversal-ASK (PR-ASK) and the Frequency Shift Keying (FSK). The amplitude modulations considered are those of UHF systems. The Wisp-Moo makes use of the backscatter of the signal reflected by the antenna, modulating this signal in amplitude with an ASK-OOK.

Generally, in the RFID systems the reader set the communication between itself and the tag, defining the encoding for communicating with the tag and imposing to the tag the encoding to use for replying. Differently from the other RFID tags, the WISP forces the system to work with MILLER 4, then the reader must be opportunely set. Encoding and modulation are used similarly both in the Europe and in the USA. They only differ on the backscatter frequency.

5.4. The control system

The control system is composed of five main components:

1. the proposed wearable sensors network and a central unit (BCU), which is able to transmit the data via radio with TETRA;
2. personal radio interface for data and voice communication with the operators;
3. Closed Circuit Television (CCTV) installed in the port perimeter, which should be integrated with the sensors system. The CCTV must be able to react to the problems detected by the wearable sensors network and to distinguish if such problems are false alarms or actual problems. Furthermore, this system can be used to control whether the workers are wearing the safety clothes appropriately;
4. interface with the terminals of the operators and of the guest operators within the area of interest;
5. the control system, the main block, is an aggregator of the system.

The control system works as follows: the moving of the workers is signalled to the control room; each worker position is identified by a marker, whose colour indicates whether he is wearing the correct clothes and/or whether he is in proximity of a danger. The RFID tags allow to know

whether the worker is wearing the mandatory safety clothes, whereas the accelerometer integrated into the WISP allows to understand whether the helmet is correctly worn. This is necessary since the worker is inclined to unwear the helmet because it is cumbersome or because in summer it is hot.

The accelerometer [44][49] is a device able to detect and measure a linear acceleration. The model integrated in our sensor is three-axial and is able to detect the different acceleration values along the three axes X, Y, Z, measured in m/s^2 . Such accelerator is a sensor equipped with a test mass, which is constrained in a way that it can only rotate around an axe perpendicular of its input axe; when an acceleration is applied to the sensor, the test mass is deflected with respect to its zero with a quantity proportional to the specific strength applied along the input axe.

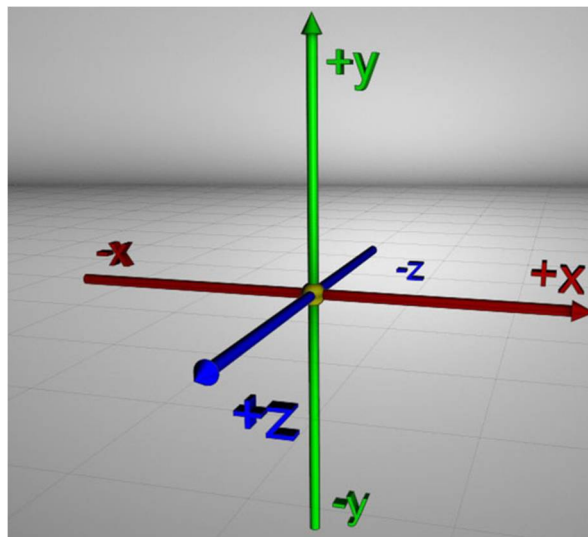








Fig. 5.7: Axes and rotation angle of a sensor.

On the basis of the reference system shown in Fig. 5.7, when a strength is applied to the device, the value acquired by the accelerometer will be positive or negative depending on the moving of the sensor. Table 5.2 summarizes the orientations and the accelerations which allow to define the positioning of the helmet.

The accelerometer detects the total acceleration on the device mass (specific strength), which is the algebraic sum of the acceleration produced by external strengths and by the earth's gravitation (to which each body with a mass is exposed); then, even if the worker is not moving, the test mass of the accelerometer is attracted downward with respect to the equilibrium position and the output of the accelerometer will be the sum of the external acceleration (in this case is $0 m/s^2$ because the device is not moving) and the earth's gravitation ($g = 9.81 m/s^2$).

TABLE 5.2 Helmet positioning

| Position | X (m/s^2) | Y (m/s^2) | Z (m/s^2) |
|---|---------------|---------------|---------------|
|  | 0 | 9.81 | 0 |
|  | 9.81 | 0 | 0 |
|  | 0 | -9.81 | 0 |
|  | -9.81 | 0 | 0 |
|  | 0 | 0 | 9.81 |
|  | 0 | 0 | -9.81 |

When the helmet is placed in the correct position above the head, the sensor is in a flat position, and the accelerations along the three axes are [45][49]:

$$\begin{bmatrix} a_x \\ a_y \\ a_z \end{bmatrix} = \begin{bmatrix} 0 \\ 0 \\ -g \end{bmatrix} \quad (5.4.1)$$

with g the Earth's gravitation. In fact, using the presence of gravity distributed on the three axes, the orientation of the device can be calculated using the modulus of the accelerations $|a_m|$ given by:

$$|a_m| = \sqrt{a_x^2 + a_y^2 + a_z^2} \quad (5.4.2)$$

and by the following equations:

$$\alpha = \cos^{-1} \left(\left| \frac{a_x}{a_m} \right| \right), \quad \beta = \cos^{-1} \left(\left| \frac{a_y}{a_m} \right| \right) \quad (5.4.3)$$

The angles α and β are the angles that the device forms with the X and Y axes. The scaled values of α and β give the angles for roll and pitch. Some simplifications have been done in this analysis since the values have been considered as the tilt angles of the sensor with respect to the Earth's surface.

This because:

- the pitch measures the angle between the Y axe and the Earth's surface, when it rotates around the X axe, forward or back, with values comprised between -180° and $+180^\circ$, with positive values when the positive axe Y is moving towards the negative axe Z;
- the roll measures the angle between the X axe and the Earth's surface, when it is free to rotate around the Z axe, with values comprised between -90° and $+90^\circ$, with positive values when the positive axe X is moving towards the positive axe Z.

The pitch and roll angles refer to the angle between the X and Y axes of the sensor with the Earth's surface, respectively. Such angles are not sufficient to unambiguously determine the sensor's position in the space. As a consequence, an alternative method for addressing the lack of the gyroscope has been found, in order to determine the correct axial set of the sensor. The proposed method estimates the angles between the directions of the accelerations along the three axes X, Y, Z, with the direction of the total acceleration to which it is exposed the sensor. This direction results, with a good approximation, parallel to the direction of the Earth's gravitation (orthogonal to the Earth's surface).

To obtain the angle between the direction of the acceleration along an axe with the direction of the total acceleration, it is sufficient to compute the arc cosine of their ratio, as in equation (5.4.3).

Fig. 5.8 shows the evolution of a straight line walk along the Y direction of the sensor (the axes X and Y are parallel to the Earth's surface), which represents the vertical angles between the acceleration along the X (Y) axis with the total acceleration A_m (blue line) and the vertical angles between the acceleration along the X (Y) axis with the Earth's gravitation A_g (red line, with $A_g = 9.81 \text{ m/s}^2$). These angles are computed as in (5.4.3). The lines are almost totally overlapping, and this confirms the validity of the approximation introduced, that is the direction of the total acceleration can be approximated with the direction of the Earth's gravitation.

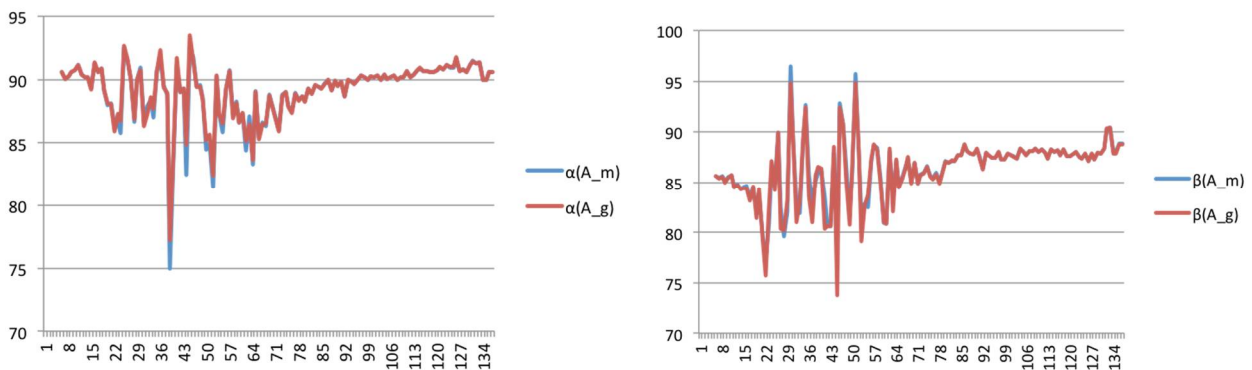


Fig. 1.8: Left: vertical angle α between the acceleration along the X axis with the total acceleration A_m and the Earth's gravitation A_g . Right: vertical angle β between the acceleration along the Y axis with the total acceleration A_m and the Earth's gravitation A_g .

For the Moo sensor lying still along the Y axis on a flat horizontal surface, the pitch and roll are equal to zero, changing when moving from 0° to 360° .

Once powered by the RF reader, the Wisp sensor send its EPC code to the reader. The EPC is 12 bytes where 6 bytes represent the three axes of the accelerometer. While the EPC codes of common RFID tags are forwarded directly to the database together with the date, time and the reader ID, the EPC codes of the Moo sensors are buffered to evaluate the sensor data before sending it to the database. The accelerometer data is stored in an array while the sensor is in the reader's range. After the sensor is out of range the data from the accelerometers is filtered over a certain amount of time in order to compensate potential errors regarding the actual movement of the user. The result of the filtering operation on the accelerometer values is compared to predefined thresholds to take the decision whether the helmet is worn in a right manner or not. The decision and the mean values of the accelerometers are written in the centralized database.

The results obtained by the mesh of these information on the central monitor bring to the situation shown in Fig. 5.9.

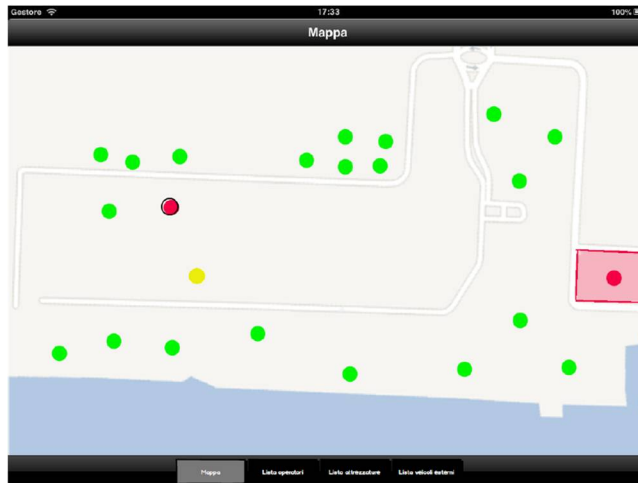


Fig. 5.9: Planimetry of the area under surveillance.

The worker signalled with a red light will be analysed to evaluate because the alarm started. The mean of the lights are as follows:

- green light: the sensor is working correctly;
- yellow light: the sensor is not working correctly, but it is active;
- red light: the sensor is not working;

In Figs. 5.10-5.11 are shown an example of the different lights: the right shoe of the worker is damaged and it is signalled with a yellow light. Furthermore, the lack of the helmet has been detected and it is signalled with a red light. Therefore, the worker is requested to go to the central for changing the clothes. If a worker is in a dangerous area or he is not wearing the mandatory clothes, a light red and a signal alarm alert the dangerous situation on the planimetry. Through the utilization of the cameras the worker will be identified and requested to solve the problems identified.



Fig. 5.10: General control room.



Fig. 5.11: Worker screen.

Chapter 6

Antennas Design

In this chapter, the design of a specific wearable antenna for RFID is presented. Section 6.1 discusses the design of a patch composed of several "side by side" conductive "threads of textile". In Section 6.2 the capacitance and inductance parameters of the antenna are calculated. Since the microwave model does not allow the design of a wearable antenna with a good approximation, in Section 6.3 a specific microwave model for coupled lines has been designed.

6.1. Multi-conductor transmission lines

I considered a patch panel such as that shown in Fig. 6.1, which can be represented as a multi-conductor transmission line (with appropriate boundary conditions) to which I applied the equations of the transmission lines considering N-dimensional voltage $\vec{V}(z)$ and current $\vec{I}(z)$ arrays and introducing the static capacitance C and inductance L matrices of the structure.

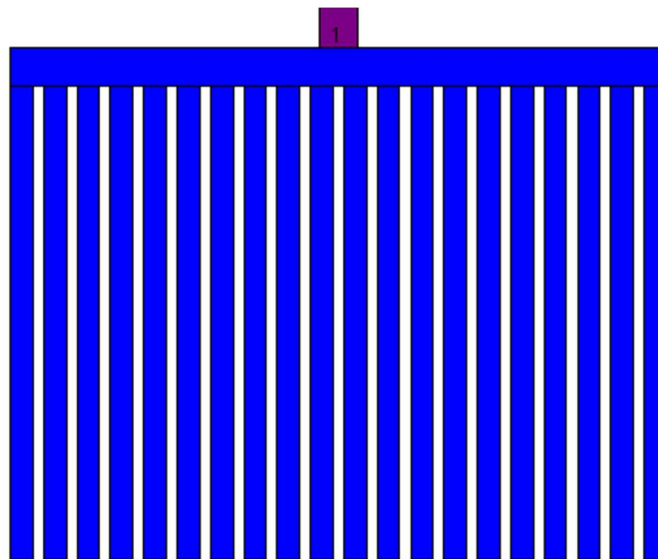


Fig. 6.1: Multi-conductor patch.

The analyzed structure is an inhomogeneous dielectric which supports quasi-TEM modes.

Starting from the equations (6.1.1) of a n conductors system:

$$\left\{ \begin{array}{l} -\frac{d\underline{V}(z)}{dz} = j\omega\mu_0\underline{L}_N\underline{I}(z) \end{array} \right. \quad (6.1.1a)$$

$$\left\{ \begin{array}{l} -\frac{d\underline{I}(z)}{dz} = j\omega\varepsilon_0\underline{C}_N\underline{V}(z) \end{array} \right. \quad (6.1.1b)$$

with \underline{C}_N and \underline{L}_N the normalized matrices of C and L, respectively $\underline{C}_N = 1/\varepsilon_0 \cdot \underline{C}$ and $\underline{L}_N = 1/\mu_0 \cdot \underline{L}$.

The first derivative of equation (6.1.1b) was computed whit respect to z:

$$-\frac{d^2\underline{I}(z)}{dz^2} = j\omega\varepsilon_0\underline{C}_N \frac{d\underline{V}(z)}{dz} \quad (6.1.2)$$

Then, equation (6.1.1a) was replaced in equation (6.1.2):

$$-\frac{d^2\underline{I}(z)}{dz^2} + \omega^2\varepsilon_0\mu_0\underline{C}_N\underline{L}_N\underline{I}(z) = 0 \quad (6.1.3)$$

with $\beta^2 = \beta_0^2\underline{L}_N\underline{C}_N$ and $\beta_0 = \omega\sqrt{\varepsilon_0\mu_0}$

and equation (6.1.3) becomes:

$$-\frac{d^2\underline{I}(z)}{dz^2} + \beta^2\underline{I}(z) = 0 \quad (6.1.4)$$

By considering the following relations:

$$\sqrt{\varepsilon_0\mu_0} = \frac{1}{c_0} \quad \omega = 2\pi f \quad \beta_0 = \frac{2\pi f}{c_0}$$

Equation (6.1.1a) and (6.1.1b) can be written in the following form:

$$\left\{ \begin{array}{l} \underline{V}(z) = -\frac{1}{\omega\varepsilon_0\underline{C}_N} \frac{d\underline{I}(z)}{dz} \end{array} \right. \quad (6.1.5a)$$

$$\left\{ \begin{array}{l} -\frac{d^2\underline{I}(z)}{dz^2} + \beta_0^2\underline{L}_N\underline{C}_N\underline{I}(z) \end{array} \right. \quad (6.1.5b)$$

I have to find the solution of this second order differential equation, which is as follows:

$$I(z) = I_0 e^{-j\beta_k z}$$

with β_k^2 the eigenvalues of the matrices $\beta_0^2 \underline{L}_N \underline{C}_N$.

In our case:

$$\beta_k = \beta_0 \cdot \sqrt{\lambda_k} \quad (6.1.6)$$

where λ_k (with k ranging from 1 to n) are the eigenvalues of the matrix $\underline{L}_N \underline{C}_N$ whose size is nxn.

Furthermore, I indicate with \underline{I}_k the eigenvector corresponding to the eigenvalue λ_k .

The current can be written in its traveling-wave form as:

$$\underline{I}(z) = \sum_{k=1}^n (I_k^+ e^{-j\beta_k z} + I_k^- e^{j\beta_k z}) \cdot \underline{I}_k$$

with I_k^- and I_k^+ appropriate scalars.

By expanding the exponentials, the traveling-wave forms of current and voltage are obtained:

$$\left\{ \begin{array}{l} \underline{I}(z) = \sum_{k=1}^n (I_k^+ \cos(\beta_k z) - I_k^+ j \sin(\beta_k z) + I_k^- \cos(\beta_k z) + I_k^- j \sin(\beta_k z)) \cdot \underline{I}_k \end{array} \right. \quad (6.1.7a)$$

$$\left\{ \begin{array}{l} \underline{V}(z) = j \frac{1}{\varepsilon_0} \underline{C}_N^{-1} \left(\sum_{k=1}^n j \beta_k (I_k^+ \cos(\beta_k z) + I_k^+ j \sin(\beta_k z) - I_k^- \cos(\beta_k z) + I_k^- j \sin(\beta_k z)) \cdot \underline{I}_k \right) \end{array} \right. \quad (6.1.7b)$$

Grouping the cosine and sine term in (6.1.7a):

$$\underline{I}(z) = \sum_{k=1}^n (\cos(\beta_k z) \cdot [I_k^+ + I_k^-] + j \sin(\beta_k z) \cdot [I_k^- - I_k^+]) \cdot \underline{I}_k \quad (6.1.8)$$

By knowing the current and voltage in a point $z = l$, it is possible to express the (6.1.8) as

$$\underline{I}(z) = \sum_{k=1}^n (\cos(\beta_0 \sqrt{\lambda_k} (z - l)) \cdot [A_k(l)] + j \sin(\beta_0 \sqrt{\lambda_k} (z - l)) \cdot [B_k]) \cdot \underline{I}_k \quad (6.1.9)$$

with:

$$\begin{aligned} [I_k^+ + I_k^-] &= I_{Ak}(l) \\ [I_k^- - I_k^+] &= B_k \end{aligned} \quad \beta_k = \beta_0 \sqrt{\lambda_k}$$

Then, equation (6.1.7) can be written in its stationary form as:

$$\left\{ \begin{aligned} \underline{I}(z) &= \sum_{k=1}^n \left(\cos(\beta_0 \sqrt{\lambda_k}(z-l)) \cdot [I_{Ak}(l)] + j \sin(\beta_0 \sqrt{\lambda_k}(z-l)) \cdot [B_k] \right) \cdot \underline{L}_k \end{aligned} \right. \quad (6.1.10a)$$

$$\left\{ \begin{aligned} \underline{V}(z) &= j \frac{1}{\varepsilon_0} \underline{C}_N^{-1} \left(\sum_{k=1}^n \left(\beta_0 \sqrt{\lambda_k} \left(-\sin(\beta_0 \sqrt{\lambda_k}(z-l)) \right) \cdot [I_{Ak}(l)] + j [B_k] \beta_0 \sqrt{\lambda_k} \cos(\beta_0 \sqrt{\lambda_k}(z-l)) \right) \right) \underline{L}_k \end{aligned} \right. \quad (6.1.10b)$$

6.2. Calculation of L and C parameters

From equation (6.1.6) there is the necessity of the computation of the matrices \underline{C}_N and \underline{L}_N to solve the equations $\underline{I}(z)$ e $\underline{V}(z)$. For simplicity, it is more practical to compute only the matrix of capacitances \underline{C} . In fact, if the structure was in the air, the matrix \underline{L}_N would be the inverse of the matrix \underline{C} in the air. To evaluate the values of the capacitances, the energy has been computed by using a finite difference numerical technique [50].

To calculate the field of a microstrip (Fig. 6.2), and therefore the capacitance per unit length, the following system has to be solved:

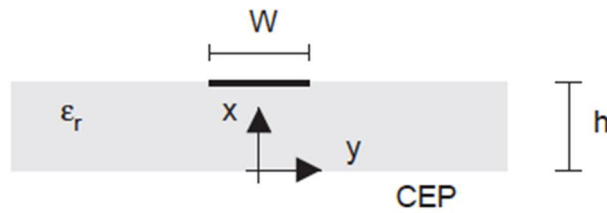


Fig. 6.2: Microstrip geometry.

$$\begin{cases} \nabla_t \cdot (\varepsilon \nabla_t \phi) = 0 & (6.2.1a) \\ \phi(x, 0) = \phi(x, \infty) = 0 & (6.2.1b) \\ \phi(x, h^-) = \phi(x, h^+) & (6.2.1c) \end{cases}$$

The solution ϕ is a function of the continuous variables x and y . To solve (6.2.1) with the finite differences method, I firstly accept to evaluate this structure only at the points of a regular grid (Fig 6.3) with equal spacings Δx and Δy (they could also be different).

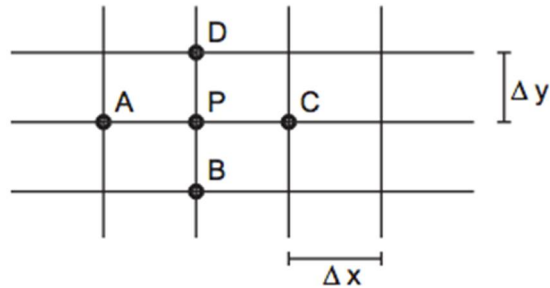


Fig. 6.3: Regular grid for microstrip.

Sample points must be along the metallic strip and on the interface (as shown in Fig 6.4). Thereafter, the partial differential equations were replaced by a system of linear equations that bind the values that the unknown function assumes in the nodes of the considered subset. The higher the number of nodes, the more accurate is the representation. The accuracy of the representation also depends on the system's order and on the shape chosen. The dielectric internal points are processed independently to ϵ_r , while the interface points are more critical and are processed in opportunity manner.

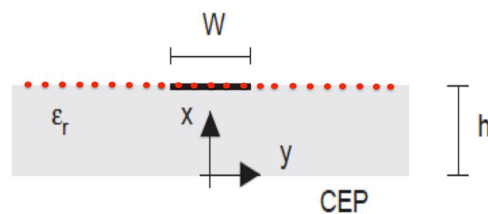


Fig. 6.4: Interface sampling.

o INNER POINTS

I consider the generic inner point as shown in Fig (6.3), and the (6.2.1a) becomes:

$$\nabla_t^2 \phi = \left(\frac{\partial^2 \phi}{\partial x^2} + \frac{\partial^2 \phi}{\partial y^2} \right) = 0 \tag{6.2.2}$$

Writing the potentials A and C according to the second-order Taylor pynomial I have:

$$\left\{ \begin{array}{l} \phi_A = \phi_P + \left(\frac{\partial \phi}{\partial x} \Big|_P (-\Delta x) + \frac{1}{2} \frac{\partial^2 \phi}{\partial x^2} \Big|_P (-\Delta x)^2 \right) \\ \phi_C = \phi_P + \left(\frac{\partial \phi}{\partial x} \Big|_P (\Delta x) + \frac{1}{2} \frac{\partial^2 \phi}{\partial x^2} \Big|_P (\Delta x)^2 \right) \end{array} \right. \quad (6.2.3a)$$

$$\left\{ \begin{array}{l} \phi_A = \phi_P + \left(\frac{\partial \phi}{\partial x} \Big|_P (-\Delta x) + \frac{1}{2} \frac{\partial^2 \phi}{\partial x^2} \Big|_P (-\Delta x)^2 \right) \\ \phi_C = \phi_P + \left(\frac{\partial \phi}{\partial x} \Big|_P (\Delta x) + \frac{1}{2} \frac{\partial^2 \phi}{\partial x^2} \Big|_P (\Delta x)^2 \right) \end{array} \right. \quad (6.2.3b)$$

Similar expressions are obtained in the y direction. By adding the two contributions:

$$\frac{\partial^2 \phi}{\partial x^2} \Big|_P = \frac{1}{(\Delta x)^2} (\phi_A + \phi_C - 2\phi_P) \quad (6.2.4a)$$

$$\frac{\partial^2 \phi}{\partial y^2} \Big|_P = \frac{1}{(\Delta y)^2} (\phi_B + \phi_D - 2\phi_P) \quad (6.2.4b)$$

and therefore :

$$\nabla^2 \phi \Big|_P = \frac{\phi_A + \phi_C + \phi_B + \phi_D - 4\phi_P}{(\Delta x)^2} \quad \text{with } \Delta x = \Delta y \quad (6.2.5)$$

In each point P inside the dielectric, the Laplace equation may be replaced by the second member of this relation equalled to zero (with an error that depends on the fourth derivative of ϕ multiplied by Δx^4 and Δy^4). Then, it is:

$$\phi_P = \frac{\phi_A}{4} + \frac{\phi_C}{4} + \frac{\phi_B}{4} + \frac{\phi_D}{4} \quad (6.2.6)$$

o POINT IN THE INTERFACES

I consider the red points shown in Fig. 6.5, and I apply the (6.2.1a) to a surface cut in half by the separation surface which allows to obtain the conditions of connection between dielectrics. I obtain $\int \varepsilon \nabla_t \phi d\vec{l}$ extended to the traced rectangle (Fig. 6.5).

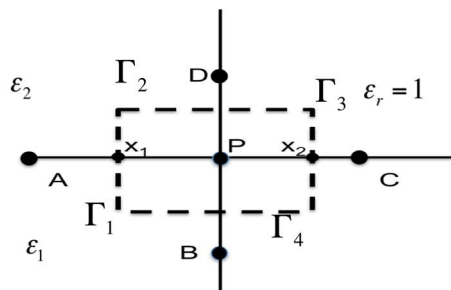


Fig. 6.5: Closed patch integral of the surface between the dielectric.

$$\int \varepsilon \nabla_t \phi d\vec{l} = \int_{\Gamma_1} \frac{\partial \phi}{\partial n} \varepsilon dl + \int_{\Gamma_2} \frac{\partial \phi}{\partial n} \varepsilon dl + \int_{\Gamma_3} \frac{\partial \phi}{\partial n} \varepsilon dl + \int_{\Gamma_4} \frac{\partial \phi}{\partial n} \varepsilon dl \quad (6.2.7)$$

Since the derivative is constant in all the 4 integrals, it can be brought out of the integral:

$$\int \varepsilon \nabla_t \phi d\vec{l} = \frac{\partial \phi}{\partial n} \Big|_{\Gamma_1} \int_{\Gamma_1} \varepsilon dl + \frac{\partial \phi}{\partial n} \Big|_{\Gamma_2} \int_{\Gamma_2} \varepsilon dl + \frac{\partial \phi}{\partial n} \Big|_{\Gamma_3} \int_{\Gamma_3} \varepsilon dl + \frac{\partial \phi}{\partial n} \Big|_{\Gamma_4} \int_{\Gamma_4} \varepsilon dl \quad (6.2.8)$$

Each of the four terms of equation (6.2.2) is solved separately:

$$\begin{aligned} \frac{\partial \phi}{\partial n} \Big|_{\Gamma_1} \int_{\Gamma_1} \varepsilon dl &= \frac{\partial \phi}{\partial n} \Big|_{\Gamma_1} \left(\int_{\Gamma_1 x_1} \varepsilon_1 dl_1 + \int_{\Gamma_2 x_1} \varepsilon_2 dl_2 \right) = \frac{(\phi_A - \phi_P)}{\Delta x} \cdot \left(\varepsilon_1 \frac{\Delta x}{2} + \varepsilon_2 \frac{\Delta x}{2} \right) \\ &= \frac{1}{2} (\phi_A - \phi_P) \varepsilon_1 + \frac{1}{2} (\phi_A - \phi_P) \varepsilon_2 \end{aligned} \quad (6.2.9a)$$

$$\begin{aligned} \frac{\partial \phi}{\partial n} \Big|_{\Gamma_2} \int_{\Gamma_2} \varepsilon dl &= \frac{\partial \phi}{\partial n} \Big|_{\Gamma_2} \left(\int_{\Gamma_2 x_1} \varepsilon_2 dl_2 + \int_{\Gamma_3 x_2} \varepsilon_2 dl_2 \right) = \frac{(\phi_D - \phi_P)}{\Delta x} \cdot \left(\varepsilon_2 \frac{\Delta x}{2} + \varepsilon_2 \frac{\Delta x}{2} \right) \\ &= (\phi_D - \phi_P) \varepsilon_2 \end{aligned} \quad (6.2.9b)$$

$$\begin{aligned} \frac{\partial \phi}{\partial n} \Big|_{\Gamma_3} \int_{\Gamma_3} \varepsilon dl &= \frac{\partial \phi}{\partial n} \Big|_{\Gamma_3} \left(\int_{\Gamma_3 x_2} \varepsilon_1 dl_1 + \int_{\Gamma_4 x_2} \varepsilon_2 dl_2 \right) = \frac{(\phi_C - \phi_P)}{\Delta x} \cdot \left(\varepsilon_2 \frac{\Delta x}{2} + \varepsilon_1 \frac{\Delta x}{2} \right) \\ &= \frac{1}{2} (\phi_C - \phi_P) \varepsilon_2 + \frac{1}{2} (\phi_C - \phi_P) \varepsilon_1 \end{aligned} \quad (6.2.9c)$$

$$\begin{aligned} \frac{\partial \phi}{\partial n} \Big|_{\Gamma_4} \int_{\Gamma_4} \varepsilon dl &= \frac{\partial \phi}{\partial n} \Big|_{\Gamma_4} \left(\int_{\Gamma_4 x_2} \varepsilon_1 dl_2 + \int_{\Gamma_3 x_1} \varepsilon_1 dl_2 \right) = \frac{(\phi_B - \phi_P)}{\Delta x} \cdot \left(\varepsilon_1 \frac{\Delta x}{2} + \varepsilon_1 \frac{\Delta x}{2} \right) \\ &= (\phi_B - \phi_P) \varepsilon_1 \end{aligned} \quad (6.2.9d)$$

I have therefore:

$$\frac{1}{2} [(\phi_A - \phi_P) \varepsilon_1 + (\phi_A - \phi_P) \varepsilon_2] + [(\phi_D - \phi_P) \varepsilon_2] + \frac{1}{2} [(\phi_C - \phi_P) \varepsilon_2 + (\phi_C - \phi_P) \varepsilon_1] + [(\phi_B - \phi_P) \varepsilon_1] \quad (6.2.10)$$

and the equation for ϕ_P is :

$$\phi_P = \frac{\phi_A}{4} + \frac{\phi_D \varepsilon_2}{2(\varepsilon_1 + \varepsilon_2)} + \frac{\phi_B \varepsilon_1}{2(\varepsilon_1 + \varepsilon_2)} + \frac{\phi_C}{4} \quad (6.2.11)$$

which generalizes the equation valid for the homogeneous dielectric.

The linear system obtained is infinite. To achieve an equivalent finite system, it can be noticed that the field decreases with the increase of $|\mathbf{x}|$ and therefore it can be assigned $\phi = 0$ to the points with $|\mathbf{x}|$ sufficiently high (which is equivalent to enclose the structure in a box of CEP). Obviously, in order to prevent errors, the box must be chosen sufficiently long.

Once ϕ is known, the capacitances can be obtained by computing the energy of the structure:

$$W_e = \frac{1}{2} CV^2 = \frac{1}{2} \int \epsilon |e|^2 dS \Rightarrow C = \int \epsilon |e|^2 dS \quad (6.2.12)$$

with V the voltage (imposed) between the strip and the ground plane.

Equation (6.2.12) is used both in the presence or absence of the dielectric, with the two different electrical fields. The same technique can be used for N microstrips, using multiple configurations of voltages from which the capacitances can be computed by solving a linear system.

Through finite differences, the capacitances were computed (both in the air and in the dielectric) of a four-conductor structure (Fig. 6.6), by neglecting the capacitances between non-adjacent lines. Only explicit structures with equal strips, with equal external gaps, and with internal gaps equal or different to external gaps were considered.

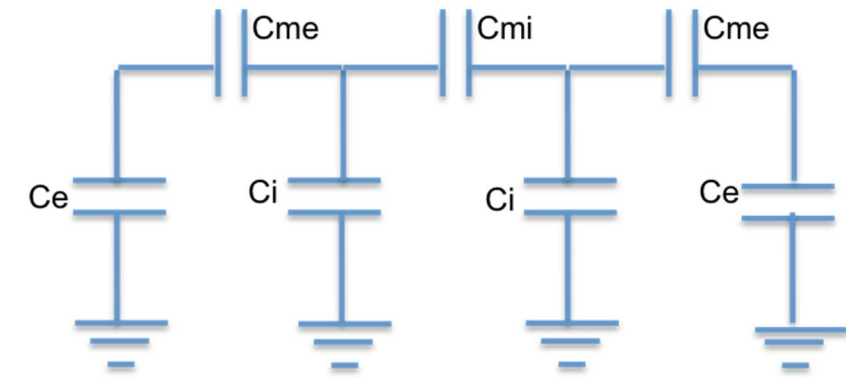


Fig. 6.6: Equivalent circuit of a 4 parallel conductor system.

Once the energy is evaluated with the finite difference method described, it is found that

$$W_k = \frac{1}{2} [\underline{v}_k]^T \begin{bmatrix} C_e + C_{me} & -C_{me} & 0 & 0 \\ -C_{me} & C_i + C_{me} + C_{mi} & -C_{mi} & 0 \\ 0 & -C_{mi} & C_i + C_{me} + C_{mi} & -C_{me} \\ 0 & 0 & -C_{me} & C_e + C_{me} \end{bmatrix} [\underline{v}_k] \quad (6.2.13)$$

with \underline{v}_k the voltage vector chosen. The (6.2.13) is a linear system of equations in capacities. Since it has four unknowns capacities, it requires four configurations, to write a linear system with four equations in the four unknowns capacities, which can be summarized in a system of the type:

$$\underline{A} \cdot \underline{C} = \underline{W}$$

with A depending (nonlinearly) by $\underline{v}_k, i = 1, \dots, 4$.

The four setups of voltages used must be "independent". Therefore, I tried to find four vectors v that would guarantee a well-conditioned matrix A. Since the matrix A is a symmetric matrix, the four eigenvectors were computed (see the Appendix) with the Matlab symbolic tool, and are as follows:

$$v_1 = \begin{bmatrix} -1 \\ -A \\ A \\ 1 \end{bmatrix} \quad v_2 = \begin{bmatrix} -1 \\ B \\ -B \\ 1 \end{bmatrix} \quad v_3 = \begin{bmatrix} 1 \\ -C \\ -C \\ 1 \end{bmatrix} \quad v_4 = \begin{bmatrix} 1 \\ D \\ D \\ 1 \end{bmatrix}$$

It can be noticed that the two terms of each eigenvector are always known while the other two have symmetries. Then, by using an iterative method the four optimal eigenvectors were evaluated to obtain a good conditioning.

The values of the four-line structure were then used as an approximation to obtain the matrix C of a N conductors system (Fig. 6.7). The internal capacitances were approximated with the value of the C_i of the 4-conductors, and all mutual internal capacitances were approximated with C_{mi} . Similarly, the two external capacitances were approximated with C_e and the two mutual external capacitances were approximated with C_{me} .

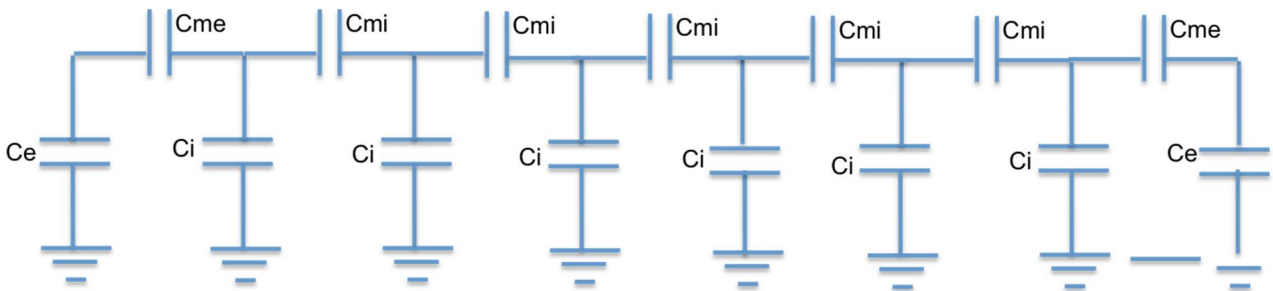


Fig. 6.7: Circuital representation.

Obviously, the 4-conductors structure used to approximate the values must have the same geometric characteristics (gap and strip width).

For generic n- conductors systems, the matrix C_n is as follows:

$$C_N = \begin{bmatrix} C_e + C_{me} & -C_{me} & 0 & \dots & 0 & 0 & 0 & 0 & 0 \\ -C_{me} & C_e + C_{me} + C_{mi} & -C_{mi} & 0 & \dots & 0 & 0 & 0 & 0 \\ 0 & -C_{mi} & C_i + 2C_{mi} & -C_{mi} & 0 & 0 & 0 & 0 & 0 \\ 0 & 0 & -C_{mi} & C_i + 2C_{mi} & -C_{mi} & 0 & 0 & \dots & 0 \\ 0 & 0 & 0 & \vdots & \vdots & \vdots & 0 & 0 & 0 \\ \vdots & \vdots & \vdots & 0 & -C_{mi} & C_i + 2C_{mi} & -C_{mi} & 0 & 0 \\ 0 & 0 & 0 & \vdots & 0 & -C_{mi} & C_e + C_{me} + C_{mi} & -C_{me} & -C_{me} \\ 0 & 0 & 0 & 0 & 0 & 0 & -C_{me} & C_e + C_{me} \end{bmatrix}$$

The matrix C_{an} can be represented similarly to C_n ; they only differ on the subscript A.

6.3. Proposed model for coupled lines

Since the microwave model does not allow the design of a wearable antenna with a good approximation, in this section a specific microwave model for coupled lines has been designed, on the basis of the full model of coupled lines proposed in [51].

I considered a generic patch with N identical conductors (Fig. 6.8) of which I evaluate the input impedance Z_{in} .

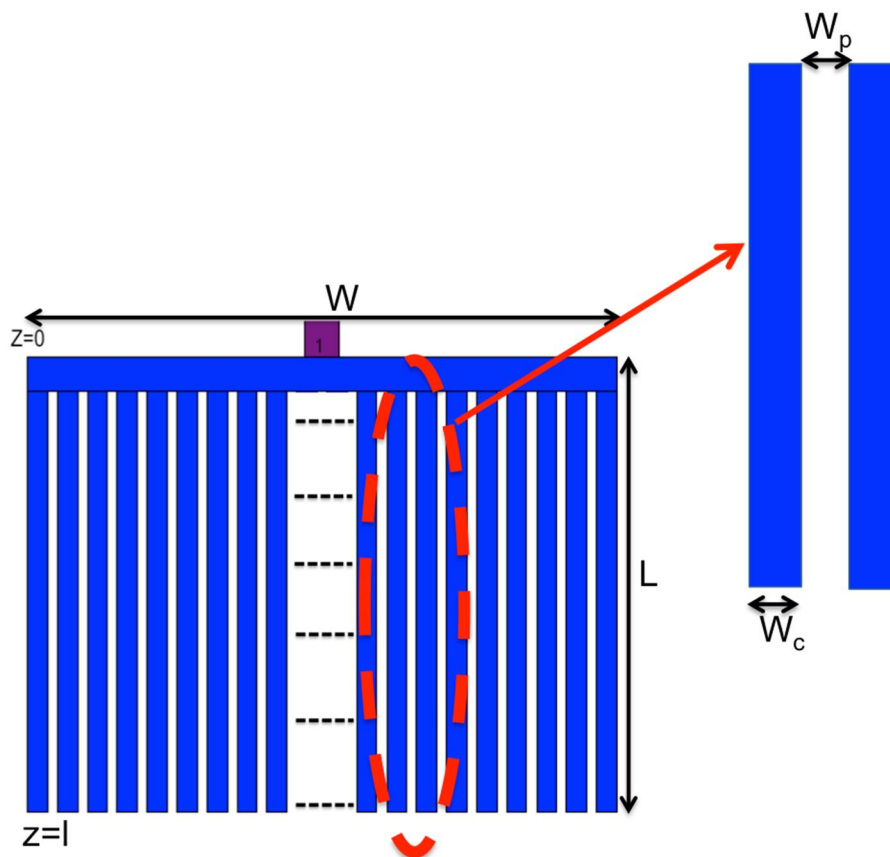


Fig. 6.8: Multi-conductor structure.

To do this, I use the system of equations (6.1.10) written in an appropriate manner. The transverse

line in the top requires that the initial voltages on each conductor are identical.

$$\underline{V}(0) = \begin{bmatrix} 1 \\ 1 \\ \vdots \\ 1 \end{bmatrix}_{1 \cdot n} \cdot V_g$$

Consequently, I know the supply voltages that are set as a term known in the (6.1.10b) for $z = 0$:

$$\underline{1} \cdot V_g = \frac{1}{j\omega\varepsilon_0} \underline{C}_N^{-1} \left\{ \sum_{k=1}^n \left(\underline{I}_{Ak}(l) \beta_0 \sqrt{\lambda_k} \sin(\beta_0 \sqrt{\lambda_k} l) + j \underline{B}_k \beta_0 \sqrt{\lambda_k} \cos(\beta_0 \sqrt{\lambda_k} l) \right) \cdot \underline{I}_k \right\} \quad (6.3.1)$$

The voltage in $z=l$ can be expressed as:

$$\underline{V}(l) = \underline{Z}_{irr} \cdot \underline{I}(l) = \underline{Z}_{irr} \cdot \sum_{k=1}^n \underline{I}_{Ak}(l) \cdot \underline{I}_k \quad (6.3.2)$$

where \underline{Z}_{irr} is the diagonal matrix of the irradiation impedance of the conductors (neglecting the coupling).

$$\underline{Z}_{irr} = \text{diag}(R_e)$$

R_e is a generic resistance of the conductor, since all the conductors are equal to each other; this impedance must be equal to:

$$R_e = nR_{irr}$$

$$R_{irr} = 2R_{in} \quad \text{dove} \quad R_e = \frac{1}{2} 90 \left(\frac{\lambda_0}{W} \right)^2$$

Substituting eq.(6.3.2) in eq.(6.1.10b) I obtain the second equation of the system to be solved:

$$\underline{Z}_{irr} \cdot \sum_{k=1}^n \underline{I}_{Ak}(l) \cdot \underline{I}_k = j \frac{1}{\omega\varepsilon_0} \underline{C}_N^{-1} \left\{ \sum_{k=1}^n \left(j \underline{B}_k \beta_0 \sqrt{\lambda_k} \right) \cdot \underline{I}_k \right\} \quad (6.3.3)$$

I have to solve the system composed of equations (6.3.2) and (6.3.3) as follows:

$$\left\{ \text{diag}(nR_{irr}) \sum_{k=1}^n [L_{Ak}(l)] \cdot \underline{I}_k = j \frac{1}{\omega \varepsilon_0} \underline{C}_N^{-1} \left\{ \sum_{k=1}^n (j \underline{B}_k \beta_0 \sqrt{\lambda_k}) \cdot \underline{I}_k \right\} \right. \quad (6.3.4a)$$

$$\left. \left\{ \underline{1} \cdot V_g = \frac{1}{j \omega \varepsilon_0} \underline{C}_N^{-1} \left\{ \sum_{k=1}^n (\underline{L}_{Ak}(l) \beta_0 \cdot t_n(l) + j \underline{B}_k \beta_0 \cdot h_n(l)) \cdot \underline{I}_k \right\} \right. \right. \quad (6.3.4b)$$

$$\text{With: } t_n(l) = \sqrt{\lambda_k} \sin\left(\beta_0 \sqrt{\lambda_k} l\right), h_n(l) = \sqrt{\lambda_k} \cos\left(\beta_0 \sqrt{\lambda_k} l\right)$$

From eq. (6.3.4) the \underline{I}_k is obtained.

$$\begin{bmatrix} \underline{L}_{A1} \\ \underline{L}_{A2} \\ \vdots \\ \underline{L}_{An} \end{bmatrix} = \begin{bmatrix} \text{diag} \left(\frac{1}{\sqrt{\lambda_k}} \right) [\underline{L}_1 \ \underline{L}_2 \ \dots \ \underline{L}_n]^{-1} \left(-\frac{\omega \varepsilon_0}{\beta_0} \right) \underline{C}_N^{-1} \text{diag}(nR_{irr}) [\underline{L}_1 \ \underline{L}_2 \ \dots \ \underline{L}_n] \end{bmatrix}^{-1} \begin{bmatrix} \underline{B}_1 \\ \underline{B}_2 \\ \vdots \\ \underline{B}_n \end{bmatrix} \quad (6.3.5)$$

and from eq.(6.3.4b) \underline{B}_k is obtained that is replaced in eq.(6.3.5)

$$\begin{bmatrix} \underline{B}_1 \\ \underline{B}_2 \\ \vdots \\ \underline{B}_n \end{bmatrix} = \left(\begin{array}{c} j \underline{C}_N^{-1} [\underline{L}_1 \ \underline{L}_2 \ \dots \ \underline{L}_n] \text{diag}(t_n(l)) [\underline{L}_1 \ \underline{L}_2 \ \dots \ \underline{L}_n]^{-1} \text{diag} \left(\frac{1}{nR_{irr}} \right) \left(-\frac{\beta_0}{\omega \varepsilon_0} \right) \underline{C}_N^{-1} [\underline{L}_1 \ \underline{L}_2 \ \dots \ \underline{L}_n] \text{diag}(\sqrt{\lambda_k}) + \\ -\underline{C}_N^{-1} [\underline{L}_1 \ \underline{L}_2 \ \dots \ \underline{L}_n] \text{diag}(h_n(l)) \end{array} \right)^{-1} \frac{\omega \varepsilon_0 V_g}{\beta_0} \begin{bmatrix} 1 \\ 1 \\ \vdots \\ 1 \end{bmatrix} \quad (6.3.6)$$

Now the admittance can be evaluated:

$$Y = \frac{\sum \underline{I}(0)}{\underline{V}(0)} = \frac{\sum \underline{I}(0)}{V_g} \quad (6.3.7)$$

The current is equal to:

$$\begin{aligned} \underline{I}(0) = & \underline{L}_k \text{diag} \left(\frac{h_n(l)}{\sqrt{\lambda_k}} \right) \left[\left(-\frac{\beta_0}{\omega \varepsilon_0 V_g} \right) \underline{C}_N^{-1} \underline{L}_k \text{diag}(t_n(l)) + \frac{1}{V_g} \underline{C}_N^{-1} \underline{L}_k \text{diag} \left(\frac{h_n(l)}{\sqrt{\lambda_k}} \right) \underline{L}_k^{-1} \underline{C}_N^{-1} \text{diag}(nR_{irr}) \underline{L}_k \right]^{-1} \begin{bmatrix} 1 \\ 1 \\ \vdots \\ 1 \end{bmatrix} + \\ & -j \underline{L}_k \text{diag} \left(\frac{h_n(l)}{\sqrt{\lambda_k}} \right) \left[\left(-\frac{\beta_0}{\omega \varepsilon_0 V_g} \right) \underline{C}_N^{-1} \underline{L}_k \text{diag}(t_n(l)) \underline{L}_k^{-1} \text{diag} \left(\frac{1}{nR_{irr}} \right) \left(-\frac{\beta_0}{\omega \varepsilon_0} \right) \underline{C}_N^{-1} \underline{L}_k \text{diag}(\sqrt{\lambda_k}) + \left(-\frac{\beta_0}{\omega \varepsilon_0 V_g} \right) \underline{C}_N^{-1} \underline{L}_k \text{diag}(h_n(l)) \right]^{-1} \begin{bmatrix} 1 \\ 1 \\ \vdots \\ 1 \end{bmatrix} \quad (6.3.8) \end{aligned}$$

At this point, it is necessary that the imaginary part of the admittance is equal to zero. Then, the patch length which allows to fulfill this condition must be evaluated. This function is not analytically solvable, then the bisection numerical technique (see the Appendix) is used, which is a

common mathematical technique for computing the resonance. This can be replaced in (6.2.11), from which, simplifying the voltage Vg the I(0) becomes:

$$I(0) = \underline{I}_k \text{diag} \left(\frac{h_n(l)}{\sqrt{\lambda_k}} \right) \left[\left(-\frac{\beta_0}{\omega \varepsilon_0} \right) \underline{C}_N^{-1} \underline{I}_k \text{diag} (t_n(l)) + \underline{C}_N^{-1} \underline{I}_k \text{diag} \left(\frac{h_n(l)}{\sqrt{\lambda_k}} \right) \underline{I}_k^{-1} \underline{C}_N^{-1} \text{diag} (nR_{irr}) \underline{I}_k \right]^{-1} \begin{bmatrix} 1 \\ 1 \\ \vdots \\ 1 \end{bmatrix} +$$

$$-j \underline{I}_k \text{diag} \left(\frac{h_n(l)}{\sqrt{\lambda_k}} \right) \left[\left(-\frac{\beta_0}{\omega \varepsilon_0 V_g} \right) \underline{C}_N^{-1} \underline{I}_k \text{diag} (t_n(l)) \underline{I}_k^{-1} \text{diag} \left(\frac{1}{nR_{irr}} \right) \left(-\frac{\beta_0}{\omega \varepsilon_0} \right) \underline{C}_N^{-1} \underline{I}_k \text{diag} (\sqrt{\lambda_k}) + \left(-\frac{\beta_0}{\omega \varepsilon_0} \right) \underline{C}_N^{-1} \underline{I}_k \text{diag} (h_n(l)) \right]^{-1} \begin{bmatrix} 1 \\ 1 \\ \vdots \\ 1 \end{bmatrix} \quad (6.3.9)$$

from which:

$$Y = \sum \underline{I}(0) \quad (6.3.7)$$

The length of the patch evaluated must consider the extensions due to boundary effects. Since the conductors are very close together, these extensions may be calculated as in the case of the rectangular patch [52]. Thus this length obtained which allows to have an imaginary part of the impedance is the effective length. This means that the actual length will be equal to:

$$L_{real} = L_{eff} - 2\Delta L \Rightarrow \Delta L = 0.412h \frac{(\varepsilon_{eff} + 0.3) \left(\frac{W}{h} + 0.264 \right)}{(\varepsilon_{eff} - 0.258) \left(\frac{W}{h} + 0.8 \right)} \text{ con } \varepsilon_{eff} = \frac{1}{2} \left[(\varepsilon_r + 1) + (\varepsilon_r - 1) \frac{1}{\sqrt{1 + \frac{12h}{W}}} \right]^{-1/2}$$

where L_{eff} is the length evaluated with mathematic method.

Chapter 7

Experimental Results

In this chapter, the model for coupled lines discussed in Chapter 6 is validated. In Section 7.1 the geometry of the antenna under test is presented. In Section 7.2, for validating the circuital model, a generic patch composed of the classic FR4 substrate has been studied. Since the model composed of 20 conductors connected in parallel obtained good results, in Section 7.3 I conducted further tests with the aim of verifying that such a model is also adaptable to a generic number of conductors connected in parallel. Once the model was validated, in Section 7.4 I studied a wearable patch using the jeans as the substrate. Validation was performed by comparing the results obtained from the circuital model with the patch realized with the software Prelude.

7.1. Geometry of antennas under test

The working frequency used in the simulations is 900 MHz. For this frequency the wavelength of a rectangular patch is about 16 cm. I started with a width of the patch (W) shorter than $\frac{\lambda_0}{2}$ due to the low frequency (which would have made a patch $\frac{\lambda_0}{2}$ too long too long).

Obviously, the full patch and the multi-conductor patch have the same width. The width used for the tests was previously set and was kept constant for all the different structures analysed for the validation of the model.

Parameters and design variables used for the simulations are:

- multi-conductor patch: n conductors connected in parallel;
- total width of the patch is fixed: $W = 102.383$ mm;
- width of the single patch inside the structure: W_c ;
- width of the gap between the two conductors: W_p ;
- points for gap discretization (for estimating C with the finite-difference method): N ;
- substrate: FR4 with $\epsilon_r = 4.3$;
- metallic patch: copper;

- substrate thickness: $h=3\text{mm}$;
- length extension: $\Delta L=1.39522\text{mm}$;
- characteristic impedance for rectangular patch: $Z_{in}= 296.640215-0.009501217j$.

A generic n-conductor patch is shown in Fig. 7.1.

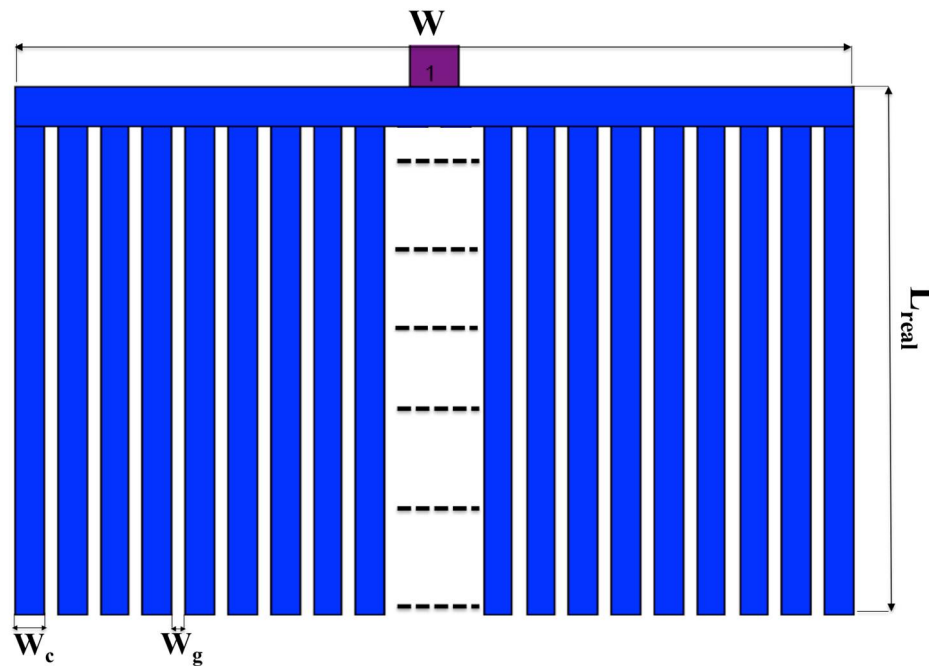


Fig. 7.1: Geometry of a n-conductor patch.

7.2. First validation

The aim of this section is to make a first validation of the model and evaluate how the various parameters affect the accuracy. Using the data described in Section 7.1, the specific data for this first test validation are:

- number of conductors: $n=20$;
- width of the single conductor: $W_c=3.51027\text{mm}$;
- width of the gap: $W_g= 1.69356 \text{ mm}$;
- FDFD discretization points: $N=16$;

The patch shown in Fig. 7.2 is obtained.

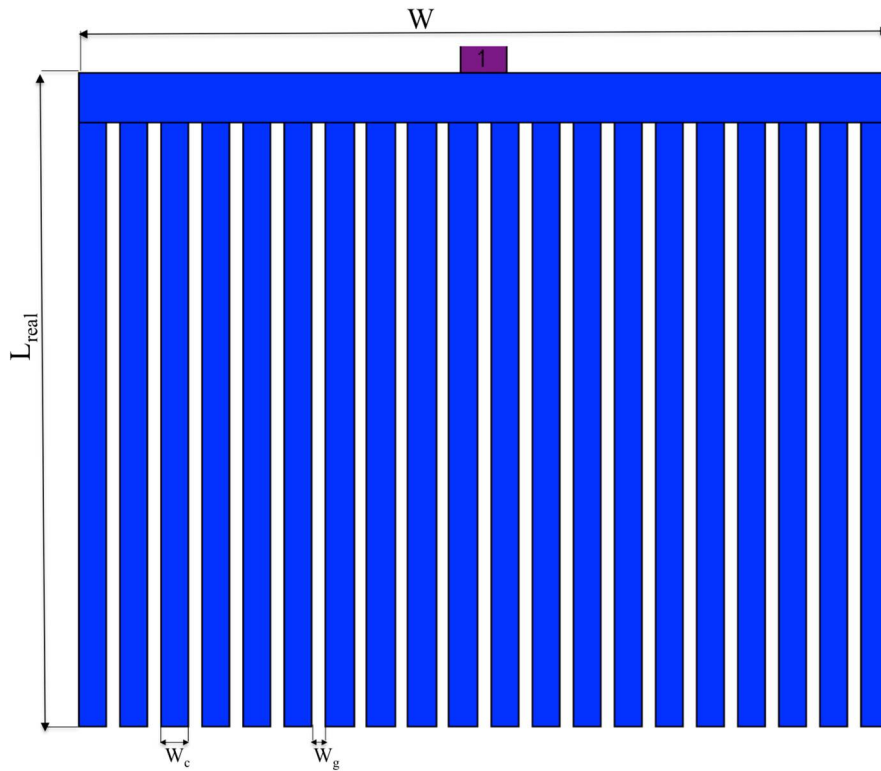


Fig. 7.2: 20-conductor patch.

Using 16 points for the discretization on the gap (this value was chosen by evaluating the graph showing the capacitance in function of the points, see Appendix for details) the capacitances of the structure are evaluated (using the method described in Chapter 6), obtaining:

| Normalized capacities [C/ε ₀] | |
|--|---------|
| C _e | 34.979 |
| C _i | 33.4538 |
| C _{mi} | 1.77141 |
| C _{me} | 1.46481 |

| Normalized capacities [C _A /ε ₀] | |
|--|---------|
| C _{Ae} | 9.71228 |
| C _{Ai} | 8.62274 |
| C _{Ami} | 1.48427 |
| C _{Ame} | 1.07662 |

From these values it was possible to determine the length and the impedance of resonance which are summarized in TABLE 7.1:

TABLE 7.1: Parameters of resonance – first test (n=20 and N=16).

| L_{efficace} [mm] | ΔL [mm] | L [mm] | L_{real} [mm] | Error I % | Z | Z_{real} | Errore Re(Z)% |
|-------------------------------|--------------------|-------------|---------------------------|--------------|----------------------------|--------------------|------------------|
| 84.9994 | 1.39522 | 82.209 | 82.24761 | 0.046944 | $3.8040e+02 - 4.8592e-09i$ | $369.63+0.007219i$ | 2.91372 |

The results are very promising. In fact, the values obtained with the circuital model are in agreement with those obtained experimentally with the software Prelude, so that there is an error on the evaluation of the length of 0.05% approximately. A similar error can be noticed in the determination of the real part of the impedance for which an error smaller than 3% is evaluated. Then, experimental results validate the proposed model.

However, in the analysis done, the R_{in} that has been chosen for the circuital evaluation of the model, is approximate. In order to assess whether this choice is suitable for the proposed model, the influences on I_{ris} has been evaluated.

By varying the resistance from a minimum of 200 Ω to a maximum of 400 Ω it is found that I_{ris} varies less than 0.0002%. Therefore, I can state that the behaviour at the resonance is very well reconstructed with a diagonal R (thus neglecting the couplings between the terminations of conductors).

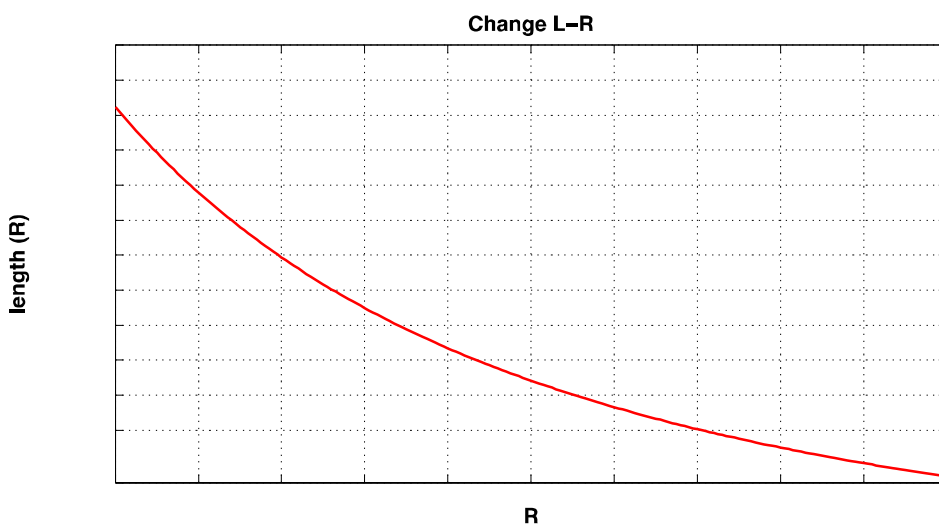


Fig. 7.3: Rirr in function of the length.

A second test has been performed using the same parameters used in the first test but choosing 36 points for the discretization on the gap instead than 16. Then with $N = 36$, the following results have been obtained:

- capacities evaluation:

| Normalized capacities [C/ε ₀] | |
|--|---------|
| C _e | 35.8715 |
| C _i | 34.5043 |
| C _{mi} | 1.50307 |
| C _{me} | 1.32046 |

| Normalized capacities [C _A /ε ₀] | |
|--|---------|
| C _{Ae} | 9.81292 |
| C _{Ai} | 9.35496 |
| C _{Ami} | 1.35536 |
| C _{Ame} | 1.04425 |

TABLE 7.2 summarizes the results obtained:

TABLE 7.2: Parameters of resonance – second test (n=20 and N=36).

| <i>L_{efficace}</i> [mm] | <i>ΔL</i> [mm] | <i>L</i> [mm] | <i>L_{real}</i> [mm] | <i>Error</i> I % | <i>Z</i> | <i>Z_{real}</i> | <i>Errore</i> Re(Z)% |
|-------------------------------------|-------------------|------------------|---------------------------------|---------------------|--------------------------|-------------------------|-------------------------|
| 84.80004 | 1.39522 | 82.0096 | 82.24761 | 0.289382 | 3.6120e+02 - 1.5381e-09i | 369.63+0.007219i | 2.28066 |

Evaluating these results, it can be noticed that the number of discretization points influences the capacitance calculation and the length and the impedance of the patch realized with the circuital model. In this case, the error on the length and also on the impedance are still good, but compared to the previous case a slight increase of the error on the length can be noticed. Since the aim of the analysis is to make the error on the length as close as possible to zero, 16 discretization points are the optimum choice.

By keeping fixed the width of the single conductor and of the total patch, the width of the gap has been increased, obtaining a 12-conductor patch. Then, the parameters used for this test are:

- number of conductors: n=12;
- width of the single conductor: W_c = 3.51027mm;
- width of the gap: W_g = 5.4781 mm;
- FDFD discretization points: N=16;

It is obtained the patch show in Fig. 7.4.

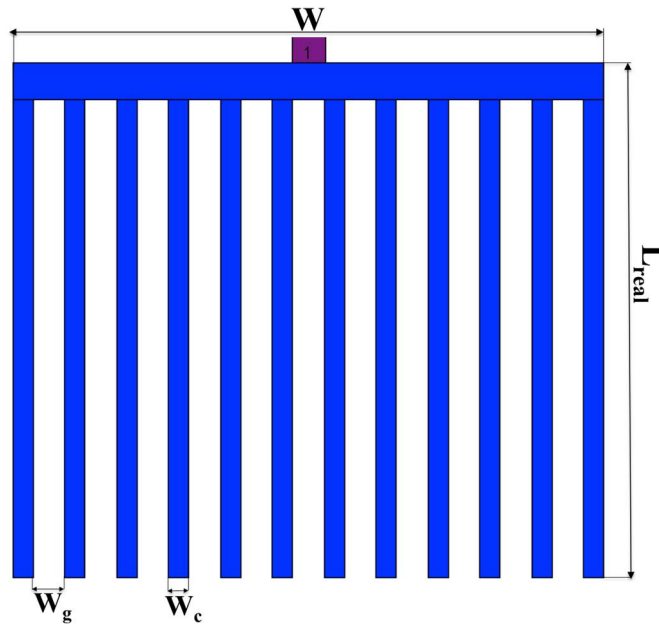


Fig. 7.4: 12-conductor patch.

The capacities evaluated from this patch are:

| Normalized capacities [C/ε ₀] | |
|--|---------|
| C _e | 36.2201 |
| C _i | 35.9409 |
| C _{mi} | 0.2747 |
| C _{me} | 0.2007 |

| Normalized capacities [C _A /ε ₀] | |
|--|---------|
| C _{Ae} | 10.4382 |
| C _{Ai} | 10.0482 |
| C _{Ami} | 0.4522 |
| C _{Ame} | 0.2933 |

TABLE 7.3 summarizes the results obtained:

TABLE 7.3: Parameters of resonance – third test (n=12 and N=16).

| L _{eff} [mm] | ΔL [mm] | L [mm] | L _{real} [mm] | Error 1 % | Z | Z _{real} | Error Re(Z) % |
|--------------------------|------------|-----------|---------------------------|--------------|-----------------------|-------------------|------------------|
| 87.35 | 1.39522 | 84.55956 | 83.42976 | 1.35419 | 504.89e - 2.9237e-09i | 507.407-0.00641i | 0.4985 |

Comparing the results obtained between the 20-conductor patch and the 12-conductor patch, it can be noticed that in the case of 12 conductors the width of the gap larger than the width of the single patch causes lower accuracy in the calculation of the mutual capacitances. Then, higher error values are obtained on the evaluation of the length of the patch, for which an error of 1.35419% has been obtained instead of an error of 0.046944% obtained with the previous test.

7.3. Test with different multi-conductor

In this section, the results of further tests are presented. The number of conductors and the width of the conductors are the parameters of interest.

The parameters considered for the two different cases are:

- CASE 1
 - number of conductors: $n=40$;
 - width of the single conductor: $W_c = 1.73042\text{mm}$;
 - width of the gap: $W_g = 0.850419\text{ mm}$;
 - number of discretization points on the gap: $N=16$;
- CASE 2
 - number of conductors: $n=80$;
 - width of the single conductor: $W_c = 0.850419\text{mm}$;
 - width of the gap: $W_g = 0.425954\text{ mm}$;
 - number of discretization points on the gap: $N=16$;

Figs. 7.5 and 7.6 show the 40-conductor and the 80-conductor patch, respectively.



Fig. 7.5: 40-conductor patch.

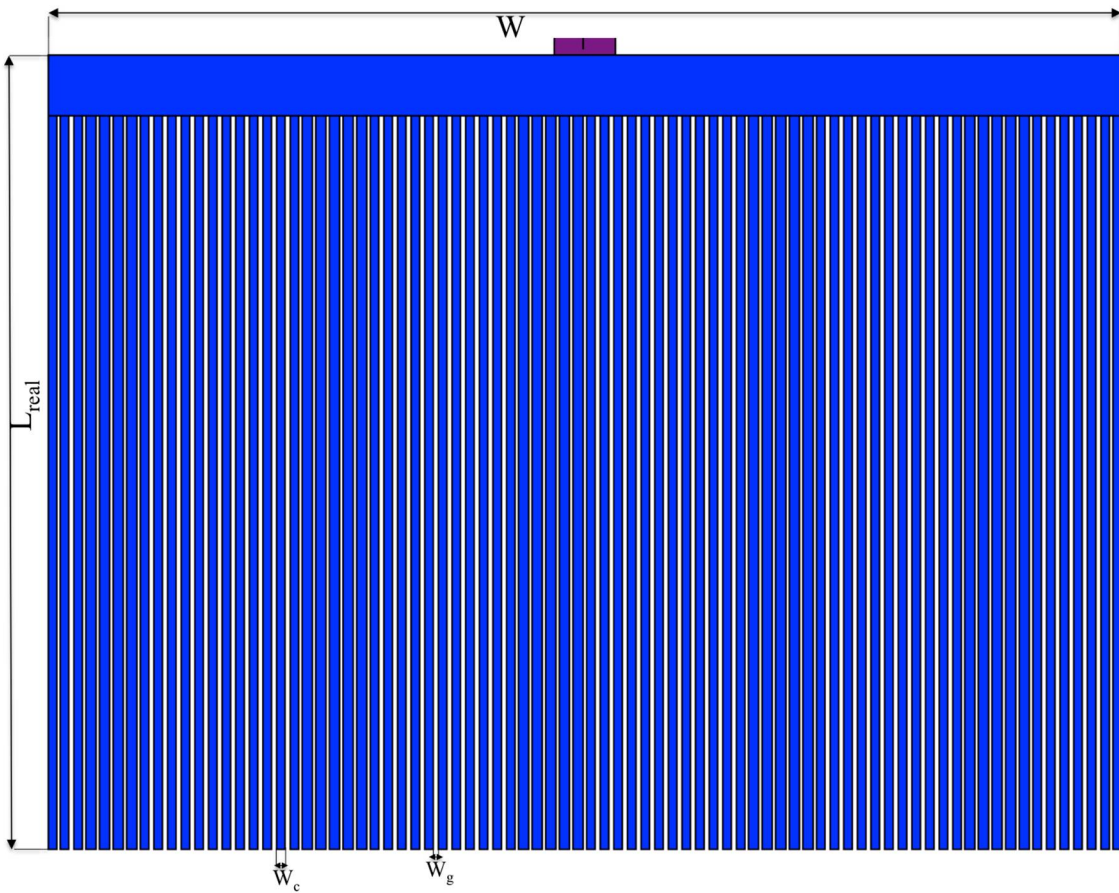


Fig. 7.6: 80-conductor patch.

As in the previous case, the error on the length and on the impedance obtained with the circuital model have been evaluated. Then, the results obtained are compared with those obtained with the software Prelude. Table 7.4 summarizes the results obtained:

TABLE 7.4: Parameters of resonance.

| $L_{efficace}$ [mm] | ΔL [mm] | L [mm] | L_{real} [mm] | Error I % | Z | Z_{real} | Errore Re(Z) % |
|------------------------|--------------------|-------------|--------------------|--------------|----------------------------|------------------------------|-------------------|
| 84.81004 | 1.39522 | 82.0196 | 81.9365 | 0.101432 | $3.6060e+02 - 3.7671e-11i$ | $352.488-0.008548i$ | 2.30135 |
| 84.70004 | 1.39522 | 81.9096 | 81.4095 | 0.6143018 | $3.7258e+02 + 4.3269e-09i$ | $378.572484+0.00607$ 8785 | 1.582916 |

From Table 7.4 it can be noticed that increasing the number of conductors and consequently decreasing the size of the conductors (while maintaining the width of the gap smaller than the width of the conductor), the error on the length remains nearly zero, with a lower accuracy than in the case of 20 conductors but still a low error that validates the model used. The same result is evaluated in the calculation of the impedance where the error is, however, also in this case less than 3%.

7.4. Test with substrate wereable

Once validated the circuital model for a classic substrate (FR4), a textile substrate has been chosen with regard to the application of the antenna on the human clothes. The parameters used for this test are:

- number of conductors: $n=80$;
- width of the total patch: $W=143.4\text{mm}$, $L=125.829$;
- width of the single patch: $W_c=1.2\text{ mm}$;
- with of the gap: $W_g=0.6\text{ mm}$;
- number of discretization points: $N=16$;
- substrate: jeans with $\epsilon_r=1.7$;
- metallic patch: conductive ink with Electric Conductivity: $2.5e+007$; $Mue: 1$;
- thickness of the substrate: $h=3\text{mm}$
- characteristic impedance for rectangular patch: $Z_{in}=(231.25228+0.0068794359i)\Omega$

By using the optimum number of discretization points (N=16) previously computed, the capacitances have been computed:

| Normalized capacities [C/ε ₀] | |
|--|---------|
| C _e | 15.1455 |
| C _i | 13.9582 |
| C _{mi} | 1.51184 |
| C _{me} | 1.14327 |

| Normalized capacities [C _A /ε ₀] | |
|--|---------|
| C _{Ae} | 9.71228 |
| C _{Ai} | 8.62274 |
| C _{Ami} | 1.48427 |
| C _{Ame} | 1.07662 |

From the evaluation of the capacities we are able to calculate the length and the impedance with the circuital model and with Prelude, which are summarized in TABLE 7.5.

TABLE 7.5: Parameters of resonance.

| <i>L_{efficace}</i> [mm] | <i>ΔL</i> [mm] | <i>L</i> [mm] | <i>L_{real}</i> [mm] | <i>Error</i> 1% | <i>Z</i> | <i>Z_{real}</i> | <i>Errore</i> Re(Z)% |
|-------------------------------------|-------------------|------------------|------------------------------|--------------------|--------------------------|-------------------------|-------------------------|
| 130.1 | 1.70786 | 126.68428 | 125,53778 | 0.913271 | 3.6060e+02 - 3.7671e-11i | 353.066-0.006199i | 2.13388 |

Using a specific textile material for the realization of a wearable patch, the error on the length remains still good since it is lower than 1. The error on the impedance is a little more higher than 2%.

Therefore, the idea of generalizing the transmission line model (studied for the rectangular patch) is a good solution for the case of a generic patch composed of n conductors connected in parallel. Furthermore, this model also fits for the design of wearable antennas.

Chapter 8

SAR: Specific Absorption Rate

The wearable sensors are placed very close to the human body [53]. These sensors are equipped with an antenna for transmitting wireless the acquired information by irradiating a transmission power. In this Chapter, I focused on the possible biological issues which may arise on the human body from the use of these sensors. In Section 8.1 the Specific Absorption Rate (SAR) is introduced. In Section 8.2 simulations have been conducted for evaluating the effects on the human body, and especially on the head, of the wearable antenna realized with different materials.

8.1. SAR for different cases of study

A very important parameter for evaluating the biological effect of electromagnetic waves on the human body is the calculation of Specific Absorption Rate (SAR). SAR is the RF power absorbed per unit mass of biological tissue [54]:

$$SAR = \frac{(\sigma + \omega \epsilon_0 \epsilon_r'') E^2}{\rho} \frac{W}{Kg} \quad (8.1.1)$$

with E the RMS value of the electric field measured in V/m, σ the electrical conductivity of the biological tissue, ω the angular frequency, ϵ_r'' the imaginary part of complex permittivity and ρ the mass density. The SAR depends on induced electrical fields and electrical properties of human body biological tissue.

SAR's equation can also be written as follows [55]:

$$SAR = \frac{d}{dt} \left(\frac{dW}{dm} \right) = \frac{d}{dt} \left[\frac{dW}{\rho(dV)} \right] = \frac{\sigma}{2\rho} |E|^2 \quad (8.1.2)$$

Both σ and ρ depend on the type of the analyzed tissue, but ρ is frequency independent and it is different for each considered tissue. The biological effects are different and depend on the part of

the human body which is irradiated. The 70% of the human body's weight consists of water. It is evident that the body's response to the stimulus depends on the electromagnetic properties and the amount of water. The response of any biological structure also depends on the type of stimulus to which it is subject. One of the constituent variables of the electromagnetic wave is the frequency; when the frequency is low, the dielectric properties of the tissues show a strong dependency with the structural properties and are, therefore, extremely variable. When the frequency is higher, for example a hundred MHz, the answer is determined by the properties of dispersion and by the conductivity of the water molecule which is the effect of the electrolytes dissolved in the interior. The percentage of water within the tissues determines the classification of tissue into three categories:

- tissue with very high water content (90% or more) such as blood, body fluids, and cerebrospinal fluid;
- tissue with high water content (80%) as skin, brain, spleen, liver;
- tissue with low water content (50% or less) such as tendons, fat, bones.

To understand the possible harmful effect of electromagnetic wave at a given frequency, it is necessary to fully describe the electrical characteristics of biological tissue, which are the relative dielectric constant of the conductivity of each type of tissue. In this study, I focused on the head because it is the part on which the sensor is placed. In fact, a sensor is placed on the helmet of the worker, therefore the head would be the point of the human body that would absorb more radiation.

For this study, I based on the different models of the human body suggested in the literature. The human head modeling which I used is constructed with respect to the FCC, IEEE and IEC standards. In this model, I considered only the human brain's tissue as it is the largest part in the head. Usually, several types of tissues are considered: brain, viscera, airways, digestive tract, glands and muscles.

In Fig.8.1 a typical model head, the CST [56], is shown.

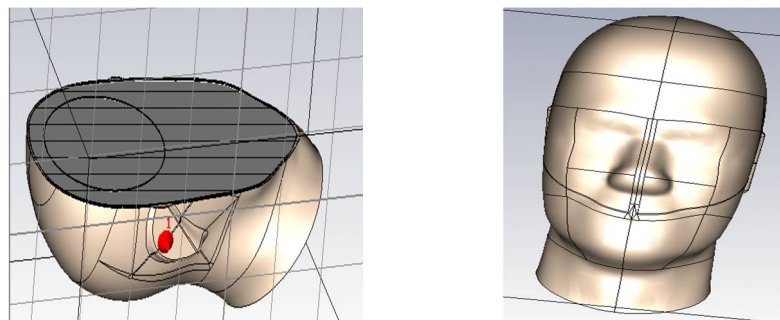


Fig. 8.1: CST model head.

To evaluate the SAR, in the literature there are several software which simulate different models of human bodies realistically. These models have often high computational costs and very accurate models have quite expensive licenses. These software allow the calculation of the SAR by solving Maxwell's equations.

The equations can be solved using analytical and numerical techniques, by using the following methods:

- a) Finite Difference Time Domain algorithms (FDTD);
- b) methods of finite difference time domain (radiation from an antenna in the presence of complex dielectric);
- c) Method Of Moments (M.O.M.);
- d) Multiple Multipole Method (M.M.P.);
- e) Finite Element Method (FEM);
- f) Analytical models.

Among the various models I considered:

- RemCom (Visible Human Project)
- Poser 6 from E-Frontier
- Sam
- Hugo (Cst)
- Norman

The difference between the various models is the number of simulated tissues, the frequency range used and the type of simulated body. Some models simulate the body of a generic man (i.e. medium size and medium build), others simulate an entire family (a man, a woman and a teenager). In some cases they can also simulate in detail the surrounding environment in order to be more precise. This suggests that these models can be more accurate, but the price to pay is a higher computational cost. The same thing occurs when simulating only the head instead of the whole human body.

There are several models of the head which vary by size and type of used materials. Many models that simulate the architecture of the human body and therefore also of the head are available. Among them:

- Phantom POPEYE V5.X [57]: it is a structure with anatomical features similar to those of humans, and has been designed to be used in particular tests for which the effects of electromagnetic performance on the body cannot be neglected;
- SAM Head Phantom [58], designed for the evaluation of radiation and total radiated power on the human head. There are three interesting head models,

-
- SAMV 4.5 E is a light and strong model of the head with the presence of an anatomically precise ear with ear canal, designed to assess radiation and total radiated power by devices such as hearing aids, wireless headphones, and Bluetooth devices;
 - SAMV 4.5BS is a model of the head that consists of an extremely lightweight solid. This model was filled with solid material Broadband (Compatible with 3.2VCTIA), and it turns out to be 30% lighter than the Phantom filled with liquids containing sugar (in fact it has a weight of 7 kg). In this model there is a positioner for hands (high precision and easy to use);
 - SAMV 4.5 is the last of these head model and is compatible with the simulation of all tissue fluids, including solvents such as recipes DGBE. Haa volume of 7.2l;
 - Hugo [59-60] is a 3D model of the human body that can be used for simulations of electromagnetic fields.

During these studies I have evaluated simpler models than the models mentioned above, but for our frequencies of interest these simplified models still provide very good results, but with reduced computational costs in terms of memory usage and processing time.

Firstly, I tried to use a simplified model of the whole human body, because, in the proposed wearable sensors network the antennas are distributed from the head to the toe, then throughout the body. One of the basic concepts is that SAR should be inversely proportional to the distance, and directly proportional to the output power of the device emitting the electromagnetic field. Only checking these initial conditions a model that satisfy the required specifications can be created.

For the first simplified model used to calculate the whole body SAR I used the model description in [61]. Then I have extended the concept of “representation of a limb as the whole body”, and I rounded the whole body to a cylinder composed solely of a material with medium-high water content (representing the muscle tissue), neglecting all biological anisotropy in order to maximize the dose quantity. In fact, the body is relevant as a “whole”, taking into consideration that the antennas are distributed all over the body [62].

In this case the parameters for simulation are:

- frequency: 900 MHz with a circular antenna polarization;
- gain: 6 dBi;
- density: $\sigma = 0,65$ S/m;
- electrical conductivity: $\rho = 1306$ kg/m³.

The SAR calculated as a function of the reader’s distance from the human body in function of three different transmitting powers is shown in Fig. 8.2.

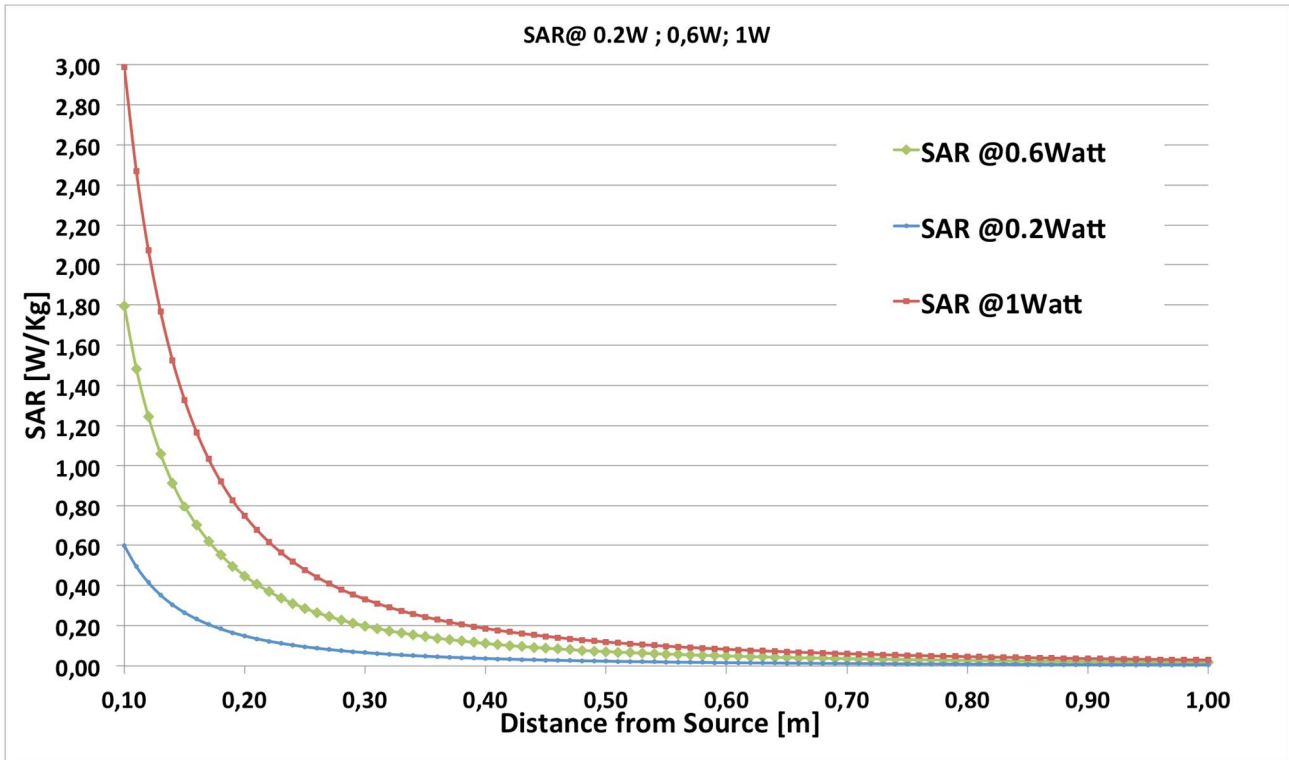


Fig. 8.2: SAR (W/kg) vs. distance from the human body for varying reader powers.

The most restrictive international limits for the SAR are those imposed by the FCC in the US, which states a limit value of SAR=1.6 W/kg. The IEC (International Electrotechnical Commission) recommends a slightly higher value of 2 W/kg, valid for the EU, South Korea and Japan. From Fig. 8.2 it can be observed that the FCC limit can be reached for a value of 0.6 W of radiated power only at a distance of 10 cm from the human body. For 0.2 W the FCC limit is not a problem, which is not the case for 1 W of radiated power where the SAR limit is reached at around 20 cm.

In the second simulation I used the Hugo model with appropriate variations. I focused on the head as it is the part most subject to an EF. In fact, in addition to the sensor, in some cases the operator may also use the radio/telephone, or may use another sensor such as a headset placed in his ear.

TABLE 8.1 Dielectric constants of the materials used in the simulations.

| | ϵ_r | Electrical Conductivity [S/m] |
|-------|--------------|-------------------------------|
| Skin | 31.29 | 8.0138 |
| Bone | 12.661 | 3.8591 |
| Brain | 38.111 | 10.31 |

In this simulation, I considered a sensor that operates at a frequency of 900 MHz. I have simulated an exposure scenario modelling the sensor as a perfectly conducting box with a monopole antenna and using the simplified head model. The head model was approximated by taking into account only the presence of skin and skeleton surface and it was enriched adding the brain and then approximated with a half spherical cap. In the simulation, I have moved the sensor from the head to a distance of 10 cm, and then I calculated the SAR in these conditions with CST.

In this case the SAR is shown in Fig. 8.3. This simulation refers to an exposure to electromagnetic waves of one person's head. At a distance of less than 2 cm there can be problems of power consumption and so it is necessary to be more careful.

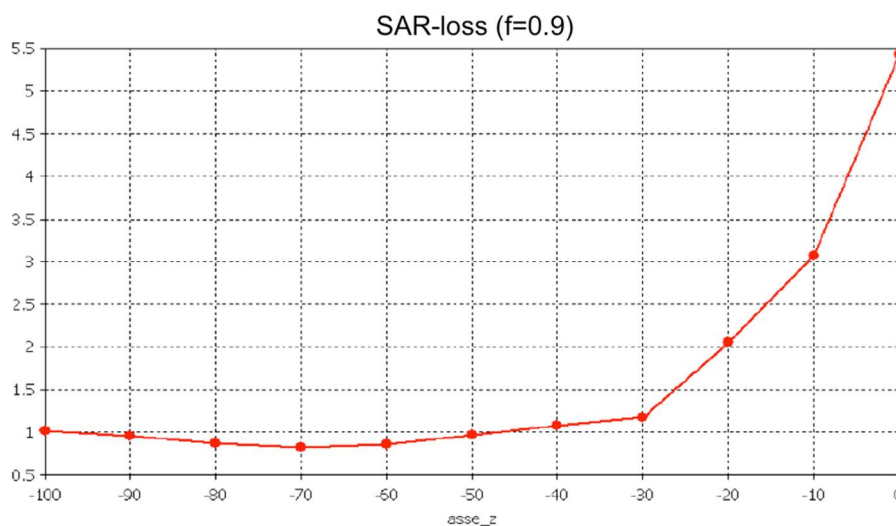


Fig. 8.3: Evaluation of the SAR at $f=900\text{MHz}$ changing the position of the sensor between 0 cm and 10 cm.

8.2. Wearable Rectangular Patch Antenna

In recent years, many research groups have shown a great interest in the study of integrating antenna in the garments, and there are currently many systems integrated in the clothes which offer functions such as monitoring of life signs, positioning, temperature etc. [63]-[64]-[65]. The wearable antenna should have features like light weight, conformal, easy to hide, and it should not affect the user's health. Synthetic or natural materials are used as substrate to manufacture the textile or cloth-based wearable antennas. For this use there are different textiles.

In this research I have studied the importance of wearable sensor at 900 MHz frequency. This particular sensor is very suitable for this application and do not create problem to the human body because the range of frequency respects the SAR (Specific Absorption Rate) constraints [62]-[55]. This research exploits the potential of textile materials for use in this new application. The important aspect of these antennas is that chip antennas are not invasive, they are small and light weight and do not disturb the movements of the person wearing them. The flexibility of textile materials is a real challenge for antenna designers. A continuous progress in material development together with a constant evolution in the field of electronics enable the integration of technologies into garments in order to increase their functionalities. The aim of this analysis is to present a rectangular patch microwave antenna composed of different materials. The materials used for simulation are materials that can be integrated into the garments. It is very important to evaluate the potential dosimetry effects on the human body. The antenna and the body have been simulated with CST microwave.

I considered the rectangular patch. The major characteristic of this particular antenna are the length and the width. In order to calculate these lengths I used the equation [52]:

$$W = \frac{c}{2f} \sqrt{\frac{2}{(1 + \epsilon_r)}} \quad (8.2.1)$$

where c is the speed of the light, ϵ_r is the dielectric constant of the substrate, and f is the working frequency.

The equation to calculate antenna's length is:

$$L = L_{eff} - 2\Delta \quad (8.2.2)$$

where :

$$L_{eff} = \frac{c}{2f\sqrt{\epsilon_{eff}}}, \Rightarrow \Delta L = 0.412h \frac{(\epsilon_{eff} + 0.3) \left(\frac{W}{h} + 0.264\right)}{(\epsilon_{eff} - 0.258) \left(\frac{W}{h} + 0.8\right)} \quad (8.2.3)$$

and ϵ_{eff} is the relative permittivity:

$$\epsilon_{eff} = \frac{1}{2} \left[(\epsilon_r + 1) + (\epsilon_r - 1) \frac{1}{\sqrt{1 + \frac{12h}{W}}} \right]^{-1/2} \quad (8.2.4)$$

whith h is the substrate's thickness.

The main parameters are:

- resonant frequency at 900MHz and at -10dB above 1% that is to $Bw > 9$ MHz;
- cross polar evaluated on cuts at 0° and a 90° in the Band $900\text{ MHz}+Bw$ and $900\text{ MHz}-Bw$ of less than -10dB;
- patch's material: conductive ink;
- substrates: 2 different substrates have been considered: jeans fabric and polyacetal.

The design of the antenna is represented in Fig. 8.4.

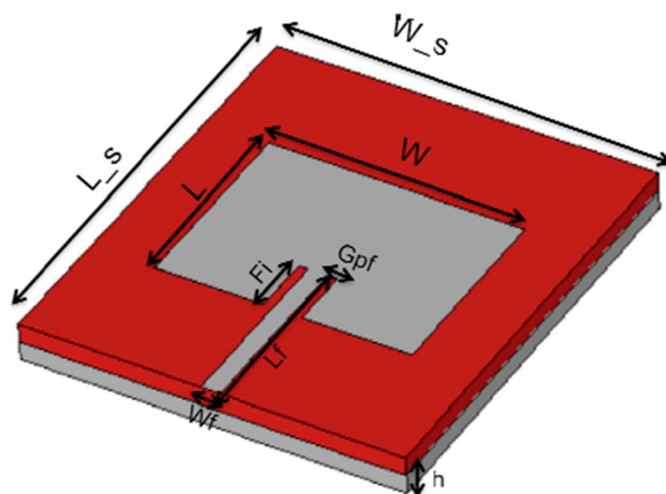


Fig. 8.4 Geometry of rectangular patch antenna.

In Table 8.2 the dimensions and parameters of the patch antenna at the frequency of 900 MHz are summarized.

TABLE 8.2 Dimensions and parameters of the patch antenna at the frequency of 900 MHz.

| Parameter | Substrate jeans | Substrate polyacetal |
|--------------|-----------------|----------------------|
| W | 124.5 mm | 110 mm |
| L | 140.5 mm | 90 mm |
| Ws | 156.5mm | 114 mm |
| Ls | 150.5 mm | 128 mm |
| Gpf | 11.3 mm | 15 mm |
| Lf | 36 mm | 40 mm |
| Mt | 0.1 mm | 0.1 mm |
| Fi | 18.5 mm | 21 mm |
| h | 3 mm | 3mm |
| Wf | 8.7 mm | 9 mm |
| ϵ_r | 1.7 | 3.8 |
| Tan δ | 0.02 | 0.08 |

In all antennas the patch is in conductive ink. The physics parameter of the substrate I refer are reported in [65],[66].

In my simulation I used the jeans fabric and the polyacetal: the jeans is a soft and easy tissue to use on the garment; the polyacetal is a particular material, it is a combination of PTFE febers uniformly distributed, the material has a lower stiffness, but it improves the flow ability greatly reducing the coefficient of friction. I have simulated the three different antenna in CST, and I have analyzed the antennas with the particular substrates (polyacetal and jeans). In TABLE 8.3 the dimension, gain, band, and S11 of the substrates are summarized.

TABLE 8.3 Results of simulation for different materials.

| Substrate | S11(dB) | B [MHz] | Bw (MHz) -10dB | Dimension patch LxW [cm] | Gain (dB) |
|-----------|---------|------------------|-----------------|--------------------------|-----------|
| Jeans | -25.83 | 890.375 - 919.25 | 19.25 | 12.45x14.05 | 3.931 |
| FR4 | -23.45 | 880.10 – 919.81 | 19.81 | 8.5x9 | 4.82 |
| Polycetal | -23.23 | 883.33 – 916.67 | 16.67 | 12.8x11.4 | 4.622 |

In Fig. 8.5, the field distribution at 900MHz + Bw and a 900MHz –Bw for two different cut at 0° and a 90° are shown.

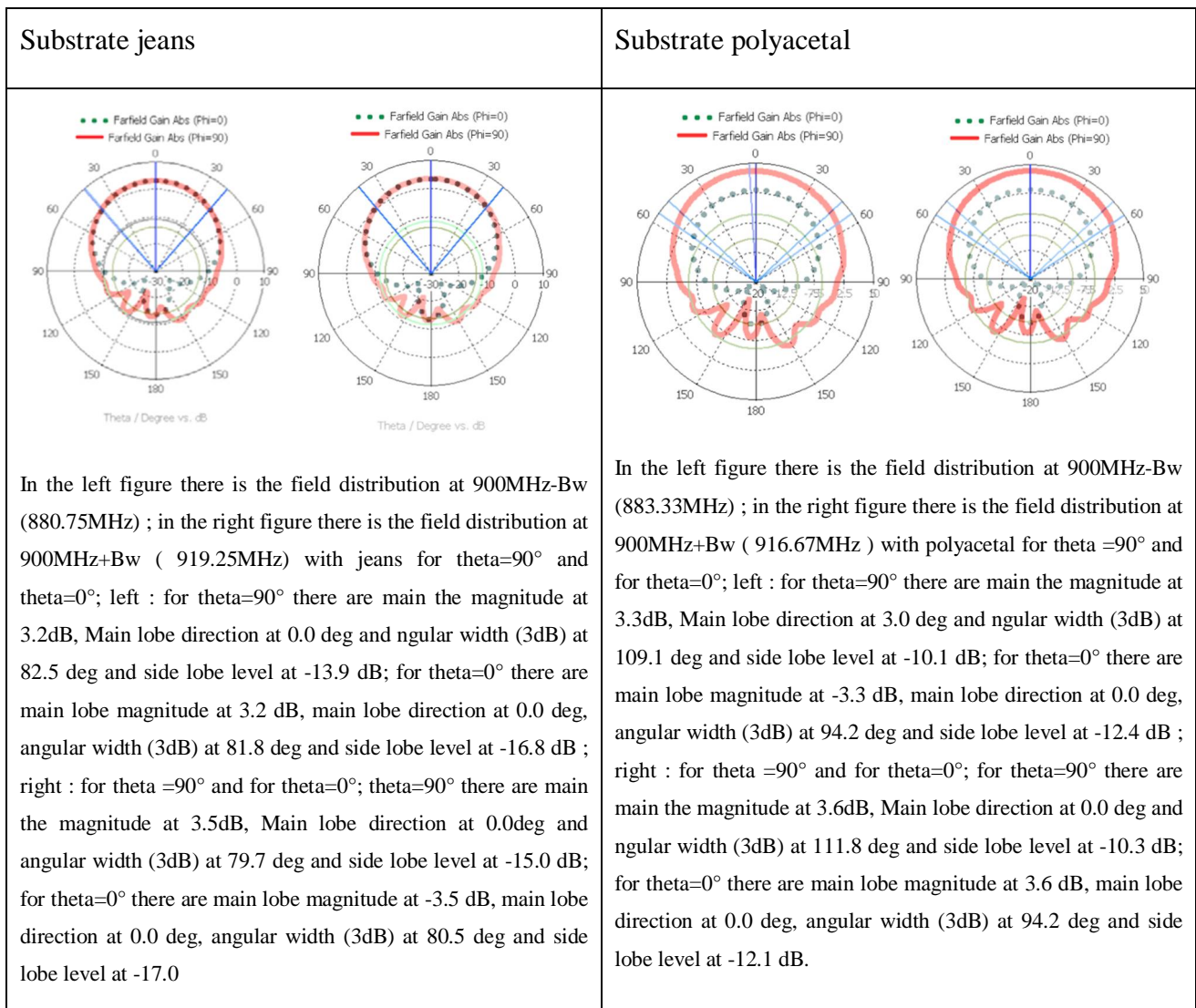


Fig. 8.5: Field distribution at 900MHz + Bw and at 900MHz –Bw for two different cut at 0° and a 90°.

From the data reported in Table 8.3 it is evident that the specific bandwidth to -10dB exceeding 1% was observed in the two cases 19.25 MHz and 16.67 MHz, by the fact that in the two bands of interest the response is below -15 dB. From the graphs of Fig. 8.5 it can be seen that both the cut at 0° and to 90° have components with lower lobes in -10. With regard to the gain, from Table 8.3 it can be seen that the use of Polyacetal provide a higher value of gain.

Even for this type of analysis the SAR is a very important factor to be calculated. It is very important because the evaluation of the Specific Absorption Rate (SAR) is the dosimetric quantity

of interest. For these simulations I used a cylinder to approximate the human body (35 cm high; 38 cm radius; filled with saline solution 1% (S/m)).

I have evaluated the SAR with and without the saline solutions.

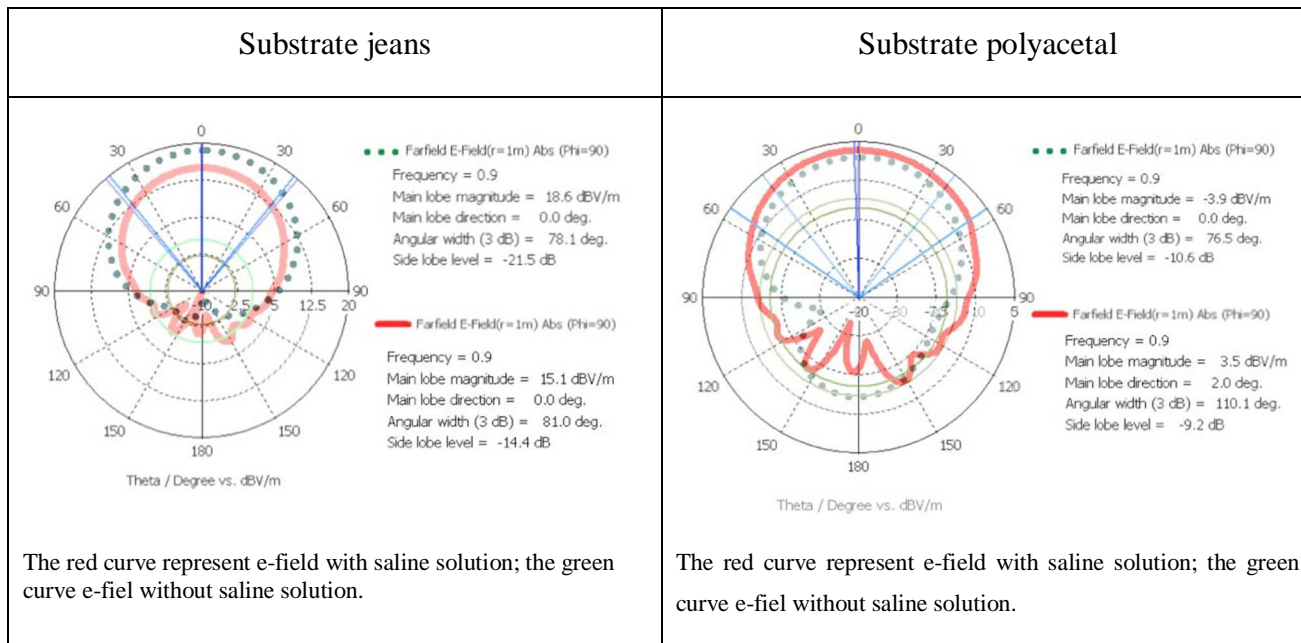


Fig. 8.6: Far Field for different substrate with and without saline solution.

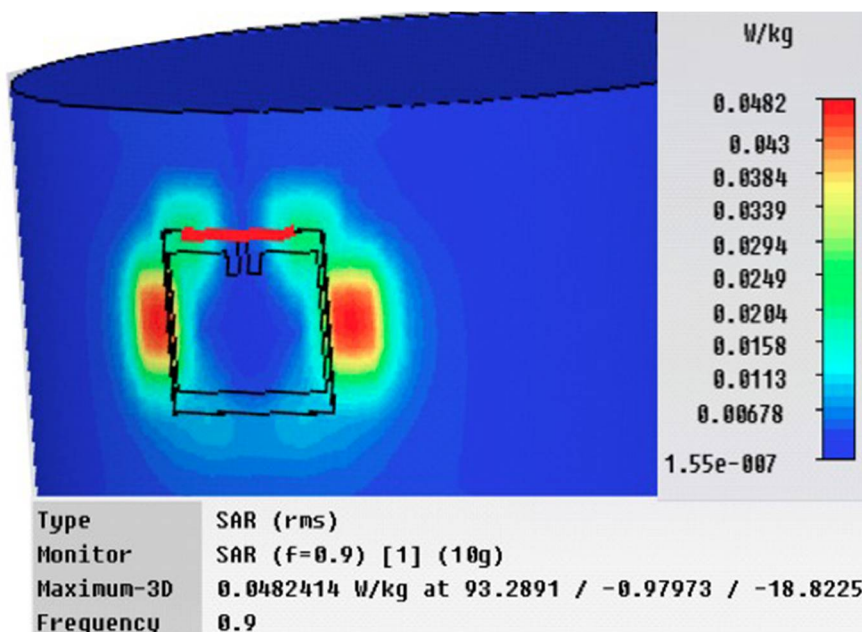


Fig. 8.7: SAR for substrate jeans.

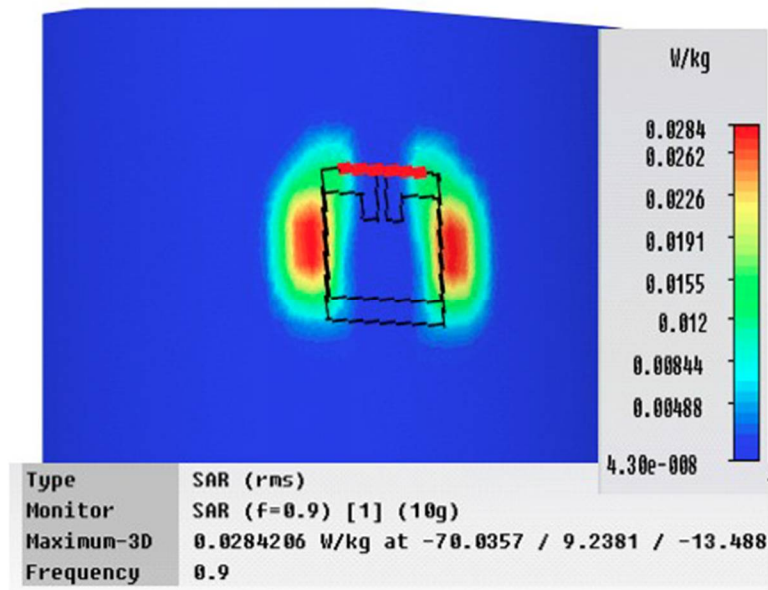


Fig. 8.8: SAR for substrate polyacetal.

The max SAR for polyacetal substrate is 0.0284 W/kg and for jeans is 0.0482 W/kg, and both these values respect the international limits for the SAR (the ones imposed by the FCC in the US, which states a limit value of SAR=1.6 W/kg). The IEC (International Electrotechnical Commission) recommends a slightly higher value of 2 W/kg , valid for the EU, South Korea and Japan

Chapter 9

Conclusion and future works

In this thesis three main topics have been addressed:

1. In the first part, I studied a control system for an industrial area that ensures greater safety for workers. Specifically it is considered the port of Cagliari (the fourth largest commercial port of Italy imported). To ensure greater safety and fewer accidents in industrial areas, the proper use of PPE plays an important role. Through the study of state-of-the-art control systems for the safety of vehicles and people, I decided to integrate the infrastructure with the study of a wearable sensor network characterized by passive RFID and a particular type of passive sensor, the WISP.

The proposed wearable sensor network is composed of four sensors placed on the PPE. Specifically, one RFID is placed in the jacket, two RFID tags are placed in the shoes and a WISP tag with accelerometer is placed on the helmet of the worker. The data acquired in real-time by the sensors is read by several gates placed in the considered area. The gates are connected to the panel via the Ethernet network. The RFID sensors allow to identify the presence of the PPE on the body of the workers. The WISP allows to evaluate not only the presence of the PPE but whether the PPE is correctly worn, thanks to the accelerometer integrated into the WISP. The server computes a comparison between the coordinates acquired by the accelerometer with threshold values which allow to identify the position of the helmet in space, and then to assess whether it was or was not worn properly. At the same time, a system for the monitoring of the vehicles is developed, which is able to interoperate with the system for the monitoring of the workers.

The data acquired by the monitoring system is sent to a control centre which allows the identification in real time of vehicles and people.

2. In the second part, I designed a circuital model for the realization of the particular wearable antennas which are the nodes the proposed wearable sensor network. Differently from conventional sensors, wearable sensors ensure a higher level of comfort, and provide higher electromagnetic performance. Furthermore, textile materials are easily available. Microstrips are good candidates for these applications

because they mainly radiate perpendicularly to the planar structure, and their ground plane allows a good shielding on the body tissues. Therefore, I have designed specific antennas for RFID, that unlike the classical microstrip antennas have the radiating surface composed of several "side by side" conductive "threads of textile". Since the microwave model does not allow the design of an antenna with these characteristics with a good approximation, a specific microwave model for coupled lines has been designed. For validating the circuital model, a generic patch composed of the classic FR4 substrate has been studied. Since the model composed of 20 conductors connected in parallel obtained good results, I conducted further tests with the aim of verifying that such a model is also adaptable to a generic number of conductors connected in parallel. Once the model was validated, I studied a wearable patch using the jeans as the substrate. Validation was performed by comparing the results obtained from the circuital model with the patch realized with the software Prelude.

3. In the last part, the possible biological issues which may arise on the human body from the use of these sensors have been analysed. The Specific Absorption Rate (SAR) has been considered and simulations have been conducted for evaluating the effects on the human body, and especially on the head, when irradiated with the electromagnetic waves generated by the wearable antenna at 900 MHz. Dosimetric effects have been evaluated in function of the distance from the body, in order to define a safe distance for placing the antenna on the human body. By varying the distance from 0 cm to 10 cm, the results show that a distance of 2 cm respects the international limits for the SAR. The same analysis has been performed using a simplified model of the head, and results respecting the international limits for the SAR were obtained. Finally, it was investigated the SAR for the sensors wearable textile designed with the proposed model of coupled lines. The SAR has been evaluated also for full patches with different textile substrates, whose surface is larger than that of the proposed model of coupled lines. Therefore, if the SAR values evaluated for the full patch are satisfying, the SAR values for the model of coupled lines will surely be acceptable. For these simulations, a simplified model of the human body has been used, whereas for the wearable substrate the polyacetal (particular plastic material, but flexible enough to be adapted to the shape of the garment) and the jeans have been used. Results show that the SAR for the proposed wearable antennas with these substrate respect the international limits for the SAR.

Future works will focus on the prototype of the proposed patch and on the evaluation of these sensors for the proposed real-time monitoring system of the port area.

Appendix

10.1. Computation of the eigenvectors

Starting from the impedance relation:

$$Z = \frac{\beta}{\omega} C^{-1}$$

the matrix C can be described as:

$$C_N = \begin{bmatrix} C_e + C_{me} & -C_{me} & 0 & 0 \\ -C_{me} & C_i + C_{me} + C_{mi} & -C_{mi} & 0 \\ 0 & -C_{mi} & C_i + C_{me} + C_{mi} & -C_{me} \\ 0 & 0 & -C_{me} & C_e + C_m \end{bmatrix}$$

Then the eigenvectors of C_N^{-1} can be computed:

$$V_1 = \begin{bmatrix} -1 \\ \frac{\left(C_e - C_{me} - 2C_{mi} + \sqrt{C_e^2 - 2C_e C_{me} - 4C_{mi} C_e + C_{me}^2 + 4C_{mi} C_{me} + 4C_{me}^2 + 4C_{mi}^2} \right)}{2C_{me}} \\ \frac{\left(C_e - C_{me} - 2C_{mi} + \sqrt{C_e^2 - 2C_e C_{me} - 4C_{mi} C_e + C_{me}^2 + 4C_{mi} C_{me} + 4C_{me}^2 + 4C_{mi}^2} \right)}{2C_{me}} \\ 1 \end{bmatrix}$$
$$V_2 = \begin{bmatrix} -1 \\ \frac{\left(C_e - C_{me} - 2C_{mi} + \sqrt{C_e^2 - 2C_e C_{me} - 4C_{mi} C_e + C_{me}^2 + 4C_{mi} C_{me} + 4C_{me}^2 + 4C_{mi}^2} \right)}{2C_{me}} \\ \frac{\left(C_e - C_{me} - 2C_{mi} + \sqrt{C_e^2 - 2C_e C_{me} - 4C_{mi} C_e + C_{me}^2 + 4C_{mi} C_{me} + 4C_{me}^2 + 4C_{mi}^2} \right)}{2C_{me}} \\ 1 \end{bmatrix}$$

$$V_3 = \begin{bmatrix} 1 \\ \frac{(C_{me} - C_e + \sqrt{C_e^2 - 2C_e C_{me} + C_{me}^2 + 4C_{me}^2})}{2C_{me}} \\ \frac{(C_{me} - C_e + \sqrt{C_e^2 - 2C_e C_{me} + C_{me}^2 + 4C_{me}^2})}{2C_{me}} \\ 1 \end{bmatrix}$$

$$V_4 = \begin{bmatrix} 1 \\ \frac{(C_e - C_{me} + \sqrt{C_e^2 - 2C_e C_{me} + C_{me}^2 + 4C_{me}^2})}{2C_{me}} \\ \frac{(C_e - C_{me} - \sqrt{C_e^2 - 2C_e C_{me} + C_{me}^2 + 4C_{me}^2})}{2C_{me}} \\ 1 \end{bmatrix}$$

The eigenvectors can be summarized as:

$$v_1 = \begin{bmatrix} -1 \\ -A \\ A \\ 1 \end{bmatrix} \quad v_2 = \begin{bmatrix} -1 \\ B \\ B \\ 1 \end{bmatrix} \quad v_3 = \begin{bmatrix} 1 \\ -C \\ -C \\ 1 \end{bmatrix} \quad v_4 = \begin{bmatrix} 1 \\ D \\ D \\ 1 \end{bmatrix}$$

For computing the four optimal eigenvectors and obtaining a good conditioning, an iterative method has been used. The following eigenvectors have been obtained:

$$v_1 = \begin{bmatrix} -1 \\ -0.84 \\ 0.84 \\ 1 \end{bmatrix} \quad v_2 = \begin{bmatrix} -1 \\ 0.6 \\ 0.6 \\ 1 \end{bmatrix} \quad v_3 = \begin{bmatrix} 1 \\ 1.46 \\ 1.46 \\ 1 \end{bmatrix} \quad v_4 = \begin{bmatrix} 1 \\ 0.3 \\ 0.3 \\ 1 \end{bmatrix}$$

10.2. Bisection method

The bisection method is the most simple numerical method to find the roots of a function. Its efficiency is low and it has the disadvantage of requiring particularly restrictive assumptions. However, it has the considerable advantage of being stable and guaranteeing the success of the operation. This method was chosen since the trend of the tangent is very unstable and the stability of such method allows to get the optimal result. To use the bisection method I proceed with the following analysis:

- I find the $[a,b]$ interval:
 - this interval is $[a, \lambda_0]$ for my choice.
 - I divide the interval $[a, b]$ in the half point c :
$$c = \frac{(a + b)}{2}$$
 - I compute $f(c)$: if this expression is zero the root is found and the iteration is stopped; otherwise the sign is evaluated :
 - if $f(c) > 0$, the right interval $[c, b]$ is neglected; I set $b = c$ and the procedure is repeated in the new interval;
 - if $f(c) < 0$, the left interval $[a, c]$ is neglected; I set $a = c$ and the procedure is repeated in the new range.

In this way the exact root should be found or alternatively a interval $[a, b] < 2\varepsilon$ where ε is required precision. The function is approximated by the straight line which passes through the points $(a, \text{sign}(f(a))), (b, \text{sign}(f(b)))$.

10.3. Discretization

The discretization is evaluated by using the finite difference method described in paragraph 2. The optimal discretization has been evaluated as composed of 16 points. Figs. 1-2 show the trends of the capacity in the air and in the dielectric for discretization values ranging from a minimum of 5 to a maximum of 36.

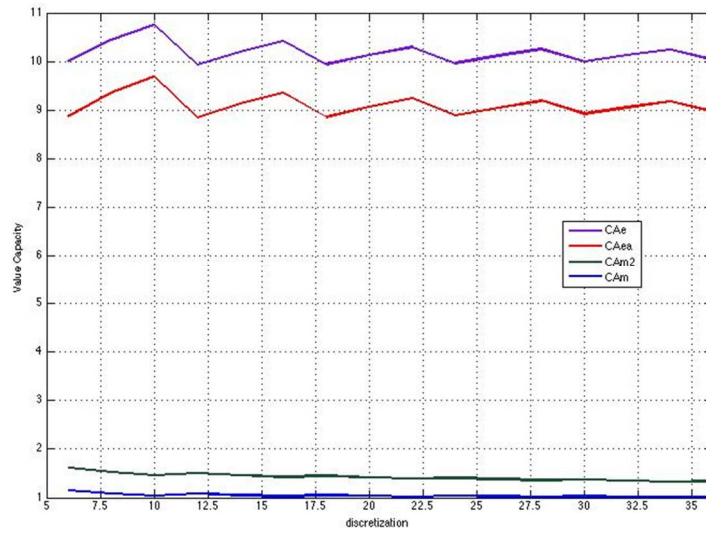


Fig. 10.1: Air capacities

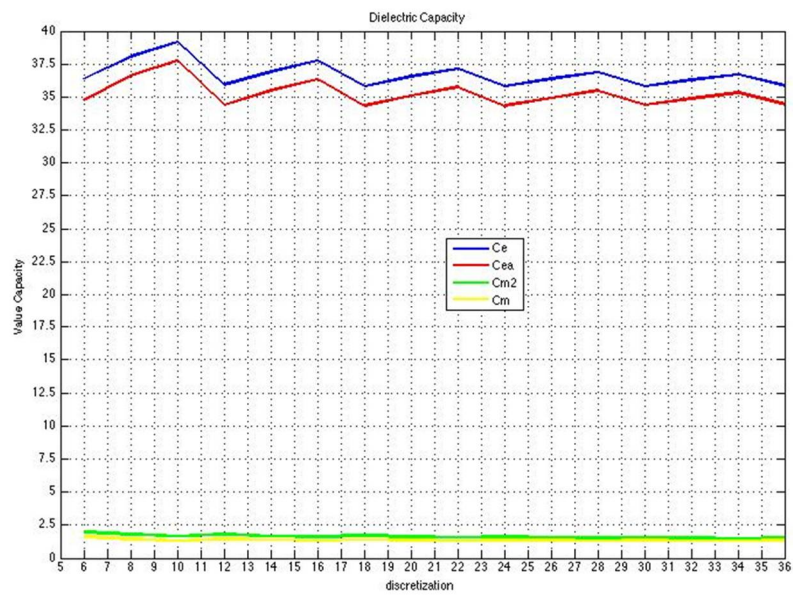


Fig. 10.2: Dielectric capacities

Acknowledgments

The research activity carried on throughout this thesis has been partially supported by the Regional Administration of Sardinia and the Port Authority of Cagliari (grants: CRP49289/Tender15, CRP49293/Tender16, CRP49297/Tender18).

Special thanks go to Daniele Giusto for the support during all my activities in these three years as PhD student.

I also would like to thank Alessandro Fanti for the support during my thesis and for the support given during the electromagnetic tests.

I would like to thank all the staff of MCLab and all the people who supported me both from a scientific and personal point of view all along this period of my life.

I thank all my friends for their invaluable friendship during these years especially Alessandro, Marzia, my “colleague” Ilenia, Silvia, Claudia, “el romano” Andrea, and Marina.

I would like to thank Claudia, Juse and Steve for their support during these months.

I want to thank my new friends Cristian for our coffee breaks, Valentina for the company, and last but not least Alessandro & Eleonora with Sebastiano and Giovanni for the time spent together.

Finally, I thank my special family (my mother Irma, my father Ignazio, my syster Francesca, my brother Sandro and my syster Luana with her husband Fabio), my little niece Sirya, my boyfriend Luca, Niky & Cucchi, Maria & Alberto for their help during all the hardest moments of my studies and life.

References

- [1] Federazione del Sistema Marittimo Italiano Censis, “Cluster marittimo e sviluppo in Italia e nelle regioni”, in IV Rapporto sull’Economia del mare, Roma, 2011;
- [2] Comunicazione della commissione al Parlamento Europeo, “Obiettivi strategici e raccomandazioni per la politica UE dei trasporti marittimi fino al 2018”, In COM(2009) 8 definitivo, Bruxelles, 2009;
- [3] Legge 28 gennaio 1994, n. 84;
- [4] International Maritime Organization, “Safety of Life at Sea”, Londra, 1974
- [5] www.imo.org;
- [6] Ministero delle Infrastrutture e dei Trasporti, “Piattaforma Tecnologica Nazionale Marittima”, Roma, 2005;
- [7] RINA et alii, “Multimodal Interoperability E-services for Logistics and Environmental Sustainability)”, 2010;
- [8] European Commission, “The EU e-Maritime initiative”, Directorate-General for Energy and Transport, 2009;
- [9] CNR et al., “Programma Ritmare. La ricerca italiana per il mare”, Programma Nazionale di Ricerca scientifica e tecnologica, 2009;
- [10] <http://www.porto.cagliari.it/>;
- [11] L. Atzori, A. Iera, G. Morabito, The Internet of Things: A survey, The International Journal of Computer and Telecommunications Networking, Volume 54 Issue 15, October, 2010;
- [12] D. Giusto, A. Iera, G. Morabito, L. Atzori (Eds.), The Internet of Things, 1662 Springer, 2010. ISBN: 978-1-4419-1673-0;
- [13] I.F.A. Vis, and R. de Koster. Transshipment of containers at a container terminal: An overview. European Journal of Operational Research Volume 147, Issue 1, 16 May 2003;

-
- [14] Recommended Minimum Safety Specifications for Quay Container Cranes, A joint initiative from TT Club, ICHCA International and Port Equipment Manufacturers Association, 2011;
- [15] <http://www.ttclub.com>;
- [16] <http://www.cict.it/index.shtml>;
- [17] Terrestrial Trunked Radio (TETRA), ETSI EN 300 392;
- [18] M. Fadda, M. Murroni, C. Perra, V. Popescu. TV white spaces exploitation for multimedia signal distribution. *Signal Processing: Image Communication*, Volume 27, Issue 8, Pages 893-899, ISSN 0923-5965, 10.1016/j.image.2012.01.014, September 2012;
- [19] Grumett S. Recording and monitoring the inspection of safety items. Great Britain, GB2460037- A. 2009-11-18;
- [20] <http://www.webgis.com/>;
- [21] INFISO D.4 Networked Enterprise & RFID INFISO G.2 Micro & Nanosystems, in: Co-operation with the Working Group RFID of the ETP EPOSS, Internet of Things in 2020, Roadmap for the Future, Version 1.1, 27 May 2008;
- [22] National Intelligence Council, Disruptive Civil Technologies – Six Technologies with Potential Impacts on US Interests Out to 2025 – Conference Report CR 2008-07, April 2008, http://www.dni.gov/nic/NIC_home.html;
- [23] <http://wisp.wikispaces.com>;
- [24] J. Pasley, “How BPEL and SOA are changing web services development”, *IEEE Internet Computing* 9(3)(2005) 60–67;
- [25] P. Spiess, S. Karnouskos, D. Guinard, D. Savio, O. Baecker, L. Souza, V. Trifa, “SOA-based integration of the internet of things in enterprise services, in: *Proceedings of IEEE ICWS 2009*”, Los Angeles, Ca, USA, July 2009;
- [26] Ning Xu, “A Survey of Sensor Network Applications”. Computer Science Department University of Southern California. 2003;
- [27] <http://ieee802.org/15>;
- [28] IEEE 802.15 Working Group for WPAN;
- [29] <http://www.ieee802.org/11>;
- [30] <http://ieee802.org/16>;
-

-
- [31] <http://www.3gpp.org>;
- [32] <http://ieee1451.nist.gov/intro.htm>;
- [33] Min Chen, Sergio Gonzalez, Athanasios Vasilakos, Huasong Cao, Victor C. M. Leung, “Body Area Networks: A Survey”, *Mobile Netw Appl* (2011) 16:171–193;
- [34] Huan-Bang Li, Ryuji Kohno. Body Area Network and Its Standardization at IEEE 802.15.BAN. *Advances in Mobile&Wireless Communications*, Volume 16, 2008;
- [35] Khalid Abu Al-Saud, Massudi Mahmuddin and Amr Mohamed, “Wireless Body Area Sensor Networks Signal Processing and Communication Framework: Survey on Sensing, Communication Technologies, Delivery and Feedback”, *Journal of Computer Science* 8 (1): 121-132, 2012;
- [36] <http://www.bluetooth.com>;
- [37] <http://www.zigbee.org>;
- [38] Movassaghi S., Arab P., Abolhasan M., “Wireless technologies for Body Area Networks: Characteristics and challenges”, *Communications and Information Technologies (ISCIT)*, 2012 International Symposium on, 2-5 Oct. 2012;
- [39] Juels A., “RFID security and privacy: a research survey”, *Selected Areas in Communications*, *IEEE Journal on* (Volume:24, Issue: 2);
- [40] M. Buettner, and D Wetherall. An Empirical Study of UHF RFID Performance. *MobiCom* 2008;
- [41] L. Sandip, *RFID Sourcebook*, IBM Press, 2006;
- [42] J.Rubio, I. Padillo, J. Espina, J. Verastegui, J. Lopez-de-Ipina, RFID in workplace safety solutions, *ITG-Fachbericht 224 – RFID Systech 2010*, pag.1-7;
- [43] D. J. Yeager, A. P. Sample, J. R. Smith. WISP: A Passively Powered UHF RFID Tag with Sensing and Computation. *RFID Handbook: Applications, Technology, Security & Privacy*, CRC Press, 2008;
- [44] D. J. Yeager, A. P. Sample, J. R. Smith. WISP: A Passively Powered UHF RFID Tag with Sensing and Computation. *RFID Handbook: Applications, Technology, Security & Privacy*, CRC Press, 2008;
- [45] C.Musu, V. Popescu, D. Giusto, “Workplace Safety Monitoring using RFID Sensors”, *Telecommunications forum (TELFOR)*, 2014, 25-27 Nov. 2014
- [46] <https://spqr.eecs.umich.edu/moo>, viewed 01.09.2014;
-

-
- [47] H.Zhang, J. Gummeson, B. Ransford, K. Fu, Moo: A batteryless computational RFID and Sensing Platform,ech. Rep. UM-CS-2011- 020, UMass Amherst Department of Computer Science, June 2011;
- [48] <http://www.impinj.com/products/readers/>;
- [49] Atzori, L.; Dessi, T.; Popescu, V.; , "Indoor navigation system using image and sensor data processing on a smartphone," Optimization of Electrical and Electronic Equipment (OPTIM), 2012 13th International Conference on , vol., no., pp.1158-1163, 24-26 May 2012, doi: 10.1109/OPTIM.2012.6231975
- [50] A. Fanti, A Generalized finite difference approach to the computation of modes, PhD Thesis, University of Cagliari , 2012.
- [51] G. Mazzarella, "CAD modeling of interdigitated structures", IEEE Trans. Educ., vol. 42, pp.81 -87 1999
- [52] C. A. Balanis, Antenna Theory Analysis and Design, John Wiley and Sons, Inc., 1997.
- [53] K.Lias, A.Hii Wee Teen, D.A.A.Mat, K.Kipli, A.S.W.Marzuki, M.H.Husin, "Biological Effect of 900MHz and 1800MHz Mobile Phones in SAR weight", Proc International Conference on Information and Multimedia Technology, 2009, pp.422-425.
- [54] L.Ahma, M.Ibrani, and E.Hamiti ,“Computation of SAR Distribution in a Human Exposed to Mobile Phone Electromagnetic Fields”, PIERS Proceedings, Xi'an, China, March 22-26, 2010, pp.1555-1557.
- [55] D.D.Arumugam, D.W.Engels, "Impacts of RF radiation on the human body in a passive RFID environment," IEEE Antennas and Propagation Society International Symposium and USNC/URSI National Radio Science Meeting, San Diego, CA, USA, 2008, pp.1- 4.
- [56] www.cst.com
- [57] Information of Phantom POPEYE V5.X . Available on: <http://www.speag.com/news-events/news/measurement/newproduct-popeye/>.
- [58] Information of SAM Head Phantom. Available on : <http://www.mcluk.org/>
- [59] HUGO. ViewTec. Ltd. [Online]. Available: <http://www.viewtec.ch/>
- [60] [meddiv/meddiv_e.html](#)
- [61] S. Valbonesi, M. Barbiroli, M. Frullone, E. Papotti, S. Vaccari, A. Vanore – “Oncological hyperthermia: working exposure assessment to RF field” – Presentato come
-

full speech al “10° International Conference of the European Bioelectromagnetic Association – EBEA2011”, Roma, 2011;

- [62] M.Sole, C.Musu, F.Boi, D.Giusto,and V. Popescu, ”RFID sensor network for workplace safety management”, ETFA 2013, pag1-4
- [63] A. Tronquo,H. Rogier, C.Hertleer, and L. VanLangenhove, “Applying textile materials for the design of antenna for wireless body area network, ” _Antennas and Propagation, 2006 EuCAP 2006, pages 1-5
- [64] P. Salonen, Y. Rahmat-Samii, and M. Kivikoski.Wearable antennas in the vicinity of human body.In Proc. of IEEE Antennas and Propagation Symposium ,volume 1, pages 467–470, Monterey, USA, Jun 2004.
- [65] S.Manzari, C.Occhiuzzi, and G.Marrocco, ” Feasibility of Body Centric Systems using passive textile RFID Tags”, IEEE Antennas and Propagation Magazine, Vol. 54, No. 4, August 2012
- [66] <http://www.kronjaeger.com/hv-old/hv/tbl/prop.html>

Related Papers

The main contribution on which some of the chapters of this thesis are based, have already been published during the PhD studies.

- [1] Sole Mariella; **Musu Claudia**; Boi Fabrizio; Giusto Daniele; Popescu Vlad, “Control System for Workplace Safety in a Cargo Terminal”, Wireless Communications and Mobile Computing Conference (IWCMC), 2013 9th International, pp. 1035 – 1039, 1-5 July 2013.
- [2] Sole Mariella; **Musu Claudia**; Boi Fabrizio; Giusto Daniele; Popescu Vlad, "RFID sensor network for workplace safety management", Emerging Technologies & Factory Automation (ETFAs), 2013 IEEE 18th Conference on , vol., no., pp.1,4, 10-13 Sept. 2013.
- [3] **C.Musu**, A.Fanti, and D.Giusto, “Dosimetry and biological effect evaluation on electromagnetic model of head”, Telecommunications forum (TELFOR), 2013, pages 663-666, 26-28 Nov. 2013.
- [4] **C.Musu**, V.Popescu, and D.Giusto, “Workplace Safety Monitoring using RFID Sensors”, Telecommunications forum (TELFOR), 2014, 25-27 Nov. 2014.
- [5] **C.Musu**, A.Fanti “Wearable Rectangular Patch Antenna for ICT Application: Dosimetry evaluation”, Telecommunications forum (TELFOR), 2014, 25-27 Nov. 2014.